NOTE TO USERS

Page(s) not included in the original manuscript and are unavailable from the author or university. The manuscript was scanned as received.

11-15

This reproduction is the best copy available.

UMI®

PROSTAGLANDIN J2-REGULATED PATHWAYS CRITICAL FOR AGGREGATION OF UBIQUITINATED PROTEINS AND NEURODEGENERATION IN A CELLULAR MODEL OF NEUROINFLAMMATION

by

ZHIYOU WANG

A dissertation submitted to the Graduate Faculty in Biochemistry in partial fulfillment of the requirements for the degree of Doctor of Philosophy, The City University of New York

2005

This Manuscript has been read and accepted by the Graduate Faculty in Biochemistry in satisfaction of the dissertation requirement for the degree of Doctor of Philosophy

4/22/05
Date

Maria Figueiredo-Pereira
Dr. MARIA FIGUEIREDO-PEREIRA
(Hunter College, **Chair of Examining Committee**)

5/3/05
Date

L. Davenport
Dr. LESLEY DAVENPORT
Executive Officer

Dr. LAUREL ECKHARDT
(Hunter College)

Dr. THOMAS SCHMIDT-GLENEWINKEL
(Hunter College)

Dr. WILLIAM TANSEY
(Cold Spring Harbor Laboratory)

Dr. PETER WERNER
(Albert Einstein College of Medicine)

Supervisory Committee

THE CITY UNIVERSITY OF NEW YORK

Abstract

PROSTAGLANDIN J2-REGULATED PATHWAYS CRITICAL FOR AGGREGATION OF UBIQUITINATED PROTEINS AND NEURODEGENERATION IN A CELLULAR MODEL OF NEUROINFLAMMATION

by

Zhiyou Wang

Adviser: Dr. Maria E. Figueiredo-Pereira

Most neurodegenerative diseases, such as Parkinson's disease (PD) and Alzheimer's disease (AD), are characterized by two hallmarks: the progressive loss of neuronal cells and the presence of inclusion bodies with aggregates of ubiquitinated proteins. However, the cellular and molecular mechanisms responsible for these two pathological characteristics remain elusive. In particular, the pathogenic role of the inclusion bodies is still widely debated.

The research described in this project addresses the hypothesis that inflammation may be a major contributor to both neuronal death and aggregation of ubiquitinated

proteins that occur in neurodegeneration. Two experimental approaches were undertaken to investigate this hypothesis:

1) To address the impact of inflammation on neuronal cells we treated human neuroblastoma SK-N-SH cells with prostaglandin J2 (PGJ2), an endogenous product of inflammation. Through high-throughput genomic and proteomic approaches we identified intracellular pathways affected by PGJ2 that may be relevant to neurodegeneration. Some of these pathways include the heat shock response, the ubiquitin/proteasome pathway and mitochondrial energy production.

2) To establish mechanisms implicated in the aggregation of ubiquitinated proteins detected in neurodegenerative disorders we focused on the sequestosome-1/p62. The latter is a protein containing a ubiquitin associated domain (UBA) at its C-terminus which confers the ability to bind polyubiquitinated proteins non-covalently. We found that PGJ2 up-regulates sequestosome 1/p62 in a time- and dose-dependent manner in human neuroblastoma SK-N-SH cells. Preventing sequestosome 1/p62 up-regulation by RNA interference abolished the aggregation but not the

accumulation of ubiquitinated proteins nor PGJ2-cytotoxicity.

In conclusion, these findings support the hypothesis that for many neurodegenerative diseases for which the root cause is unknown, products of neuroinflammation, such as PGJ2, may play a key role. Furthermore, sequestosome 1/p62 up-regulation under stress conditions, such as those induced by PGJ2, contributes to the "sequestration" of poly-ubiquitinated proteins into aggregates. However, the overwhelming accumulation of ubiquitinated proteins, rather than their aggregation, is likely to be an important contributor to neuronal death.

Acknowledgements

First of all, I would like to express my appreciation to Professor and Dr. Maria Figueiredo-Pereira for her advice, support and encouragement during my intense doctoral research endeavor for the past two and half years. As my mentor, she has constantly supervised me to remain organized and normalized on my data, précised and well-repeated on biochemical measurements, and focused on achieving my goal. Her close observations and immediate comments helped me to establish the overall direction of the research and to move forward with investigation in depth.

And most of all, I am grateful for Dr. Maria Figueiredo-Pereira, for her peer review she has contributed toward shaping this thesis.

I would like to express my sincere thanks to my thesis committee members: Dr. Thomas Schmidt-Glenewinkel, Dr. Laurel Eckhardt, Dr. Peter Werner and Dr. William Tansey. They all gave me valuable suggestions from my initial proposals through research progress. I specially thank Dr.

Werner and Dr. Tansey for their generous time to come a long distance to join my committee meetings.

I greatly thank Dr. Frida Kleiman in the chemistry department of my school for her advice to do cell fractioning experiments.

I would like to thank colleagues and organizations for sharing their resources that have been utilized to take immunofluorescence images and collect and analyze microarray datasets. The colleagues and organizations whose resources I have used in scheduling experiments reported in this thesis include: Dr. William Lloyd at the Image Facility in our department of Hunter College of the City University of New York, Mr. Anthony Galante at the Center for Applied Genomics at Newark, NJ.

I would like to thank to all those who helped and supported me during this work toward my PH.D. degree, to all my colleagues in the lab for numerous helps from them.

I would like to thank administrative staff members of the school who have been kind enough to advise and help in their respective roles.

Last, but not least, I would like to dedicate this thesis to my parents, my wife and son and my parents-in-law for their love, patience, and understanding. They allowed me to spend most of the time on this thesis.

Table of Contents

Page

Title i

Copyright Page ii

Approval Page iii

Abstract iv

Acknowledgement vii

Table of Contents x

List of Figures xv

List of Tables xviii

List of Abbreviations xix

***Chapter I* Introduction** 1

1.1 **NEUROINFLAMMATION AND NEURODEGENERATION** 3

1.1.1 Neuroinflammation 3

1.1.2 Cyclooxygenase-2 (COX-2) and Neurodegeneration 4

1.1.3 Prostagladin J2 (PGJ2) and Neurodegeneration 7

1.2 **INCLUSION BODIES IN NEURODEGENERATION** 14

1.2.1 The Ubiquitin/Proteasome Pathway (UPP) 13

1.2.2 Involvement of the UPP in

Neurodegeneration 19

1.2.3 The Role of Protein Aggregates in Neurodegeneration 21

1.2.4 The Sequestosome-1/p62 and Protein Aggregates 22

***Chapter II* Materials and Methods** 26

2.1 MATERIALS 27

2.2 CELL CULTURES 27

2.3 CELL TREATMENTS 28

2.4 MICROARAY HIGH THROUGHPUT SCREENING OF GENE INDUCTION/REPRESSION 28

2.5 COMPUTATIONAL ANALYSIS OF MICROARRAY DATA.....30

2.6 HIGH-RESOLUTION TWO-DIMENTIONAL GEL ELECTROPHORESIS 31

2.7 LIQUID CHROMATOGRAPHY TANDEM MASS SPECTROMETRY (LC-MS/MS) 33

2.8 WESTERN BLOTTING 33

2.9 RT-PCR ANALYSIS 34

2.10 IMMUNOFLUORESCENCE 34

2.11 RNA INTERFERANCE 35

2.12 CELL VIABILITY ASSAY 35

2.13 PROTEIN CONCENTRATION 36

2.14 STATISTICAL ANALYSIS 37

Chapter III **Hightroughput characterization of the response of human neuroblastoma SK-N-SH cells to prostaglandin J2, a product of inflammation: from genomics to proteomics** ... 38

3.1 Introduction 39

3.2 Results 40

3.3 Effect of PGJ2 on Differential Gene Expression in Human Neuroblastoma SK-N-SH cells 40

3.4 Functional Classification of Known Genes Differentially Expressed in Human Neuroblastoma SK-N-SH cells Upon PGJ2-Treatment 44

3.5 High-resolution two-dimensional gel electrophoresis protein pattern in human neuroblastoma SK-N-SH cells upon PGJ2-treatment 45

3.6 Two-dimensional Immunoblot Analysis of Ubiquitinated Proteins that Accumulate in Human Neuroblastoma SK-N-SH cells Upon PGJ2-Treatment 46

3.7 Discussion 47

Chapter IV **Inhibition of sequestosome 1/p62 up-regulation prevents aggregation of**

ubiquitinated proteins induced by prostaglandin J2 without reducing its neurotoxicity 53

4.1 Introduction 54

4.2 Results 58

4.3 PGJ2 induces a dose-dependent increase in sequestosome 1/p62 expression 58

4.4 PGJ2 stimulates a time-dependent increase in the levels of sequestosome 1/p62 and ubiquitinated proteins that correlates with a decrease in cell viability 59

4.5 PGJ2 promotes the formation of cytoplasmic protein aggregates containing ubiquitinated proteins, sequestosome 1/p62 and UCH-L1 60

4.6 Sequestosome 1/p62 post-transcriptional silencing prevents the cytoplasmic aggregation of ubiquitinated proteins induced by PGJ2 62

4.7 Sequestosome 1/p62 post-transcriptional silencing does not prevent PGJ2-cytotoxicity 63

4.8 Discussion 64

***Chapter V* Model** 73

***Chapter VI* Conclusions and Future Directions** 78

***Chapter VII* Reference List** 135

List of Figures

Page

Figure 1 The activity of cyclooxygenases enerates the precursors for the prostaglandin family 83

Figure 2 Metabolic pathway of PGJ2 derivation 84

Figure 3 Possible modes of action of prostaglandins of the J2 series in cells 85

Figure 4 Protein ubiquitination..... 86

Figure 5 The 26S proteasome 87

Figure 6 The structure of the 20S proteasome 88

Figure 7 Functional domains of the p62 protein..... 89

Figure 8 Scheme illustrating the two steps required for DNA hybridization on a microarray glass slide 90

Figure 9 Overall analysis of the 11 experiments carried-out for microarray analysis of the gene expression profile..... 91

Figure 10 Time course of the number of known genes 92

Figure 11 Functional classification of 465 known genes ... 93

Figure 12 Coomassie-stained acrylamide two-dimensional gel electrophoresis pattern of proteins..... 95

Figure 13 Ubiquitinated proteins..... 97

Figure 14 PGJ2 increases the expression of sequestosome 1/p62 in a dosedependent manner..... 99

Figure 15 PGJ2 increases sequestosome 1/p62 and ubiquitinated protein levels in a time-dependent manner 101

Figure 16 The time-dependent decrease in cell viability induced by PGJ2 is inversely proportional to the increase in ubiquitinated protein and sequestosome 1/p62 levels 103

Figure 17 Sequestosome 1/p62 and ubiquitinated proteins are co-localized in aggregates 104

Figure 18 Co-localization of sequestosome 1/p62 and UCH-L1.....105

Figure 19 PGJ2 increases protein aggregation in a time-dependent manner 106

Figure 20 Post-transcriptional silencing of sequestosome 1/p62 107

Figure 21 Aggregation (but not accumulation) of ubiquitinated proteins induced by treating SK-N-SH cells with 15μM PGJ2 is prevented by post-transcriptional 109

Figure 22 Post-transcriptional sequestosome 1/p62 silencing failed to prevent PGJ2 cytotoxicity...111

Figure 23 Scheme linking inflammation to neurodegeneration 112

List of Tables

Page

Table 1 Frequency and number of known genes that showed altered expression 113

Table 2 Time course of the number of known genes with significantly expression change 114

Table 3 Gene significantly up-regulated..... 115

Table 4 Gene significantly down-regulated..... 123

Table 5 Functional classification of genes that are significantly upregulated 127

Table 6 Functional classification of genes that are segnificantly downregulated 130

Table 7 Altered protein expression 133

List of Abbreviations

AA	Arachidonic Acid
AD	Alzheimer's disease
ALS	Amyotrophic Lateral Sclerosis
BCA	bicinchoninic acid
CNS	central nervous system
CFTR	cystic fibrosis transmembrane conductance regulator
COX-1	Cyclooxygenase 1
COX-2	Cyclooxygenase-2
DALIS	dendritic cell aggresome-like induced structures
DAPI	4',6-Diamidino-2-phenylindole
DMSO	dimethyl sulfoxide
15d-PGJ2	15-deoxy-Δ12,14-PGJ2
DriPs	defective ribosomal products
DTT	dithiothreitol
ERK	extracellular regulated kinase
GFP	green fluorescent protein
HD	Huntington's disease
HNE	4-Hydroxy-2-nonenal
IL-1β	interleukin-1β
JNK	Jun N-terminal kinase
LPS	lipopolysaccharide
MAPK	mitogen-activated protein kinase

MEM	minimal essential media
MPP(+)	1-methyl-4-phenylpyridinium ion
MTOC	Microtubule Organizing Center
MPTP	1-Methyl-4-phenyl-1,2,3,6-tetrahydropyridine
MTT	3-(4,5-dimethylthiazol-2-yl)-2,5-diphenyl tetrazolium Bromide
NMDA	N-methyl-D-aspartate
NSAIDs	non-steroidal anti-inflammatory drugs
PAGE	Poly-Acrylamide Gel Electrophoresis
PBS	Phosphate Buffered Saline
PD	Parkinson's disease
PGD2	Prostaglandin D2
PGE2	Prostaglandin E2
PGJ2	Prostaglandin J2
PGG2	prostaglandin G2
PGH2	prostaglandin H2
PolyQ	polyglutamine
PPARγ	peroxisome proliferator-activated receptor γ
PUFAs	polyunsaturated fatty acids
RNAi	RNA interference
RT-PCR	Reverse Transcription Polymerase Chain Reaction
SDS	Sodium dodecyl sulphate
Seq.	sequestosome 1/p62
siRNA	silencing RNA oligonucleotides

TNFα	tumor necrosis factor α
TNFβ	tumor necrosis factor β
Ub	ubiquitin
UBA	ubiquitin-associated domain
UCH-L1	ubiquitin C-terminal hydrolase L1

Chapter I

Introduction

Most neurodegenerative diseases, such as Parkinson's disease (PD) and Alzheimer's disease (AD), are characterized by two clinical hallmarks in the particular affected areas of the nervous system: the progressive loss of neuronal cells and the presence of inclusion bodies with aggregates of ubiquitinated proteins in many of the remaining neurons. The cellular and molecular mechanisms responsible for these two pathological characteristics remain elusive. Neuronal death in the Central Nervous System (CNS) is, in many cases, shown to be associated with oxidative stress or a spectrum of cytotoxic agents, such as N-methyl-D-aspartate (NMDA), pesticides, environmental contaminants, heavy metals and infectious agents. The pathogenic role of the inclusion bodies is still widely debated. Whether these inclusion bodies are protective or damaging to particular neurons is still unclear.

Since many neurodegenerative disorders found to be associated with the accumulation of ubiquitinated proteins in neuronal inclusions also exhibit signs of inflammation, we postulate that these two processes are interconnected in the neurodegenerative pathway. This project investigates possible mechanisms by which a product of inflammation, i.e. prostaglandin J2 (PGJ2), leads to the accumulation and

aggregation of ubiquitinated proteins and to neuronal death. Identification of intracellular mechanisms that link inflammation with neurodegeneration is expected to have a positive impact on the design of new therapeutic approaches for neurodegenerative disorders, such as PD and AD, which exhibit the common pathological characteristics of abnormal aggregates of ubiquitinated proteins and signs of inflammation.

1.1 NEUROINFLAMMATION AND NEURODEGENERATION

1.1.1 Neuroinflammation

One mechanism that may explain the neuronal damage observed in neurodegenerative disorders is neuroinflammation. The latter is a CNS response (Streit et al., 2004) to injury induced by a variety of insults, such as neurotoxins including trimethylin, 1-methyl-4-phenyl-1,2,3,6-tetrahydropyridine (MPTP), rotenone, lipopolysaccharide (LPS) and HIV-glycoprotein gp-120 (Viviani et al., 2004b).

In the initial stage of the reaction, astrocytes or microglia are activated to release pro-inflammatory cytokines (TNF-α, IL-1β), free radicals (nitric oxide,

superoxide, perhydroxyl), and/or anti-inflammatory mediators (TNF-β1, cyclopentenone prostaglandins) (Gao et al., 2003). As a result, several intracellular pathways are stimulated in neurons as well as glia. For example, TNF-α leads to caspase-8 mediated apoptosis and an intracellular increase in Ca^{2+} (MacEwan, 2002). Both TNF-α and IL-1β activate NF-κB and MAPK signaling pathways (Viviani et al., 2004a). Free radicals induce inflammatory reactions and oxidative stress (Djordjevic, 2004). Anti-inflammatory mediators, such as TNF-β1 and cyclopentenone prostaglandins, induce apoptosis and inhibit NF-κB (Lawrence et al., 2001).

As discussed below, increasing experimental evidence implicates neuroinflammation in the development of neurodegenerative disorders.

1.1.2 Cyclooxygenase-2 (COX-2) and Neurodegeneration

COX-2 is a central inflammatory mediator. It plays a key role in catalyzing the rate-limiting step in the biosynthesis of prostaglandins, prostacyclins and thromboxane A2 from their precursor arachidonic acid (Smith

et al., 2000). As illustrated in Figure 1 Page 83, cyclooxygenases are bifunctional enzymes that catalyze the cyclooxygenation of arachidonic acid to prostaglandin G2 (PGG2) followed by the hydroperoxidation of PGG2 to prostaglandin H2 (PGH2) (Kulkarni et al., 2000) with the generation of free radicals as by-products. Specific reductases, isomerases and synthases then convert PGH2 to other prostaglandins and thromboxane A2.

The brain expresses cyclooxygenase-1 (COX-1) and COX-2 under normal physiological conditions but COX-2 levels are dynamically regulated by pro-inflammatory signals and by physiological neuronal plasticity involving, for example, NMDA receptor activation (Yamagata et al., 1993). The cellular levels of COX-2 are dynamically regulated by pro-inflammatory mediators via the transcriptional activation of, for example C/EBP-β and NF-κB (Wu, 2005).

There seems to be a close correlation between COX-2 up-regulation and neurodegeneration. For instance, COX-2 is up-regulated in neurofibrillary tangle-containing and damaged neurons in the frontal cortex (Pasinetti and Aisen, 1998) or hippocampal pyramidal layer of AD patients (Ho et al., 1999), and the spinal cord of ALS patients (Yasojima

et al., 2001). In addition, increased cyclooxygenase activity indicated by a higher level of PGE2, was detected in the substantia nigra of brains of PD patients (Mattammal et al., 1995).

The role of cyclooxygenase activity in neurodegeneration is further supported by the finding that its inhibition attenuates neuronal degeneration. For example, the cyclooxygenase inhibitor sodium salicylate significantly limits 1-methyl-4-phenylpyridinium ion (MPP^+)-induced striatal dopamine depletion (Sairam et al., 2003), blocks the degeneration of dopamine-containing neurons induced by LPS (Araki et al., 2001) and inhibits TNF-α-induced activation of NF-κB (Manna et al., 1999).

More strikingly, treatment of AD patients with non-steroidal anti-inflammatory drugs (NSAIDs), which are cyclooxygenase inhibitors, slows the progression of the disease proportionally to the duration of the treatment (Stewart et al., 1997). However, this effect is controversial and still under investigation.

In summary, these studies support the notion that there is a connection between cyclooxygenase activity, most likely

involving COX-2, and neurodegeneration.

1.1.3 Prostaglandin J2 (PGJ2) and Neurodegeneration

Interestingly, prostaglandin J2 (PGJ2), which is one of the products of cyclooxygenases, exhibits both anti-inflammatory and pro-inflammatory properties. PGJ2 plays a role as an anti-inflammatory agent by inhibiting NF-κB (Rossi et al., 2000), blocking the production of pro-inflammatory mediators such as inducible nitric oxide synthase (iNOS), TNF-α, IL-1β, suppressing IL-1β-induced COX-2 expression (Sawano et al., 2002) and limiting LPS-induced microglia and astrocyte activation (Giri et al., 2004). However, it also stimulates the production of pro-inflammatory mediators, such as IL-8, in activated T cells (Harris et al., 2002) and activates COX-2 promoters (Meade et al., 1999).

PGJ2 is derived from PGD2, the major prostanoid made in the mammalian CNS (Figure 2, Page 84). PGD2 is produced by PGD2 synthases, which are enzymes that carry out the isomerization of PGH2 to PGD2 (Urade and Hayaishi, 2000). PGD2 readily undergoes *in vivo* and *in vitro* non-enzymatic dehydration to generate PGJ2, which is further converted to

Δ12-PGJ2 and 15-deoxy-$^{\Delta}$12,14-PGJ2 (15d-PGJ2) (Kulkarni et al., 2000).

Prostaglandins are formed in regions of the brain and spinal cord in response to different types of challenges (Kaufmann et al., 1997). Their physiological concentrations in body fluids are found to be in the pico-nanomolar range (Fukushima, 1990). However, their levels rise considerably under pathological conditions such as hyperthermia, infection and inflammation, reaching the micromolar range at the site of damage (Herschman et al., 1997;Offenbacher et al., 1986;Offenbacher et al., 1986).

Synthesis of cyclopentenone prostaglandins, such as prostaglandins of the J2 series, was found to increase in the late phase of inflammation and to be associated with its resolution (Gilroy et al., 1999b). For example, the induction of COX-2 expression following carrageenin-induced pleurisy in rats, is biphasic occurring two hours and 48h after the pro-inflammatory insult. The COX-2 peak at two hours was associated with maximal PGE2 synthesis, while the 48h COX-2 peak coincided with high levels of PGD2 and 15d-PGJ2. The second COX-2 surge was significantly greater (~350%) than the first one and coincided with the anti-

inflammatory phase meant to resolve inflammation. Therefore, the concentration of prostaglandins of the J2 series may be increased in response to pro-inflammatory stimuli, particularly during the resolution phase of the inflammatory response (Gilroy et al., 1999a).

It is possible that only low levels of 15d-PGJ2 can be detected in biological fluids. 15d-PGJ2 has a short half-life and binds avidly to free sulfhydryl groups and thus most of it could be bound to intracellular proteins. Attempts to accurately measure the endogenous levels of 15d-PGJ2 should focus on assessing intracellular 15d-PGJ2/protein complexes (Gilroy et al., 2004).

Once synthesized prostaglandins of the J2 series are released or exported to the extracellular space. As they are unstable, they exert their effects near their site of synthesis thus acting as autocrine or paracrine hormones (Scher and Pillinger, 2005). As illustrated in Figure 3 Page 85, for example 15d-PGJ2 enters the cells by an active transport system (Narumiya and Fukushima, 1986). An additional transport mechanism allows 15d-PGJ2 to enter the nucleus where it regulates gene transcription. Alternatively, PGD2 that enters cells by an anionic

transporter can be dehydrated to 15d-PGJ2 within the cytoplasm.

Once inside the nucleus, the cyclopentenone prostaglandins regulate gene transcription through different transcription pathways. For example, 15d-PGJ2, one of the cyclopentenones of the J2 series, seems to be an endogenous agonist for the transcription factor peroxisome proliferator-activated receptor γ (PPARγ). The prostaglandins of the J2 series were also shown to regulate gene expression through PPARγ-independent transcription. These prostanoids were shown to activate the p38/MAPK (Li et al., 2004a); (Wilmer et al., 2001), ERK and JNK(Li et al., 2004a) pathways (Sawano et al., 2002) and to inhibit the NF-κB pathway (Wilmer et al., 2001;Rossi et al., 2000;Straus et al., 2000).

Prostaglandins of the J2 series can also exert their effects directly as reactants participating in chemical reactions. Unlike most other classes of eicosanoids, prostaglandins of the J2 series contain a cyclopentenone ring with α,β-unsaturated carbonyl groups, making them susceptible to Michael addition reactions with free sulfhydryl groups of cysteines in glutathione and cellular

disassemble the polyubiquitin chains and may edit the ubiquitination state of proteins (D'Andrea and Pellman, 1998;Wilkinson, 2000).

Covalent binding of ubiquitin to proteins marks them for degradation by the 26S proteasome (Figure 5, Page 87), a multicomponent enzymatic complex with a native molecular weight of approximately 2,000 kDa (DeMartino and Slaughter, 1999). The 26S proteasome includes two major particles: a 20S particle, known as the 20S proteasome, which is the catalytic core, and a 19S particle, known as PA700, which is the regulatory component. Association between the two particles in the cell is a dynamic process and requires ATP-hydrolysis. The 20S proteasome can associate with other regulatory particles, such as PA28, but this combination is not known to affect the degradation of ubiquitinated proteins (DeMartino and Slaughter, 1999).

The 20S particle is composed of 28 subunits arranged in a topology characterized by an αββα sandwich (Figure 6, Page 88). The four heptameric-stacked rings form a cylindrical structure with a hollow center in which proteolysis takes place (Groll et al., 1997). The 20S proteasome hydrolyzes most peptide bonds present in a protein(Orlowski et al.,

1993), and its peptide cleavage patterns are influenced by its subunit composition(Boes et al., 1994). Assembly of this particle from precursor subunits is a complex process and was shown to require the assistance of a short-lived chaperone (Ramos et al., 1998).

The 19S particle (PA700) contains at least 17 subunits, including ATPases, a de-ubiquitinating enzyme and polyubiquitin-binding subunits. It confers ubiquitin/ATP-dependency to proteolysis by the 26S proteasome (DeMartino and Slaughter, 1999). PA700 can also stimulate proteasomal degradation of non-ubiquitinated proteins such as ornithine decarboxylase, which still requires ATP hydrolysis but not ubiquitination for its proteasomal breakdown (Murakami et al., 1992). The subunits in PA700 are distributed into a lid and base arrangement, with the lid required for recognition of polyubiquitinated proteins (Glickman et al., 1998). The base, containing the ATPases, exhibits chaperone-like activity(Braun et al., 1999).

The 26S proteasome is found in the cytoplasm next to intermediate filaments of the cytoskeleton(Scherrer and Bey, 1994). It also resides in the nucleus and in association with the cytoplasmic side of the ER membrane

(Palmer et al., 1996) (Reits et al., 1997;Reits et al., 1997). Localization studies with fluorescently labeled subunits of the 20S and 19S particles demonstrated that proteasomal proteolysis occurs mainly at the nuclear envelope/rough ER site (Enenkel et al., 1999). An important function of such proteolysis is to eliminate abnormal secretory proteins residing in an ER/pre-Golgi compartment(Plemper and Wolf, 1999). Functionally inefficient, misfolded or unassembled ER proteins leave this intracellular compartment by retrograde transport through the Sec61 translocation channel. They are ubiquitinated by ubiquitin-conjugating enzymes associated with the cytosolic side of the ER membrane and then degraded by the cytosolic 26S proteasome (Plemper and Wolf, 1999). Although this ER degradation pathway appears to be non-essential for viability, its importance is underscored by its evolutionary preservation "despite strong negative selection" since disruption of this mechanism seems to be associated with many disease states (Plemper and Wolf, 1999).

The 20S proteasome was detected in all areas of the rat CNS, but higher levels were found in pyramidal cortical

neurons of layer 5 and the motor neurons of the ventral horn of the spinal cord (Mengual et al., 1996).

1.2.2 Involvement of the UPP in Neurodegeneration

Since the UPP is responsible for the turnover of many proteins required to maintain neuronal homeostasis it is conceivable that perturbations in the UPP might play a role in protein aggregation and neurodegeneration. The link between UPP and neurodegeneration was strengthened by the identification of disease-causing mutations in genes encoding several members of the UPP (McNaught et al., 2001). The first example is parkin, which encodes a 52kDa protein that is a RING-type ubiquitin (Ub) ligase (E3). Various deletions and point mutations in parkin cause autosomal recessive juvenile parkinsonism (AR-JP), one of the most common forms of familial PD-like disease (Tanaka et al., 2001). In addition, a point mutation (Ile93Met) in UCH-L1 was identified in a German pedigree composed of two affected family members (Leroy et al., 1998). UCH-L1 encodes a ubiquitin carboxyl-terminal hydrolase and is one of the most abundant proteins in the brain.

Defects in the UPP are associated not only with hereditary

forms but also with sporadic forms of neurodegenerative disorders. For instance, oxidative modification of UCH-L1 was recently identified and linked to the pathogenesis of sporadic AD and PD (Choi et al., 2004). Furthermore, a significant decline (30-50%) of proteasome activity was observed in AD patients, indicating a possible role of direct proteasome modifications and inhibition in neurodegeneration (Keller et al., 2000).

Frameshift mutants of ubiquitin B (UbB+1) were found to co-localize with neurofibrillary tangles and senile plaques in the cerebral cortex of patients with sporadic AD. The gene encoding UbB contains GAGAG motifs that are prone to GA deletions during transcription. A single dinucleotide deletion (GA) in the first GAGAG motif of UbB mRNA, produces UbB+1, which lacks the C-terminal glycine, an amino acid essential for ubiquitination (van Leeuwen et al., 1998). UbB+1 molecules may impair degradation of ubiquitinated proteins by competing with wild type ubiquitin in the interaction with the 26S proteasome.

The UPP is a major participant of the intracellular protein quality control system, which also involves molecular chaperones. The role of the UPP in neurodegeneration is even more striking when the UPP is viewed not simply as an

isolated degradation pathway but rather as a complex cascade linked to other ubiquitin-dependent processes such as signal transduction and cell cycle as well as to the chaperone system (Berke and Paulson, 2003).

In summary, the UPP is recruited for removal of proteins that are most likely modified, misfolded and ubiquitin-tagged. Disturbance of protein degradation by the UPP must have catastrophic consequences and play a critical role in neurodegeneration. In this study we investigated the effect of UPP impairment induced by PGJ2 in SK-N-SH cells. We also addressed the role of the deubiquitinating enzyme UCH-L1 on the biogenesis of protein aggregates.

1.2.3 Role of Inclusion Bodies in Neurodegeneration

The relationship between inclusion bodies containing protein aggregates and neurodegeneration is not well understood. On the one hand inclusions may be beneficial and result from an attempt of the cell to isolate a subclass of ubiquitinated proteins that are not effectively degraded. On the other hand, the inclusions may impede normal cell function contributing to cell death. The size of the aggregates maybe a critical determinant of their

toxicity (Mezey et al., 1998). Small aggregates may be protective while expanded aggregates may confer fatal effects that can contribute to neuronal cell damage.

The mechanisms leading to protein aggregation and the role of protein aggregates in the progression of neurodegeneration are unclear. In this project we address mechanisms that may lead to protein aggregation and neuronal cell death induced by prostaglandin J2, which is a product of inflammation.

1.2.4. The Sequestosome-1/p62 and Protein Aggregation

The intracellular mechanisms that promote the aggregation of ubiquitinated proteins that evade degradation by the UPP and accumulate in inclusion bodies are not well defined. To address this issue, we focused on a protein known as sequestosome-1 or p62 (here after referred to as p62 for simplicity), first isolated in human tissues by Shin and colleagues (Park et al., 1995b). p62 belongs to a family of proteins, including Mud1 and Rad23, that contain ubiquitin-associated (UBA) domains (Hartmann-Petersen et al., 2003). This sequence motif is conserved among proteins that can bind polyubiquitin chains (Hofmann and Bucher, 1996;Hofmann

and Falquet, 2001). The UBA domain enables proteins to non-covalently bind polyubiquitin chains 300 times more tightly than mono-ubiquitin (Wilkinson et al., 2001;Madura, 2002). The UBA domain forms a compact three-helix bundle with a hydrophobic surface on one side that is likely the interface for protein-protein interactions (Bertolaet et al., 2001).

The UBA domain of p62, spanning residues 386-434 at its C-terminus, is required for its non-covalent binding to poly-Ub chains (Vadlamudi et al., 1996b). Clinical screening for p62 mutations in patients with Paget disease of bone (PDB) led to the identification of a recurrent non-conservative change (P392L) in its UBA domain that was not present in control individuals (Laurin et al., 2002). PDB is a common disease characterized by focal and disorganized increases in bone turnover. In this disease, nuclear and cytoplasmic inclusion bodies are detected in osteoclasts, which are the primary cells affected by PDB(Rebel et al., 1974;Howatson and Fornasier, 1982). Additional mutations in p62 were identified in both familial and nonfamilial PDB, including both amino acid substitutions and mutations that result in total deletion of the ubiquitin-binding domain (reviewed in Roodman and Windle, 2005). Patients with truncation

mutations in p62 exhibit a more severe Paget phenotype than patients with any of the point mutations. However, it is not yet clear whether alterations in ubiquitin binding are directly related to the mechanism of pathogenesis. The PDB-associated p62 mutations could potentially affect a number of cellular processes, such as signaling, ubiquitin-dependent proteolysis and others.

Due to its high affinity for poly-ubiquitin chains, p62 was suggested to serve as a receptor for binding and storing polyubiquitinated proteins (Shin, 1998b). Interestingly, p62 contains several other structural motifs suggesting that it might participate in the formation of multimeric signaling complexes (Figure 7, Page 89). These domains include an SH2 domain that binds the tyrosine kinase $p56^{lck}$ in a phosphotyrosine-independent manner (Vadlamudi et al., 1996a), an acidic interaction domain (AID) that binds the atypical PKC ζ (Puls et al., 1997), a ZZ type ZINC finger that binds the receptor interactive protein (RIP) involved in TNFα-induced apoptosis (Sanz et al., 1999), a binding site for the RING-finger protein tumor necrosis factor receptor-associated factor 6 (TRAF6) that is an E3 ubiquitin ligase (Sanz et al., 2000;Wooten et al., 2001) and two PEST sequences, which are hydrophobic regions that

target proteins for rapid degradation by the UPP [reviewed in (Geetha and Wooten, 2002)].

p62 was detected in ubiquitin-containing intraneuronal and intraglial inclusions in a variety of neurodegenerative disorders, such as atypical Pick's disease, PD, amyotrophic lateral sclerosis (ALS) and AD (Furukawa et al., 2004b;Kuusisto et al., 2001b;Nakano et al., 2004a;Zatloukal et al., 2002b) as well as in hepatocyte Mallory bodies associated with alcoholism (Stumptner et al., 2002a). Furthermore, the expression of p62 in neuronal cells is induced by serum withdrawal conditions that trigger apoptosis and by proteasomal inhibition (Kuusisto et al., 2001d;Nakaso et al., 2004a) as well as by the expression of expanded pathologic polyglutamine repeats (Nagaoka et al., 2004b).

Overall these findings suggest that p62 is likely to be involved in the biogenesis of inclusions containing ubiquitinated proteins. In this study we investigated the role of p62 in the aggregation of polyubiquitinated proteins induced by PGJ2 in human neuroblastoma SK-N-SH cells.

Chapter II

Materials and Methods

MATERIALS - Glass oligonucleotide microarrays (65 mers) were printed at the Center for Applied Genomics, CAG (Newark NJ). The chips are Human 19K Oligo Arrays with internal controls. 3DNA® Submicro™ Oligo Expression Array Detection kits were from Genisphere Inc. (Hatford, PA). Hybridization chambers (Hybchambers) were from Genemachines (San Carlos, CA). Microarray scanner (GenePix 4100B) was from Axon Instruments (Union City, CA). PGJ2 was from Cayman Chemical Co. (Ann Arbor, Michigan). The mouse monoclonal anti-p62 (1:500) antibody was obtained from BD Transduction Lab (San Diego, CA), the goat polyclonal anti-COX-1 (1:1,000) antibody was from Santa Cruz Biotechnology (Santa Cruz, CA), the rabbit polyclonal anti-ubiquitin conjugates (1:1,500) antibody from Dako Corp. (Carpinteria, CA), and the rabbit anti-UCH-L1 (1:2,000) antibody from BIOMOL (Plymouth Meeting, PA). The Super Signal West Pico detection system and the bicinchoninic acid protein assay kit were from PIERCE (Rockford, IL). Other reagents were of the highest purity available.

CELL CULTURES - SK-N-SH cells are a human neuroblastoma cell line derived from peripheral tissue (Biedler et al., 1978). The cells are maintained at 37°C in 5% CO2 and minimal essential media (MEM) with Eagle's salts containing

5% normal fetal bovine serum, 2mM L-glutamine, 1mM sodium pyruvate, 0.4% MEM vitamins, 0.4% MEM nonessential amino acids, and 100 units/ml penicillin, 100µg/ml streptomycin.

CELL TREATMENTS - Cells were treated for a specific period of time at 37°C without (vehicle, DMSO) or with different concentrations of PGJ2 in DMSO. The drug was added drop wise directly into serum-containing medium with a gentle swirl of the culture plate. The final DMSO concentration in the medium was 0.5%. When specified, inhibitors of transcription (actinomycin D, 1.25µg/ml) or translation (cycloheximide, 6.25µg/ml) both in DMSO, were added to the culture media 1h prior to PGJ2 treatment. At the end of the indicated incubation times, the cultures were washed twice with Phosphate Buffered Saline (PBS) and the cells were harvested as previously described (Figueiredo-Pereira et al., 1998). Cell washes removed unattached cells, hence subsequent assays were performed on adherent cells only.

MICROARAY HIGHTHROUGHPUT SCREENING OF GENE INDUCTION/REPRESSION - SK-N-SH cells were treated with 20µM PGJ2 for 4, 8, 16 and 24h. At the end of each incubation, total RNA from control and PGJ2-treated cells was isolated with a QIAGEN kit (Valencia,CA) according to the

manufacture's protocol. After the final step samples were concentrated with Amicon's Microcon 30 kit and validated for total RNA integrity by agarose gel electrophoresis. Since the Genisphere Submicro kit does not label contaminating genomic DNA it is not necessary to treat the RNA sample with DnaseI prior to use.

cDNAs were generated in a reverse transcriptase (RT) reaction for two hours at 42°C using 5μg of the total RNA per sample in a 20μl reaction volume with the reverse transcriptase Superscrip II from Invitrogen (Carlsbad, CA). For each microarray chip two consecutive hybridizations were performed with fluorescent probes from the 3DNA Submicro™ Oligo Expression Array Detection Kit (Genisphere) following the manufacture's specifications, as shown in Figure 8, page 90. Briefly, in the first hybridization reaction the solution containing the mixture of cDNAs obtained from control and treated cells was loaded onto an oligo array glass chip, which was subsequently incubated overnight at 55°C in an HybChamber from Genemachines (San Carlos, CA). In the second hybridization reaction Cy3 (green) and Cy5 (red) fluorescent probes were used to label the cDNAs from control and PGJ2-treated cells, respectively, with the 3DNA Submicro ™ Oligo

Expression Array Detection Kit. The second hybridization was carried out for 3 hours at 65°C in HybChambers from Genemachines (San Carlos, CA). This cDNA co-hybridization provides a measure of the relative gene expression levels defined as a fold-difference between two cell populations.

Differential signals emitted by Cy3 and Cy5 probes were obtained after scanning the microarray chip with the Axon Scanner (GenePix 4100B) where the signals from Cy3 labeled cDNAs from control (untreated) cells and those from Cy5 labeled cDNAs from treated cells were captured. The signal to background ratio for each spot on the glass microarray chip was calculated and normalized with the Axon GenePix Pro software.

COMPUTATIONAL ANALYSIS OF MICROARRAY DATA - Computational analysis of the microarray data generated was performed with the GeneSpring SoftWare at the Center for Applied Genomics (Newark, N.J.). Differential expression profiles of 18,325 human genes spotted on each array were generated by determining unequal signals emitted by the Cy3 and Cy5 probes after fluorescence laser scanning. Experimental clustering and ANOVA analysis with a p-value of 0.05 were also performed with this software.

HIGH-RESOLUTION TWO-DIMENTIONAL GEL ELECTROPHORESIS - SK-N-SH cells cultured to 90% density in 100mm dishes were treated with vehicle (DMSO, control) or 20μM PGJ2 for 24 hours consistent with the microarray analysis. To obtain similar protein concentration, control or PGJ2 treated cells in each dish were harvested in 100 or 70μl buffer containing 1% SDS and 10mM Tris, pH 7.5, respectively. To inactivate proteases and denature proteins completely, samples were boiled in a water bath for 5 min immediately after the harvest followed by mild sonication. Total lysates from control and PGJ2-treated cells were sent to Kendrick Laboratory Inc. (Madison, WI) for 2D-gel electrophoresis analysis of the protein content. Equivalent amounts of protein (200μg per sample) from control- and PGJ2-treated cells were separated in the first dimension according to their isoelectric point along a linear immobilized pH gradient (3/10) following the method of O'Farrell (O'Farrell, 1975). Briefly, isoelectric focusing was carried out in glass tubes of inner diameter 2.0mm using 2% pH 3.5-10 (Amersham Pharmacia Biotech, Piscataway, NJ) for 9600 volt-hrs. One μg of an IEF internal standard, tropomyosin, was added to each sample. This protein migrates as a doublet with a polypeptide spot of MW 33,000

and pI 5.2; an arrow on the stained gels marks its position.

In the second dimension, the proteins were separated according to their molecular mass using standard SDS-PAGE. Briefly, the pH gradient gels from the first dimension were equilibrated for 10 min in a buffer containing 10% glycerol, 50mM DTT, 2.3% SDS and 62.5 mM Tris, ph 6.8. The gels were then sealed to the top of a stacking gel overlaying a slab gel (10% acrylamide, 0.75 mm thick). And the SDS slab gel electrophoresis was carried out for 4 hours at 12.5 mA/gel followed by staining and drying. The bands for molecular weight standards appear at the basic edge of the Coomassie blue-stained acrylamide slab gel. The gel was dried between sheets of cellophane with the acid edge to the left.

Two gels were run in parallel for each sample. One gel was stained with Coomassie blue. This gel was used for mass spectrometry (MS) analysis of the protein spots of interest following the protocol established by the Rockefeller University Protein Resource Center. To determine which proteins are ubiquitinated upon PGJ2-treatment, the other gel was transferred to transfer buffer (12.5 mM Tris,

pH8.8, 86 mM Glycine, 10% MeOH) and transblotted onto PVDF membrane overnight at 200 mA and approximately 100 volts/two gels. The PVDF blots were probed with the anti-ubiquitin conjugates antibody (1:1,500 dilution, DAKO, CA).

The 2D-gel spot patterns obtained from control- and PGJ2-treated cells were compared. Some of the protein spots detected only in the gel obtained from PGJ2-treated cells and not in the corresponding control gel were carefully select for mass spectrometry analysis.

LIQUID CHROMATOGRAPHY TANDEM MASS SPECTROMETRY (LC-MS/MS): The protein spots of interest were excised from the 2D-gel and analyzed by LC-MS/MS following the protocol from the Rockefeller University Protein Resource Center where the MS analysis was performed.

WESTERN BLOTTING - Following the indicated treatments, cell extracts were prepared as described previously (Figueiredo-Pereira et al., 1998). 5-50 μg of protein/lane, were analyzed by SDS Poly-Acrylamide Gel Electrophoresis (SDS-PAGE). Detection of the proteins of interest was by western blotting and the antigens were visualized by a horseradish peroxidase method utilizing the Supersignal West PICO

chemiluminescent substrate (Pierce, Rockford, IL). Semi-quantitative analysis of protein detection was done by image analysis with the ImagePC program from National Institute of Health (NIH) as described (Pereira et al., 1992).

RT-PCR ANALYSIS - Total RNA was isolated with the RNeasy Kit from QIAGEN (Valencia,CA). To perform RT-PCR, 1µg of RNA/sample was reverse-transcribed in a 25µl reaction (Omniscript RT Kit from Qiagen, Valencia, CA). 2µl of the resultant cDNA was amplified with gene specific primers using the Taq PCR core Kit from QIAGEN (Valencia, CA). The human specific PCR primers were for *p62* (forward: *CTGCCCAGACTACGACTTGTGT* and reverse: *TCAACTTCAATGCCCAGAGG*) and for *gapdh* (forward: *CCACCCATGGCAAATTCCATGGCA* and reverse: *TCTAGACGGCAGGTCAGGTCCACC*). The *p62* PCR was performed as follows: 5-min at 95°C, then 30 cycles of 30-sec at 95°C, 1-min at 52°C and 47-sec at 72°C with a final extension at 72°C for 5-min. All PCR products were run on 2% agarose gels and stained with ethidium bromide.

IMMUNOFLUORESCENCE - SK-N-SH cells were fixed in ice cold methanol:acetone (1:1) at -20°C and co-incubated with the antibodies listed in each figure. The secondary antibodies

(1:50) were Texas Red-labeled donkey anti-rabbit or fluorescein-labeled donkey anti-mouse (Jackson Laboratories, Inc.). Slides were mounted with Vectashield medium containing 4',6-Diamidino-2-phenylindole (DAPI) (Vector). Cell staining was visualized with an OPTIPHOT-2 fluorescence microscope (NIKON).

RNA INTERFERANCE - Human p62 specific siRNAs (19-25 nucleotides, proprietary sequence) were obtained from Santa Cruz Biotech. (Santa Cruz, CA). SK-N-SH cells in 6-well plates or 8-chamber tissue culture slides grown to 50% confluence in both serum- and antibiotic free media were transfected with the p62 specific siRNAs (100nM) following the protocol specified by Santa Cruz Biotech. (Santa Cruz, CA). Four hours after transfection, the cells were treated with PGJ2 (15μM) without removal of the siRNA-containing media. Prior to the PGJ2-treatment, 5% fetal bovine serum was added to the cell culture media. Following 24h of incubation with PGJ2 the cells were harvested for western blot analysis or fixed for immunofluorescence analysis.

CELL VIABILITY ASSAY - Cell viability was assessed by a modified Mosmann's method (Mosmann, 1983). 3-(4, 5-dimethylthia-zol-2-yl)-2, 5-diphenyl tetrazolium bromide

(MTT) at a final concentration of 0.5mg/ml was dissolved in the SK-N-SH cell culture media containing 5% fetal bovine serum. The incubation media of SK-N-SH cells grown in 24-well plates was removed and the cells in each well were incubated with 0.5ml of the MTT solution for 1h at 37°C in 5% CO_2. The supernatant was aspirated and 0.4ml of a solution of 0.04M HCL in isopropanol was added and gently shaken to dissolve the precipitated formazan dye. 150µl of each sample was transferred into a well of a 96-well plate and the absorbance was read at 550nm and 620 nm with a spectrophotometer (BIOTEK Power 200). The results were expressed as the difference between the values obtained at the two wavelengths.

PROTEIN CONCENTRATION - The Bicinchoninic Acid (BCA) Reagent Kit (Pierce, IL) was applied to analyze the protein concentration of cell lysates. The assay was set-up in a 96-well plate. To establish a standard curve, 25µl of SDS buffer (1% SDS, 0.01M Tris-EDTA, pH 7.5) or 25µl of each of standard solutions containing 0.1mg/ml, 0.2mg/ml, 0.4mg/ml, 0.8mg/ml and 2.0mg/ml of Bovine Serum Albumin in the same SDS buffer were added in duplicates to each well. For the unknown samples, 22.5µl of the same SDS buffer and 2.5µl of

each sample were added to each well to establish a 1:10 dilution. 200µl of the assay solution was then added to each well, followed by incubation at 37°C for 30 minutes. The assay solution was prepared by adding one volume of 4.0% $CuSO_4$ (Reagent B, provided in the Kit) to 50 volumes of the Bicinchoninic Acid solution (Reagent A, provided in the kit). After incubation, the absorbance of each well was read with a spectrophotometer (BIOTEK Power 200) at 562nm.

STATISTICAL ANALYSIS - Statistical significance was estimated using one-way ANOVA with the Tukey-Kramer multiple comparison test.

Chapter III

Hightroughput characterization of the response of human neuroblastoma SK-N-SH cells to prostaglandin J2, a product of inflammation: from genomics to proteomics

INTRODUCTION

Advancements in gene cloning techniques and gene expression analyses provide compelling evidence linking the ubiquitin/proteasome pathway (UPP) with the turnover of many proteins required to maintain neuronal homeostasis. Findings from studies on hereditary forms of neurodegeneration, such as autosomal recessive juvenile parkinsonism and early-onset autosomal recessive familial PD, provide direct evidence that the manifestation of these disorders results from genetic defects in enzymes that are essential components of the UPP. Consequently, these findings support the notion that UPP impairment is a critical event associated with the neurodegenerative process.

A fundamental characteristic of neurodegenerative disorders is the accumulation and aggregation of ubiquitinated proteins in neuronal inclusions, such as neurofibrillary tangles in Alzheimer's disease (AD) and Lewy bodies in Parkinson's disease (PD). The identity of most ubiquitinated proteins that accumulate in neuronal inclusions, the mechanisms causing this protein aggregation and its role in the progression of neurodegeneration are unknown. We postulate that under harmful conditions, such

as those induced by inflammation, the cell may rely on the UPP to remove abnormal proteins thus promoting neuronal homeostasis.

In this study, by microarray analysis we analyzed the gene expression profile of human neuroblastoma SK-N-SH cells treated with a product of inflammation, prostaglandin J2 (PGJ2). In addition, by high-resolution two-dimensional gel electrophoresis and mass spectrometry we identified some of the proteins that are up-regulated in SK-N-SH cells treated with PGJ2. These studies, involving potent bioinformatics analysis, led to the development of a comprehensive picture of intracellular pathways altered by inflammation and that may play an important role in neurodegeneration.

RESULTS

Effect of PGJ2 on Differential Gene Expression in Human Neuroblastoma SK-N-SH cells - We compared by microarray analysis the expression profile of 18,325 human genes in untreated SK-N-SH cells with cells treated with 20μM PGJ2 for 4, 8, 16 and 24h. We carried-out a time course study to establish which of the changes detected in gene expression occur under short- or long-term treatment with 20μM PGJ2.

The investigation at each time point was repeated three times, except for the 16h time point that was repeated two times. Arrays were scanned with the GenePix 4000B Axon Scanner with the accompanying software. The laser intensities were adjusted to bring the brightest spot below saturation when the data were analyzed.

Computational analysis of the microarray data generated was performed in collaboration with the Center for Applied Genomics (Newark, N.J.) with the GeneSpring Software from Silicon Genetics (Redwood City, CA). The GeneSpring software offers powerful classification tools for comparing gene profiles between samples. It provides hierarchical clustering of groups of genes according to expression profiles, behavior under different experimental conditions and within functionally related groups, such as energy metabolism, proteolysis, heat shock, nuclear protein, transcription/translation and others.

Anomalous spots were flagged for exclusion. In addition, to achieve more stringent selection of significant changed genes we filtered out the genes with a threshold below 1.5-fold expression change. In addition, the ANOVA test performed with the GeneSpring software was used to assess

the statistical significance of changes that occurred consistently in the triplicate or duplicate experiments performed for each time point. Only p values <0.05 were considered statistically significant, meaning that no more than 5% false-positive genes were included in the significantly changed gene list.

A total of 18,325 genes were evaluated over four time points, 4, 8, 16 and 24h upon treatment with 20μM PGJ2 (Figure 9, page 91). Although the sequences of these genes are known, not all of them have known functions. According to a standard annotation from Compugen database (http://www.cgen.com, commercially available) genes were divided into groups of known and unknown genes. From the 18,325 genes tested there were 14,519 genes known and 3,806 genes unknown (79.2% and 20.8%, respectively). Of the 18,325 genes 2,084 were filtered out because their expression levels declined below the noise level and a total of 16,241 genes were found to be expressed in the SK-N-SH cells. We found that 993 genes, 6% of the total of 16,241 genes expressed in the SK-N-SH cells, showed statistical significance and at least a 1.5-fold increase or a 1.5-fold decrease in expression at one or more of the four time points after acute treatment with 20μM PGJ2. Of

these, 866 (87.2%) were known genes and 127 (12.8%) were unknown. Of the known genes, 35.5% were primarily down-regulated and 64.5% were up-regulated, whereas of the unknown genes, 29.7% were down-regulated and 70.3% were up-regulated. Many known genes have significantly altered expression at multiple time points (Table 1, page 113).

A longitudinal study generated a picture of the distribution of the known genes with significantly altered expression over all time points against untreated controls (Figure 10, page 92). PGJ2 treatment significantly induced changes in gene expression that lasted for at least 24h. Up-regulation was dominant over down-regulation at all time points (Figure 10, page 92). The overall profile of the time course of altered genes showed that the changes in gene expression occurred as early as four hours and reached the peak levels at 24h.

The number of times that a gene is differentially expressed over the multiple time points could be an indication of the relative effect of PGJ2 on the gene. Approximately 73.0% of the genes, among the 866 genes that exhibited statistically significant changes, were changed at only one time point,

whereas the remaining 27.0% were differentially expressed at more than one time point (Table 1, page 113).

Functional Classification of Known Genes Differentially Expressed in Human Neuroblastoma SK-N-SH cells Upon PGJ2-Treatment - As shown in Tables 3, page 115 and 4, page 123, 314 known genes were identified as being at least 1.5-fold up-regulated and 151 known genes were down-regulated by at least 1.5-fold upon PGJ2-treatment for 24h, respectively. Of the known genes, 67.5% were primarily up-regulated and 32.5% were down-regulated.

The 465 known genes differentially expressed after 24h of treatment with PGJ2, were classified into 19 functional groups (18 classified and 1 unclassified) based on the annotation of genes used in the CAG microarray chips and Compugen's Source database. This classification is relative since, due to their multiple functions, some genes can be included in more than one functional group. The number and percentage of gene in each group are shown in Figure 11, page 93. The percentage of genes significantly up- or down-regulated within each of the functional groups is shown in Figure 11, page 93.

Completion of the microarray studies revealed changes in the expression of genes that provide potential clues to the etiology of neurodegeneration associated with pro-inflammatory conditions.

High-resolution two-dimensional gel electrophoresis protein pattern in human neuroblastoma SK-N-SH cells upon PGJ2-treatment - To investigate alterations in protein levels induced by PJG2, we performed comparative high-resolution, two-dimensional gel electrophoresis experiments on protein samples obtained from control and PGJ2-treated SK-N-SH cells. Proteins from SK-N-SH cell lysates were resolved by isoelectric focusing on pH gradient (3.5-10) disc gels followed by second-dimensional separation by SDS-PAGE on 10% acrylamide slab gels. Total proteins (200μg/gel) in the two-dimensional gels were visualized by staining with Coomassie blue. Comparison of protein patterns in the Coomassie blue-stained two-dimensional gels revealed at least 7 distinct protein spots on the two-dimensional gel from PGJ2-treated cells that were absent or present in significantly lower levels in the two-dimensional gel from control cells (Figure 12, page 95). Semi-quantification results showed that the intensity levels of these spots

were increased by 5-fold to ~37-fold in PGJ2-treated cells compared to controls (Table7, page 134).

Two-dimensional Immunoblot Analysis of Ubiquitinated Proteins that Accumulate in Human Neuroblastoma SK-N-SH cells Upon PGJ2-Treatment - In an attempt to identify proteins that are polyubiquitinated in response to PGJ2-treatment, protein samples from control and PGJ2-treated SK-N-SH cells were analyzed by two-dimensional gel electrophoresis followed by western blotting probed with an anti-ubiquitinated protein antibody. The high molecular mass ubiquitin-positive smear showed little appreciable resolution, but the lower molecular mass ubiquitin species were somehow resolved into vertical series of spots separated by approximately 9kDa (Figure 13, page 97). These series, most likely represent polyubiquitinated proteins with increasing numbers of ubiquitins (n>4) in the chain. The isolated longitudinal series that is highly visible in the PGJ2-treated samples (*brackets*, Figure 13, page 97), may represent unanchored polyubiquitin chains, which can be pre-assembled prior to attachment to a target protein. This is based on the fact that the smallest spot is close to that of monoubiquitin (approximately 9kDa). Clearly, the levels of unanchored polyubiquitin chains is significantly

higher in the PGJ2-treated cells than in controls. A strategy to improve the resolution of the spots corresponding to ubiquitinated proteins is currently under exploration.

DISCUSSION

Relevant genes predominantly up-regulated upon PGJ2-treatment

Heat shock genes - Three heat shock genes, Hsp70, Hsp90 and Hsp110 are among the 15 top genes that exhibit the greatest level of up-regulation in SK-N-SH cells treated for 24h with 20μM PGJ2. In particular, Hsp 70 (HSP70B'/HSPA6) appeared as the most highly expressed gene of all. This data strongly indicates the active involvement of the heat shock response in rescuing the cell from stress induced by PGJ2, which is a neurotoxic product of inflammation. Moreover, it is consistent with the established role of heat shock gene products which are sensitive to a large variety of stress-inducing agents.

Ubiquitin/Proteasome Pathway genes - Another obvious large group of genes affected by PGJ2-treatment encode members of

the ubiquitin/proteasome pathway (UPP). This study established that ten genes encoding for 26S proteasome subunits, including subunits from the 20S and 19S particles, were up-regulated by at least 1.5-fold over control conditions. Interestingly, the proteasome 26S ATPase subunit 5 (PSMC5) was 15-fold up-regulated. PSMC5 is also known as S8, p45, SUG1, p45/SUG and TBP-1. The latter is known to be an HIV-1 Tat binding protein (Nakamura et al., 1998). In addition, this ATPase subunit is essential for the activity of the immunoproteasome, which processes peptides that are presented by the MHC class I molecule (Ferrer et al., 2004). Our studies involving microarray analysis suggests that PGJ2-treatment induces a high level of expression of the immunoproteasome in SK-N-SH cells.

In addition, SK-N-SH neuronal cells may need to increase proteasome levels to remove the overwhelming levels of oxidatively modified and/or ubiquitinated proteins generated by the PGJ2-treatment. That the proteasome plays a key role in the degradation of oxidatively modified proteins was demonstrated in human lung fibroblasts treated with hydrogen peroxide (Sitte et al., 1998). In these cells, increased protein turnover of oxidatively modified proteins was found to be mediated by the proteasome.

Additional microarray data support the need for increased levels of ubiquitination and protein degradation by the UPP upon PGJ2-treatment. Our microarray studies established that mRNA levels of the ubiquitin-conjugating enzyme E2H and the UBP ubiquitin specific protease 16 were significantly up-regulated in cells treated with PGJ2. Moreover, the mRNA levels of ubiquitin, in particular of the UbC gene, were found to be up-regulated by the PGJ2-treatment. UbC, which encodes nine tandemly repeated ubiquitins, is one of the members of the human ubiquitin multigene family (Wiborg et al., 1985). A rise in UbC levels is relevant and consistent with the increased levels of ubiquitinated proteins observed in cells treated with PGJ2 (Figure 13, page 97). Increased levels of ubiquitinated proteins may result from both an increase in protein ubiquitination as well as decreases in their degradation and de-ubiquitination. UbC is a stress inducible gene. Its up-regulation under PGJ2-induced stress conditions may be required to provide additional ubiquitin molecules to support the ubiquitination of increased levels of misfolded proteins generated by the PGJ2-treatment. Interestingly, we detected increased levels of putative non-anchored polyubiquitin chains in cells treated with

PGJ2 (Figure 13, page 97). The functional significance of this finding is currently unknown.

Energy production and ion or molecular transport channels in SK-N-SH cells may be altered by PGJ2 - Many genes encoding proteins involved in the mitochondrial energy production pathway as well as ion channels and molecular translocation were up-regulated. For example, COX-17 that is a copper chaperone specific for the mitochondrial protein cytochrome oxidase, and other genes encoding proteins also involved in cytochrome oxidase assembly were found to be up-regulated by more than 1.5-fold. The up-regulation of certain mitochondrial genes may reflect an effort by the cell to counteract the deleterious effect of prostaglandins of the J2 series on mitochondrial function (Martinez et al., 2005;Pignatelli et al., 2005).

Similarly, genes encoding for a voltage-dependent calcium channel and an H(+)-ATPase proton pump were also significantly up-regulated. Genes encoding for protein components of subcellular organelles, such as the Golgi and nucleus as well as for translocase at the outer mitochondrial membrane, were also significantly up-regulated upon PGJ2-treatment.

Enzymes and Signal Pathways activated by PGJ2 - The group of genes encoding for enzymes was one of the largest up-regulated groups of genes. Interestingly, a large number of kinases, including the inflammation inducible kinase mitogen-activated protein kinase kinase 3 (MAP2K3), were up-regulated by PGJ2. Expression of serine proteases, such as serine protease 16, and related genes including aspartic proteases, such as the lysosomal cathepsin D, were uniformly increased upon treatment with PGJ2.

Genes encoding proteins widely studied in models of neurodegeneration - Even though it is difficult to allocate particular genes to this special class, two genes relevant to this class, one for amyloid beta (A4) precursor-like protein 2 and another for regeneration associated protein 3 (RAP3), were found to be significantly up-regulated. Notably, a gene of the pro-inflammatory response encoding for the lipopolysaccharide specific response protein was also up-regulated, indicating a potential connection between neuroinflammation and neurodegeneration.

Down-regulated genes hint at mechanisms involved in PGJ2-induced cytotoxicity - A decrease in the expression of at

least five genes encoding for mitochondrial proteins, in particular NADH dehydrogenase (ubiquinone) subcomplexes, was observed in PGJ2-treated cells. These genes include NADH dehydrogenase (ubiquinone) flavoprotein 1, NADH dehydrogenase (ubiquinone) 1-α subcomplex 3, 1-β subcomplexes 7 and 10, and the ATP synthase, H+ transporting mitochondrial F1 complex. Down-regulation of these mitochondrial genes corroborates the recently described finding that prostaglandins of the J2 series induce mitochondrial dysfunction (Martinez et al., 2005;Pignatelli et al., 2005).

The stress conditions faced by the PGJ2-treated cells involve other deteriorating pathways. Additional genes found to be down-regulated by the PGJ2-treatment include dopa decarboxylase, carbonyl reductase and thioredoxin peroxidase. The two latter enzymes are known to play a role in the cellular antioxidant response. The decline of these two enzymes strongly implicates that PGJ2 impairs the antioxidant defense mechanisms in SK-N-SH cells.

Chapter IV

Inhibition of sequestosome 1/p62 up-regulation prevents aggregation of ubiquitinated proteins induced by prostaglandin J2 without reducing its neurotoxicity

INTRODUCTION

The ubiquitin/proteasome pathway plays a major role in the quality control process by eliminating mutated or abnormally folded proteins by degradation to prevent their accumulation as aggregates that often form intracellular inclusions. Notably, neurodegenerative disorders, such as Parkinson's disease, Alzheimer's disease and amyotrophic lateral sclerosis, exhibit abnormal intraneuronal inclusions containing ubiquitinated proteins [reviewed in (Arnold et al., 1998;Figueiredo-Pereira ME and Rockwell, 2001)]. The mechanisms leading to the formation of such abnormal aggregates and their role in the progression of neurodegeneration is unknown (Tran and Miller, 1999). Inclusions may arise from a cellular attempt to compartmentalize accumulated proteins preventing their interference with normal cell function. Their presence may also be cytotoxic thus contributing to neuronal cell damage. Aggregate size may be a pivotal determinant of their toxicity as their expansion may confer fatal effects (Mezey et al., 1998).

Pericentriolar structures within centrosomes were found to be deposition sites for ubiquitinated proteins that escape degradation by the ubiquitin/proteasome pathway

and were named accordingly "aggresomes" (Johnston et al., 1998b). Some of the ubiquitinated proteins shown to be deposited in aggresomes resulted from either overexpression of mutant cystic fibrosis transmembrane conductor regulator or presenilin 1 and/or from impaired protein degradation induced by treating cells with proteasome inhibitors (Johnston et al., 1998b;Wigley et al., 1999;Garcia-Mata et al., 1999). Centrosomes were shown to be associated with high levels of 26S proteasomes and also with de-ubiquitination activity (Fabunmi et al., 2000). While some studies suggest that the retrograde transport of ubiquitin protein aggregates to centrosomes is dependent on microtubule integrity (Johnston et al., 1998b), others indicate that this process may not require intact microtubules (Fabunmi et al., 2000).

Other intracellular mechanisms besides centrosome targeting may promote the aggregation of ubiquitinated proteins that evade degradation by the ubiquitin/proteasome pathway. Recently, several studies described a variety of proteins containing a ubiquitin-associated (UBA) domain [reviewed in (Hartmann-Petersen et al., 2003)]. Certain proteins with UBA domains, such as Mud1 and Rad23, non-covalently bind polyubiquitin chains 300-times more tightly than mono-ubiquitin (Wilkinson et al., 2001; (Madura,

2002). Another UBA-containing protein is the sequestosome 1, also known as p62, first isolated in human tissues by Shin and colleagues (Park et al., 1995a). Due to its high affinity for poly-ubiquitin chains, sequestosome 1/p62 was suggested to serve as a receptor for binding and storing ubiquitinated proteins (Shin, 1998a). Sequestosome 1/p62 was detected in ubiquitin-containing intraneuronal and intraglial inclusions in a variety of neurodegenerative disorders (Kuusisto et al., 2001a;Zatloukal et al., 2002a;Furukawa et al., 2004a;Nakano et al., 2004b) as well as in hepatocyte Mallory bodies associated with alcoholism (Stumptner et al., 2002b), suggesting that sequestosome 1/p62 participates in the biogenesis of inclusions containing ubiquitinated proteins. Furthermore, sequestosome 1/p62 expression in neuronal cells is induced by serum withdrawal conditions that trigger apoptosis and by proteasome inhibitors (Kuusisto et al., 2001c;Nakaso et al., 2004b) as well as by expression of expanded pathologic polyglutamine repeats (Nagaoka et al., 2004a).

In this study we show that the endogenous ligand prostaglandin J2 (PGJ2), which is a neurotoxic product of inflammation that causes the accumulation and aggregation of ubiquitinated proteins (Li et al., 2004b), also induces sequestosome 1/p62 up-regulation in a concentration- and

time-dependent manner. Sequestosome 1/p621 and ubiquitin C-terminal hydrolase L1 (UCH-L1), which is inhibited by some of the prostaglandins of the J2 series, were co-localized in the protein aggregates containing ubiquitinated proteins. Abolishing sequestosome 1/p62 up-regulation by RNA interference (RNAi) prevented the aggregation of ubiquitinated proteins. However, post-transcriptional sequestosome 1/p62 silencing failed to reduce PGJ2-cytotoxicity and PGJ2-dependent increases in ubiquitin-protein conjugates. Our data indicate that UCH-L1 impairment with the ensuing build-up of ubiquitinated proteins in conjunction with sequestosome 1/p62 up-regulation may promote "sequestration" of poly-ubiquitinated proteins into aggresome-like induced structures. However, the overwhelming accumulation of proteasome substrates in the form of poly-ubiquitinated proteins, rather than their aggregation, may be an important factor promoting cell death.

RESULTS

PGJ2 induces a dose-dependent increase in sequestosome 1/p62 expression - We determined the effect of increasing concentrations of PGJ2 on sequestosome 1/p62 expression in human SK-N-SH neuroblastoma cells. Anti-sequestosome 1/p62 immunoreactivity was detected as a 62kDa band only faintly visible in control cells. Sequestosome 1/p62 protein levels increased the most in neuronal cells treated with 15μM PGJ2 for 24h, rising to at least 24-fold above control (Figure 14A, semi-quantified in 14C). The levels of cyclooxygenase 1 (COX-1), a protein that is constitutive in these cells, were not altered by the PGJ2-treatment.

To determine if PGJ2 affects *sequestosome 1/p62* gene expression in SK-N-SH cells, we carried out RT-PCR analysis with sequestosome 1/p62 gene-specific primers. These studies revealed that PGJ2 concentrations ranging between 5 and 25μM caused a considerable elevation of *sequestosome 1/p62* mRNA levels, reaching a maximum of 2.5-fold above control upon treatment with 20μM PGJ2 (Figure 14B, semi-quantified in 14C). The *gapdh* mRNA levels did not change significantly under these conditions.

Inhibitors of transcription (actinomycin D, 1.25μg/ml) or translation (cycloheximide, 6.25μg/ml) prevented the increase in sequestosome 1/p62 protein expression induced by 15μM PGJ2, establishing that sequestosome 1/p62 up-regulation is due to *de novo* synthesis (Figure 14D).

PGJ2 stimulates a time-dependent increase in the levels of sequestosome 1/p62 and ubiquitinated proteins that correlates with a decrease in cell viability - To establish the time-dependency of the PGJ2 effect on sequestosome 1/p62 and ubiquitinated protein levels we incubated SK-N-SH cells with 15μM PGJ2 for 4, 8, 16, 24 and 48h. Notably, sequestosome 1/p62- and ubiquitinated protein-levels increased in a time-dependent and parallel manner (Figure 15). A substantial rise in the levels of these proteins was detected only after 16h of incubation. While after 48h of incubation with 15μM PGJ2 sequestosome-levels increased by as much as 19-fold those of ubiquitinated proteins reached a 7-fold maximum. COX-1 levels were not increased by PGJ2. The increase in sequestosome 1/p62 levels induced by 15μM PGJ2 upon 24h of incubation was found to range between 10- and 25-fold above control (compare Figure 14 and 15), under similar experimental conditions.

We also determined the time-dependent effect of PGJ2 on the viability of SK-N-SH cells. As shown in Figure 16, the decrease in cell viability induced by 15μM PGJ2 was inversely proportional to the increase in the levels of sequestosome 1/p62 and ubiquitinated proteins. These three events, i.e. the decline in cell viability and the rise in sequestosome 1/p62 and ubiquitinated protein levels, were clearly apparent after 16h of incubation, suggesting that the onset of these events may be closely associated.

PGJ2 promotes the formation of cytoplasmic protein aggregates containing ubiquitinated proteins, sequestosome 1/p62 and UCH-L1 - Our previous studies demonstrated that PGJ2 induces the accumulation and aggregation of ubiquitinated proteins in SK-N-SH cells (Li et al., 2004b). We also showed that some of the PGJ2 metabolites inhibit the ubiquitin C-terminal hydrolase UCH-L1 without directly affecting proteasome activity. These aggregates accumulate predominantly in the cytoplasm, with the highest aggregate density displaying a juxtanuclear distribution [Figure 17, *panels 2 and 3(B,C)* and Figure 18, *panel 2(B,C)*]. Merged images show that the cytoplasmic aggregates contain ubiquitinated proteins, sequestosome 1/p62 (Figure 17, *panels 2D and 3D*) and UCH-L1 (Figure 18, *panel 2D*). Other

less abundant protein aggregates containing ubiquitinated proteins but not sequestosome 1/p62, were detected in nuclei of PGJ2-treated cells (Figure 17, *panels 2C and 3C*). The majority of cells treated with the highest PGJ2 concentrations tested (20 and 25μM) had a round appearance. Most of the cells treated with 25μM died and were removed from the culture dishes following the PBS washing because they were no longer adherent.

No sequestosome 1/p62 or UCH-L1 aggregates were observed in control cells and staining for ubiquitinated proteins was low and evenly distributed throughout these cells (Figure 17, *panels 1B-1D*). Similar levels of UCH-L1 were detected in control and PGJ2-treated cells and its distribution was predominantly cytoplasmic (Figure 18, *panels 1C and 1D*).

No aggregates were detected after 4h of treatment with 15μM PGJ2. Co-localization of sequestosome 1/p62 and ubiquitinated proteins in PJG2-induced aggregates was observed after 8, 16 and 24h of treatment with 15μM PGJ2 (Figure 19). The increase in aggregates observed along this time (Figure 19) is in agreement with the increase in sequestosome 1/p62 and ubiquitinated protein levels detected by western blot analysis (Figure 15). Aggregate

intensity peaked after 24h of incubation with 15 μM PGJ2, a time-point at which the levels of sequestosome 1/p62 and ubiquitinated proteins were 10- and 4-fold above basal levels, respectively. The increased aggregate intensity could be due to an increase in their numbers and/or in their sizes.

Sequestosome 1/p62 post-transcriptional silencing prevents the cytoplasmic aggregation of ubiquitinated proteins induced by PGJ2 - As the cytoplasmic aggregates identified upon PGJ2-treatment contained sequestosome 1/p62, we investigated if reducing sequestosome 1/p62 up-regulation would prevent protein aggregation. Transfection of SK-N-SH cells with sequestosome 1/p62-specific siRNAs prior to PGJ2-treatment reduced sequestosome 1/p62 up-regulation by 75%, as observed by western blot analysis (Figure 20, *top panel*). The transfection reagent alone had no effect on sequestosome 1/p62 levels (Figure 20, *top panel*). As expected, sequestosome 1/p62 siRNAs did not affect the levels of the heat shock protein HSP105, which is also up-regulated by the PGJ2-treatment (Figure 20, *middle panel*). Post-transcriptional sequestosome 1/p62 silencing also failed to diminish the PGJ2-dependent increase in ubiquitinated protein levels (Figure 20, *bottom panel*).

Notably, sequestosome 1/p62 specific RNAi significantly diminished the cytoplasmic aggregation of ubiquitinated proteins. As shown in Figure 21 (*panel 2C*), aggregates of ubiquitinated proteins are clearly detected in PGJ2-treated SK-N-SH cells. The majority of the aggregates containing ubiquitinated proteins (Figure 21, *panels 2C and 2D*) are co-localized with sequestosome-aggregates (Figure 21, *panels 2B & 2D*), most of them exhibiting a juxtanuclear distribution. However, preventing sequestosome 1/p62 up-regulation by post-transcriptional silencing (Figure 21, *panel 3B*) had a significant impact on the distribution of the ubiquitinated proteins. Instead of forming juxtanuclear aggregates, the increased levels of ubiquitinated proteins were mostly dispersed throughout the cytoplasm (Figure 21, *panels 3C and 3D*). No sequestosome 1/p62- or ubiquitin-protein aggregates were visible in control SK-N-SH cells (Figure 21, *panels 1B -1D*).

Sequestosome 1/p62 post-transcriptional silencing does not prevent PGJ2-cytotoxicity - Studies by Uchida and colleagues (Kondo et al., 2001;Kondo et al., 2002;Li et al., 2004b) demonstrated that prostaglandins of the J2 series are neurotoxic. Herein, we demonstrate that sequestosome 1/p62 post-transcriptional silencing does not

prevent PGJ2-neurotoxicity (Figure 22). The transfection reagent alone or in combination with the sequestosome 1/p62-specific siRNAs was not cytotoxic in the absence of PGJ2 (Figure 22).

DISCUSSION

Protein aggregates containing sequestosome 1/p62 and ubiquitinated proteins are abundant in the cytoplasm and scarce in the nucleus of PGJ2-treated cells - In different forms of neurodegenerative disorders, intracellular aggregates with ubiquitinated proteins are detected either in the cytoplasm, such as in Parkinson's disease, or in the nucleus, such as in Huntington's disease. The cause of this differential subcellular aggregate distribution is not clear. By treating SK-N-SH cells with PGJ2, a well characterized product of inflammation, we detected the appearance of protein aggregates with an overwhelming cytoplasmic, not nuclear, distribution. These aggregates contained ubiquitinated proteins as well as sequestosome 1/p62, the levels of which are up-regulated by PGJ2. Ubiquitinated proteins were present in the cytoplasm and the nucleus, while sequestosome 1/p62-aggregates were

excluded from the nucleus in PGJ2-treated cells. That sequestosome 1/p62 is mainly a cytoplasmic protein was initially demonstrated by Shin and colleagues (Vadlamudi et al., 1996a). In fact, these investigators were the first to propose that sequestosome 1/p62 forms a "storage place" for ubiquitinated proteins (Shin, 1998a). The overabundance of sequestosome 1/p62 in the cytoplasm of PGJ2-treated cells may explain why protein aggregates containing ubiquitinated proteins and sequestosome 1/p62 prevail in the cytoplasm and not in nuclei.

An investigation of the nuclear diffusion limit in mammalian cells, including primary neurons and SK-N-SH cells, established that large molecules (molecular masses above 70kDa) cannot freely diffuse into nuclei of intact, healthy cells (Trushina et al., 2003). In our studies, most of the ubiquitin protein conjugates detected in the PGJ2-treated cells had molecular masses above 75kDa as judged by western blot analysis. It is thus unlikely that these high molecular mass ubiquitin conjugates passively diffuse from the cytoplasm into the nucleus and vice-versa. Their size may be even larger in the aggregates as they may be bound to the UBA domain of sequestosome 1/p62. The large aggregates could only passively enter the nucleus if the nuclear membrane was disrupted. Accordingly, nuclear

migration of full-length mutant huntingtin can only occur upon deterioration of the nuclear membrane (Trushina et al., 2003). These studies indicate that aggregate size, nuclear diffusion limit and nuclear membrane integrity may influence the subcellular distribution of protein aggregates in general.

Are sequestosome 1/p62 and UCH-L1 partners in the formation of cytoplasmic aggregates? - PGJ2 was shown to induce oxidative stress by causing decreases in glutathione, glutathione peroxidase and mitochondrial membrane potential as well as increases in the production of protein-bound lipid peroxidation products, such as acrolein and 4-hydroxy-2-nonenal (Kondo et al., 2001). In addition, we demonstrated that PGJ2 and its metabolite Δ12-PGJ2 induce the accumulation and aggregation of ubiquitinated proteins without decreasing proteasome activity and that Δ12-PGJ2 inhibits ubiquitin hydrolases, such as UCH-L1 and UCH-L3 (Li et al., 2004b). These events induced by prostaglandins of the J2 series may be relevant to the pathology of neurodegenerative diseases, since PGJ2 and its metabolites Δ12-PGJ2 and 15d-PGJ2, are readily produced non-enzymatically *in vivo* and *in vitro* by dehydration of PGD2,

the major prostanoid made in the CNS (Fukushima, 1990;Urade, 1997). Furthermore, UCH-L1 comprises 1-2% of the total soluble protein in brain (Wilkinson et al., 1992).

In the studies reported herein, we demonstrate that PGJ2 up-regulates sequestosome 1/p62 in a concentration- and time-dependent manner. Furthermore, we established that sequestosome 1/p62 and UCH-L1 are co-localized in predominantly cytoplasmic protein aggregates detected in SK-N-SH cells treated with PGJ2. It is conceivable that inhibition of ubiquitin hydrolases, such as UCH-L1, in conjunction with increases in the levels of oxidatively modified proteins, both events triggered by prostaglandins of J2 series, lead to an overload of poly-ubiquitinated proteins in the cells. We speculate that sequestosome 1/p62 up-regulation could constitute a protective mechanism for the storage of these poly-ubiquitinated proteins. The temporary sequestration of putative proteasome substrates would prevent it from becoming blocked by excessive substrate levels.

Sequestosome 1/p62 up-regulation is stimulated by a variety of stress conditions, such as those induced by PGJ2 demonstrated herein, or by proteasome inhibitors (Nakaso et al., 2004b) or by transfection with pathogenic forms of

polyglutamine repeats (Nagaoka et al., 2004a). The stress-dependent up-regulation of sequestosome 1/p62 combined with their ability to bind poly-ubiquitinated proteins could be a mechanism to delay the access of excessive substrates to the proteasome to prevent its blockage. The shuttling of poly-ubiquitinated proteins from the sequestosome 1/p62 to the proteasome could thus be under tight regulation.

A similar mechanism was identified in maturing dendritic cells in response to protein damaging agents (Lelouard et al., 2004). Upon stimulation with the pro-inflammatory agent lipopolysaccharide followed by treatment with the translation damaging agent puromycin, defective ribosomal products (DRiPs) are sorted into large cytosolic aggregates known as dendritic cell aggresome-like induced structures (DALIS). Unlike aggresomes, DALIS are not localized in the pericentriolar area and lack vimentin cages (Lelouard et al., 2004). In addition, DALIS contain many components of the ubiquitination machinery, including E1, E2s and E3s. When DRiPs are formed they are rapidly sequestered into DALIS where they are eventually ubiquitinated. This mechanism allows dendritic cells to regulate the degradation rate of DRiPs, an ability that is important for their immune functions (Lelouard et al., 2004).

Sequestosome 1/p62 contain seven structural motifs: an SH2 domain that binds the tyrosine kinase $p56^{lck}$ in a phosphotyrosine-independent manner (Vadlamudi et al., 1996a), an acidic interaction domain (AID) that binds the atypical PKC ζ (Puls et al., 1997), a ZZ type ZINC finger that binds the receptor interactive protein (RIP) involved in TNFα-induced apoptosis (Sanz et al., 1999), a binding site for the RING-finger protein tumor necrosis factor receptor-associated factor 6 (TRAF6) that is an E3 ubiquitin ligase (Sanz et al., 2000;Wooten et al., 2001), two PEST sequences and a UBA domain [reviewed in (Geetha and Wooten, 2002)]. Recent studies with HEK cells transfected with full-length or truncated sequestosome 1/p62 forms indicate that sequestosome 1/p62 may act as a shuttle that delivers poly-ubiquitinated proteins to the proteasome (Seibenhener et al., 2004). Notably, those studies suggest that sequestosome 1/p62 can bind poly-ubiquitin chains through the C-terminal UBA domain and the proteasome through their AID domain, which is closer to their N-terminus. The AID domain is proposed to be structurally similar to ubiquitin-like (UBL) domains, known to interact with the proteasome (Seibenhener et al., 2004). Due to their binding versatility, sequestosome 1/p62 may thus play an important role as a scaffold and/or shuttle

molecule storing poly-ubiquitinated proteins and delivering them to the proteasome in a regulated manner.

We speculate that the co-localization of UCH-L1 and sequestosome 1/p62 could provide a means to recycle ubiquitin from poly-ubiquitin chains or to elongate ubiquitin chains, the latter UCH-L1 function identified by Lansbury and colleagues (Liu et al., 2002). However, under extreme conditions the overabundance of misfolded proteins could jeopardize the recovery process and activate cellular death pathways.

Preventing protein aggregation does not abolish cytotoxicity - Most studies addressing the role of aggregate formation on cell death rely on transfection and overexpression of wild type or mutant forms of proteins, such as CFTR (Johnston et al., 1998b), α-synuclein (Tanaka et al., 2004), parkin (Cookson et al., 2003) or huntingtin (Arrasate et al., 2004), to name a few. In some cases the whole protein or its truncated fragments, as in the case of huntingtin, are fused to GFP (Arrasate et al., 2004). In addition the transfected cells, in many instances, are treated with proteasome inhibitors (Tanaka et al., 2004) or maintained in serum-free media which induces apoptosis (Arrasate et al., 2004). The studies listed above support

the notion that aggregates are beneficial to the cell and act as "neuron protection agencies" (Orr, 2004).

The studies that we report herein address the effect of an endogenous ligand (PGJ2), not proteasome inhibitors, on the intracellular distribution of endogenous, not transfected, proteins into aggregates in human SK-N-SH neuroblastoma cells. We found that preventing sequestosome 1/p62 up-regulation by RNAi does not decrease the cytotoxic effects of PGJ2. Furthermore, post-transcriptional sequestosome 1/p62 silencing inhibits aggregate formation without prevent the increase in the levels of high molecular mass ubiquitinated proteins induced by PGJ2. Our studies, therefore, support the notion that the presence of aggregates as well as sequestosome 1/p62 up-regulation in PGJ2-treated cells are not directly proportional to the loss of cell viability. Instead, the extent of neuronal cell death induced by PGJ2 seems to be relative to the levels of ubiquitinated proteins independently of their state of aggregation.

Other studies reached a similar conclusion. The amount of diffuse, non-aggregated, intracellular huntingtin-GFP fusion products accumulating in primary rat neuronal cultures maintained in serum free media was found to directly predict the degree of cell death (Arrasate et al.,

2004). Furthermore, protein aggregates generated by the transient overexpression of huntingtin or CFTR aggregation-prone fragments in HEK 293 cells, were shown to directly inhibit the ubiquitin/proteasome pathway (Bence et al., 2001). It is likely that this pathway would be inhibited by the overexpressed proteins even if they did not aggregate. Together these studies support the notion that a non-specific overload of intracellular proteins rather than their aggregation, may be a pathological event that accelerates cell death. Therapeutic strategies that promote degradation of the accumulated proteins rather than abolishing their aggregation would most likely be effective in the prevention or treatment of neurodegenerative disorders associated with protein mishandling.

Chapter V

Mechanistic model for the interaction between neuroinflammation and UPP Dysfunction in Neurodegeneration

In these studies we attempted to identify by high throughput screening methods as well as conventional biochemical analyses mechanisms leading to the development of the two hallmarks of neurodegeneration, i.e. neuronal cell death and neuronal inclusion bodies. We focused on the effects of prostaglandin J2 (PGJ2), a neurotoxic product of inflammation. Our cellular model consisted of human neuroblastoma SK-N-SH cells treated with increasing concentrations of PGJ2. Our studies yielded the identification of several PGJ2-regulated pathways that may play a significant role in neurodegeneration associated with neuroinflammation and that may be relevant to a variety of neurodegenerative disorders, such as AD and PD.

Our mechanistic model for the interaction between neuroinflammation and neurodegeneration, mediated mostly by PGJ2, is depicted in Figure 23 (page 112).

The ubiquitin/proteasome pathway (UPP) is most likely one of the major pathways affected by PGJ2 and that is associated with neurodegeneration. Protein aggregates containing ubiquitinated proteins developed in the SK-N-SH cells upon PGJ2 treatment. These aggregates could result from a combination of PGJ2-dependent intracellular events,

such as inhibition of de-ubiquitination activity as well as induction of oxidative stress and protein misfolding. The latter two events may indirectly or directly impair the proteasomal degradation of ubiquitinated proteins.

To overcome the PGJ2-mediated UPP impairment the cells initiate a putative "repair" response aimed at increasing UPP activity. This "repair" response includes up-regulation of proteasome subunits, ubiquitin and ubiquitin-conjugating as well as de-ubiuqitinating enzymes. Furthermore, up-regulation of heat shock genes may be another cellular strategy to overcome the damage inflicted by PGJ2-treatment. Moreover, it is possible that up-regulation of proteins like sequestosome 1/p62, which contain UBA domains, is part of the "repair" response to UPP impairment. Up-regulation of sequestosome 1/p62 under stress conditions, such as those induced by PGJ2, may by a means to "sequester" poly-ubiquitinated proteins into aggregates so that cell function is not jeopardized. However, if not removed, the overwhelming accumulation of ubiquitinated proteins, rather than their aggregation, is likely to contribute to neuronal death.

Besides altering UPP activity, PGJ2 affects the expression

of mitochondrial genes, such as the complex I protein NADH dehydrogenase (ubiquinone) 1α subcomplex and COX-17 (cytochrome c oxidase-17) essential for mitochondrial complex III activity. These PGJ2-dependent mitochondrial related changes in gene expression may indicate mitochondrial dysfunction and activate programmed cell death (apoptosis).

Overall, we conclude that products of neuroinflammation, such as PGJ2, might play a key role in neurodegenerative disorders associated with the accumulation of ubiquitinated proteins. A key question that remains unanswered is whether the different forms of neurodegenerative disorders share a common mechanism, i.e. neuroinflammation. If so, how can the enormously varied etiology, presentation and time course of these devastating disorders be explained? For example, while head injury is a rapid, accidental event that affects mostly young individuals, PD is characterized by damage to specific brain regions resulting in motor disturbances and chronic degeneration. This variety of disease manifestations could be correlated to the primary brain region affected by the injurious event, its severity and duration.

Much more needs to be learned about the functions of inflammation in the normal and diseased CNS. The challenge resides in dissecting the dual nature of neuroinflammation as it has both positive and negative effects differing spatially and temporally in the CNS.

Chapter VI

Conclusions and Future Directions

In this project we attempted to address the mechanisms responsible for inducing the two hallmarks of neurodegenerative disorders, i.e., neuronal cell death and accumulation of polyubiquitinated proteins into protein aggregates. Our cell model system consisted of human neuroblastoma SK-N-SH cells treated with increasing concentrations (5, 10, 15, 20 and 25μM) of prostaglandin J2 (PGJ2), a neurotoxic product of inflammation.

The results from our microarray analysis of gene expression in cells treated with 20μM PGJ2 compared to control, revealed two pathways that may be relevant to neurodegeneration and that are up-regulated by this product of inflammation: (1) the ubiquitin/proteasome pathway and (2) the heat shock response. Moreover, biochemical analysis demonstrated that sequestosome-1/p62, a scaffold protein with an UBA domain that binds polyubiquitinated proteins non-covalently, is essential for aggregation of polyubiquitinated proteins induced by the PGJ2-treatment.

Overall, our studies support the notion that in response to stress induced by products of inflammation, such as PGJ2, the cell has three strategies to deal with the abnormal

levels of misfolded and/or ubiquitinated proteins produced under such conditions:

1) The first strategy is to activate the heat shock response with the ensuing up-regulation of heat shock proteins, in an attempt to refold or "repair" the misfolded proteins.

2) If this strategy fails, for example because too many oxidatively modified or misfolded proteins are produced, then the cell would resort to the second strategy: attach polyubiquitin chains to the modified/misfolded proteins to target them for degradation by the 26S proteasome. Concurrently, under these conditions, the sequestosome-1/p62 is up-regulated to increase the rate of delivery of the polyubiquitinated proteins to the 26S proteasome. The sequestosome-1/p62 may also delay the delivery of polyubiquitinated proteins to the 26S proteasome to prevent its overloading.

3) As a last resort, if high levels of misfolded/modified proteins are produced and they cannot be re-folded or degraded, up-regulation of the sequestosome-1/p62 may cause the "sequestration" of poly-ubiquitinated proteins into aggregates to ensure that cell function is not jeopardized.

The accumulation of polyubiquitinated proteins induced by PGJ2 is not caused by a direct inhibition of the proteasome by PGJ2, as demonstrated by previous studies from our laboratory (Li et al., 2004b) and others. However, an indirect effect cannot be ruled out, as high levels of ubiquitinated proteins may overload the proteasome and impair its activity.

The accumulation of polyubiquitinated proteins induced by PGJ2 can also be attributed to inhibition of de-ubiquitinating enzymes. Previous studies from our laboratory (Li et al., 2004b) and others have demonstrated that prostaglandins of the J2 series inhibit the ubiquitin hydrolases UCH-L1 and UCH-L3 as well as isopeptidase activity. It is also possible that PGJ2 inhibits the de-ubiquitinating activity associated with the 19S regulatory particles of the 26S proteasome. De-ubiquitinating enzymes are cysteine proteases and prostaglandins of the J2 series are known to form Michael addition reactions with free thiol groups of cysteines. Thus, it is possible that these eicosanoids induce the accumulation of polyubiquitinated proteins by preventing their de-ubiquitination, a step required prior to their degradation by the 26S proteasome.

Independently of the mechanism(s) responsible for the overwhelming accumulation of ubiquitinated proteins, our results strongly support that it is not protein aggregation per se but the impairment of the UPP that is a major contributor to cell death induced by PGJ2.

Notably, besides altering UPP activity, PGJ2 drastically down-regulates the expression of mitochondrial genes, indicating that mitochondrial dysfunction is also an important factor in the induction of apoptosis by PGJ2.

Which is the major culprit in neuronal death induced by PGJ2 and thus by inflammation? Is it impairment of the UPP or mitochondrial dysfunction? Answers to this question may arise from the evaluation of changes induced by more subtle conditions, such as treatment with lower concentrations of PGJ2 for shorter time points. Additional studies involving microarray analysis under these "reversible" milder damaging conditions may discover important clues of the relationship between inflammation and neurodegeneration.

Figure 1. The activity of cyclooxygenases generates the precursors for the prostaglandin family. Membrane lipids are broken down by phospholipase A2 (PLA2) into arachidonic acid (AA). Subsequently, cyclooxygenases (either COX-1 or COX-2) via their cyclooxygenase activity convert AA to prostaglandin G2 (PGG2) followed by the conversion of PGG2 to PGH2 via their peroxidase activity. The peroxidase step results in the production of free radicals as well. PGH2 is then converted by tissue-specific synthases to the different prostaglandins illustrated in this figure and other not shown products (Smith et al., 2000).

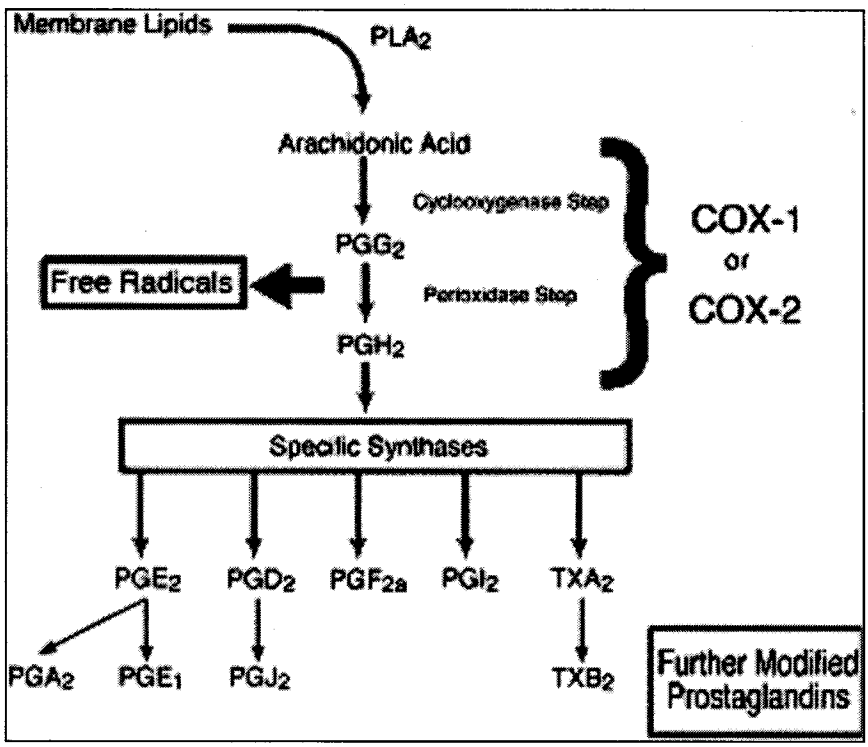

Figure 2. Metabolic pathway of PGJ2 derivation (Adapted from Zhuang et al., 2003). Notice that PGJ2 is derived from PGD2 without any involvement of enzymes.

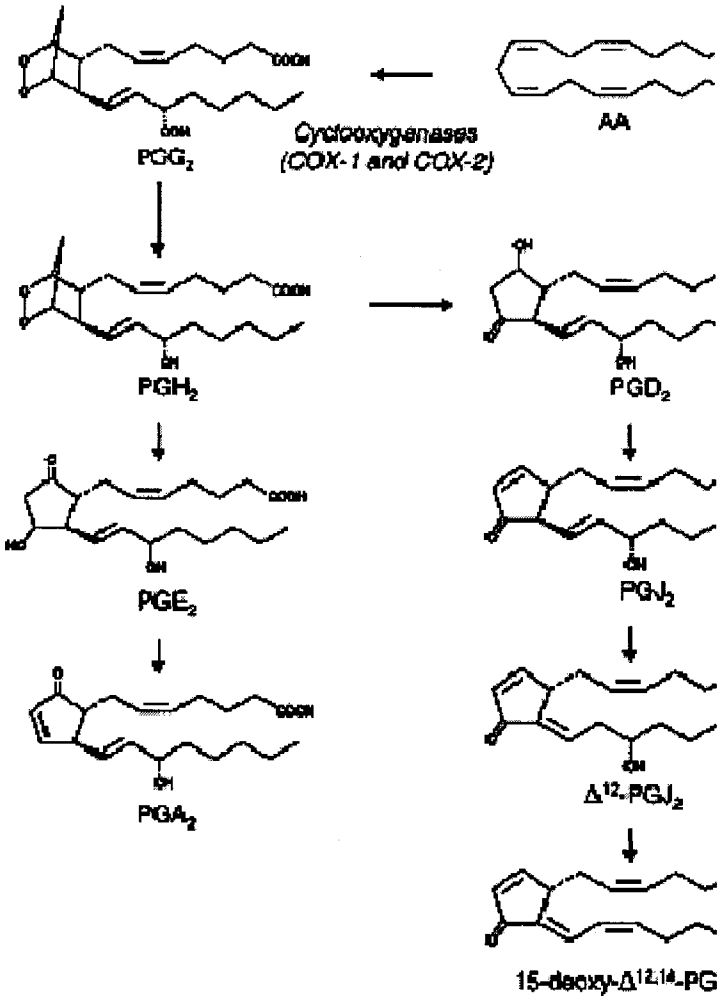

Figure 3. Possible modes of action of prostaglandins of the J2 series in cells, illustrated for 15d-PGJ2 (Harris et al., 2002a).

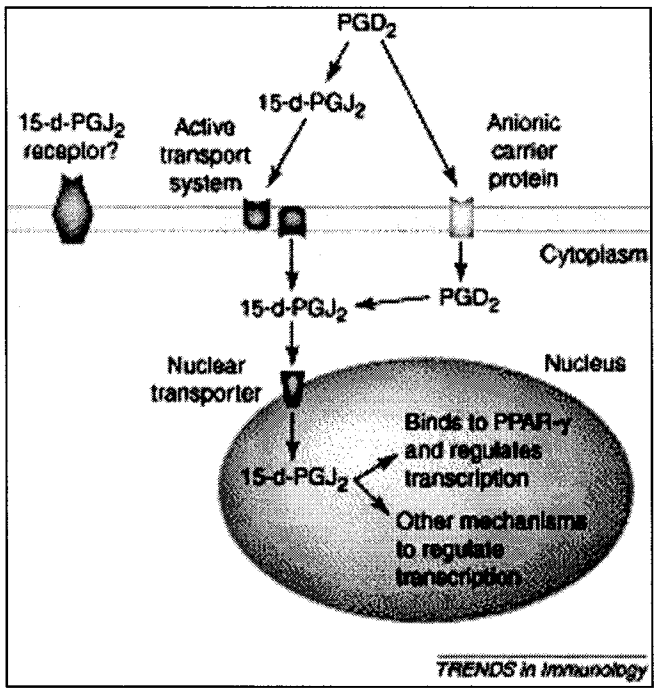

Figure 4. Protein ubiquitination. First, a high energy thioester bond is formed between ubiquitin (Ub) and a ubiquitin-activating enzyme (E1). This reaction requires ATP hydrolysis. Secondly, the activated ubiquitin is transferred to a ubiquitin conjugating enzyme (E2). Thirdly, the activated ubiquitin is ligated, via an isopeptide bond, to the protein substrate by a ubiquitin ligase (E3). Lastly, the ubiquitin chain is elongated by an ubiquitin-chain elongating factor (E4) which drives the polyubiquitin chain (poly Ub) assembly.

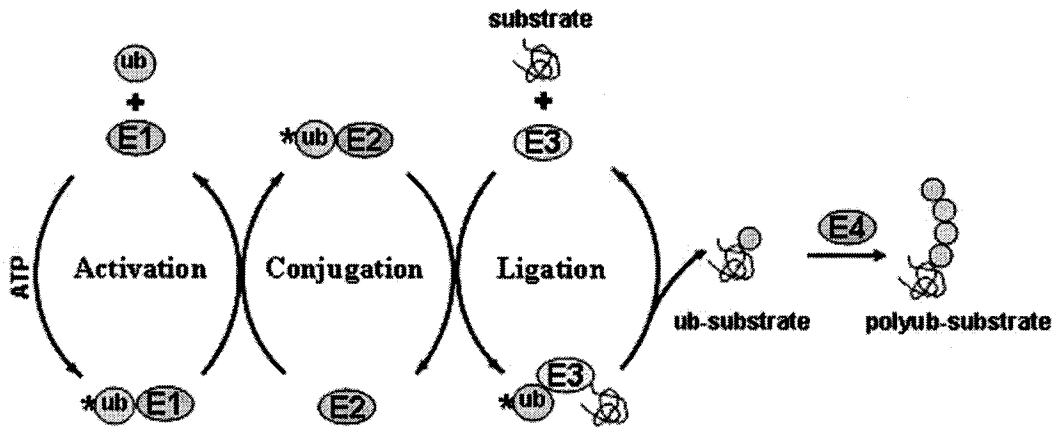

Figure 5. The 26S proteasome. Its two major particles, the 20S particle (20S proteasome) which is the catalytic core, and the 19S particle (PA700) which is the regulatory component, require ATP hydrolysis to assemble into the 26S proteasome. The midsagital view of the 20S proteasome was drawn from 1ryp.pdb (Groll et al., 1997).

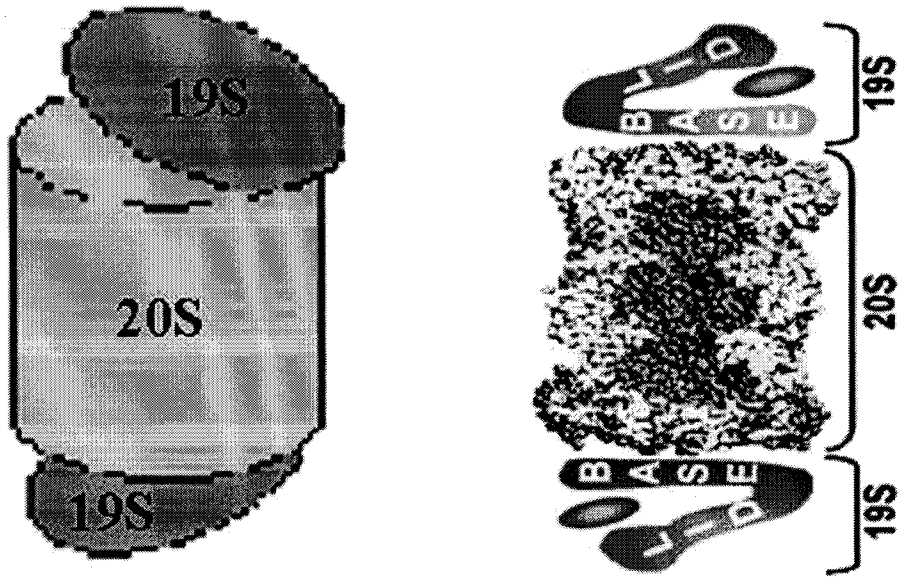

Figure 6 - The structure of the 20S proteasome (Affinity, UK). Each colored sphere represents one subunit of the 20S proteasome. The 28 subunits are arranged in a novel topology characterized by a αββα sandwich.

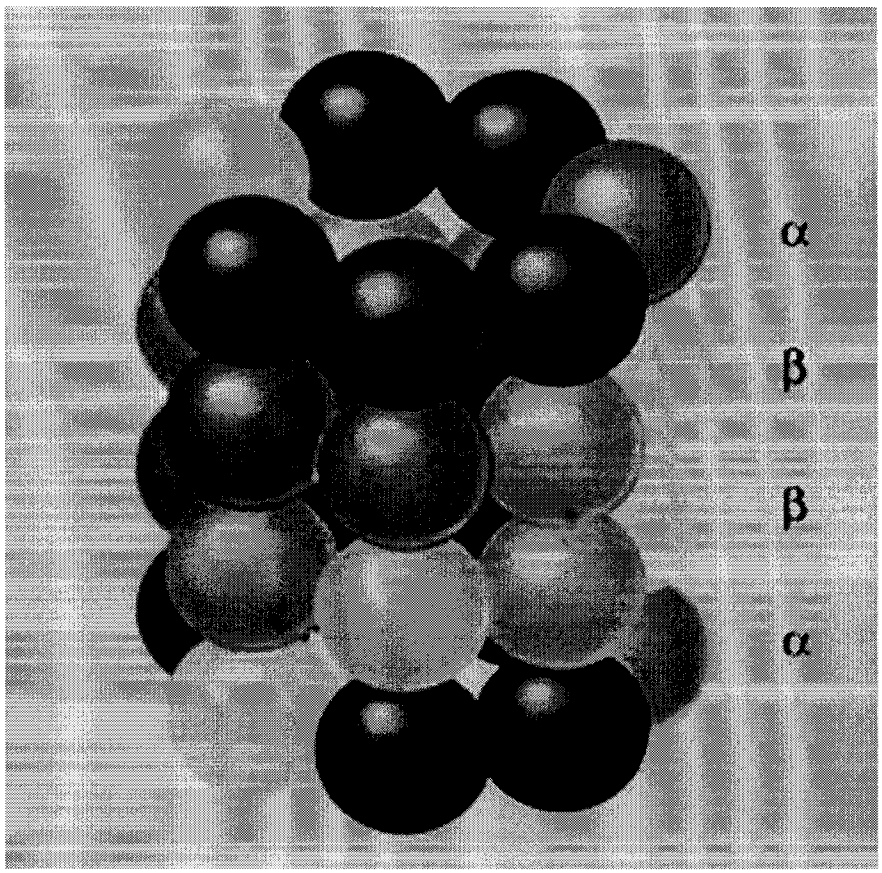

Figure 7. Functional domains of the p62 protein. SH2, AID, ZZ and TRAF6 refer to binding sites for the SH2 domain of $p56^{lck}$, aPKC, RIP and TRAF6, respectively. Mutations identified in Paget's disease of bone are shown.

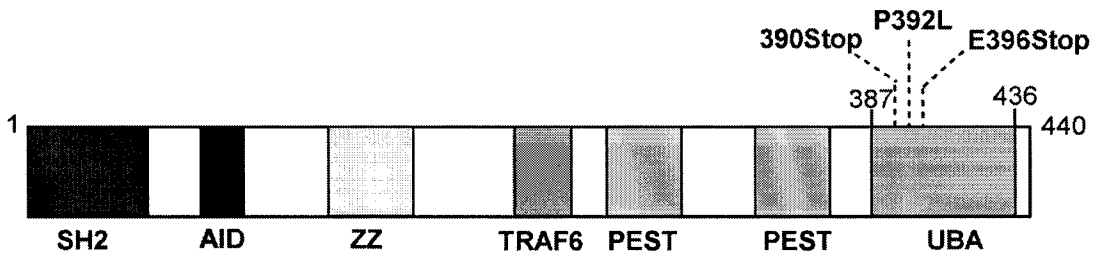

Figure 8. Scheme illustrating the two steps required for DNA hybridization on a Microarray Glass Slide.

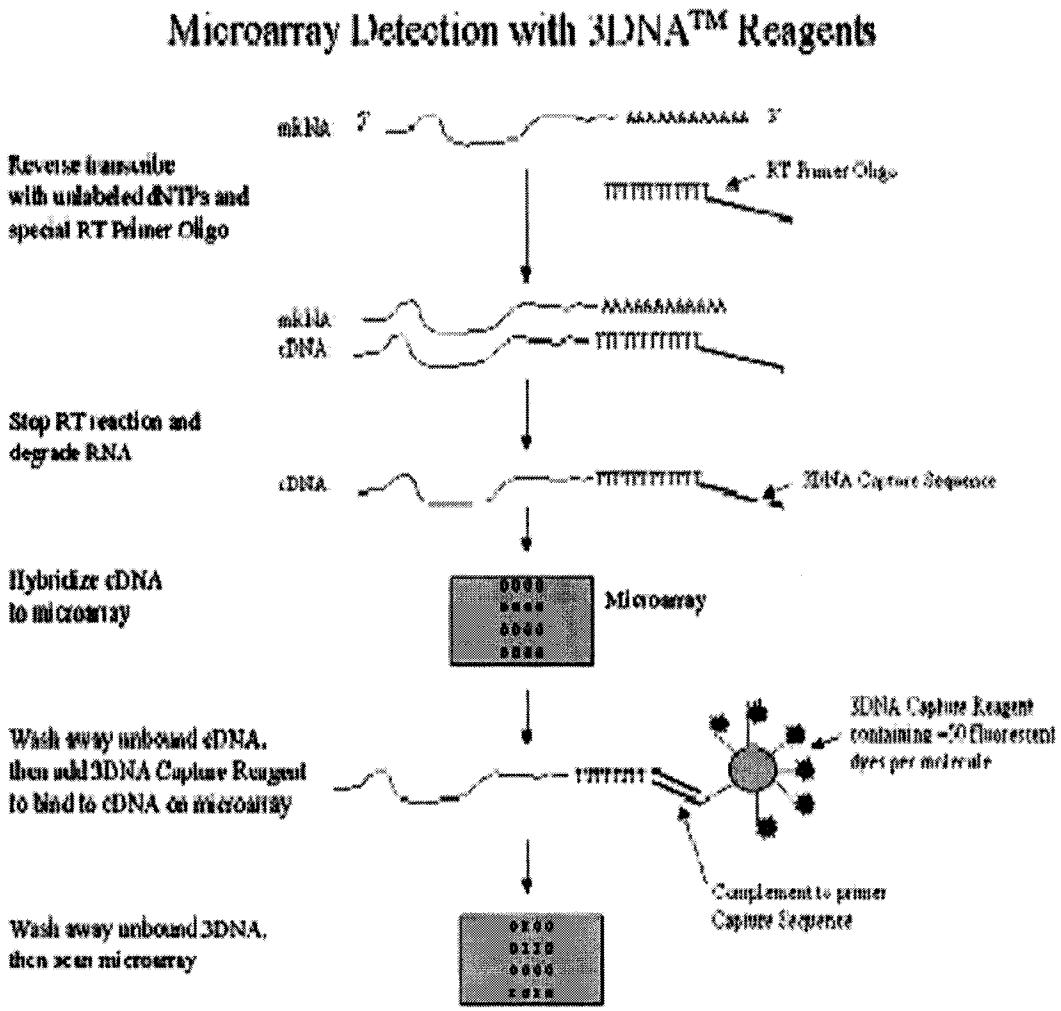

Figure 9. Overall analysis of the 11 experiments carried-out for microarray analysis of the gene expression profile in SK-N-SH cells upon treatment with 20μM PGJ2 for 4, 8, 16 and 24.

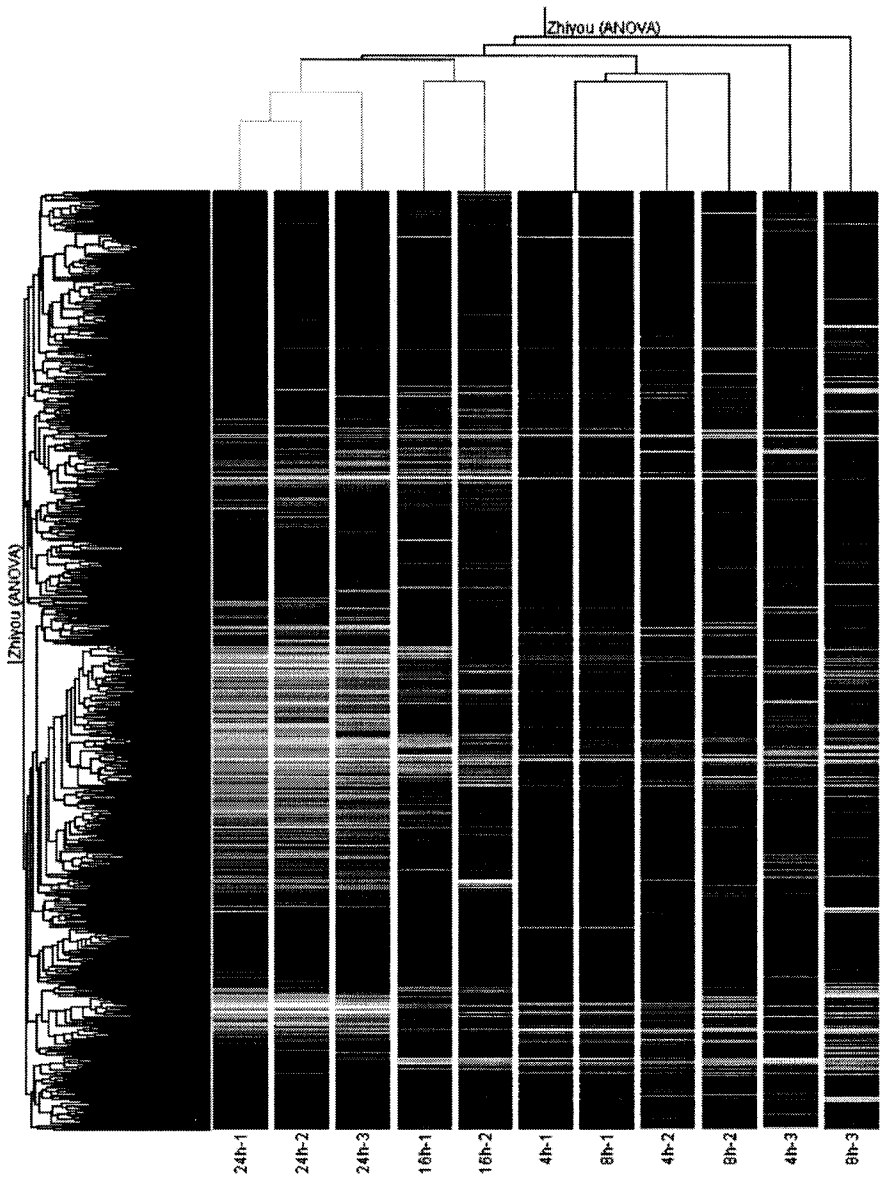

Figure 10. Time course of the number of known genes with significantly ($p<0.05$) altered expression and > 1.5-fold change. The curves depict the total number of genes with altered expression (up-regulation and down-regulation) at every time point following treatment with 20μM PGJ2. The greater number of genes was altered after 24h of treatment. Up-regulation was predominant over down-regulation at all time points.

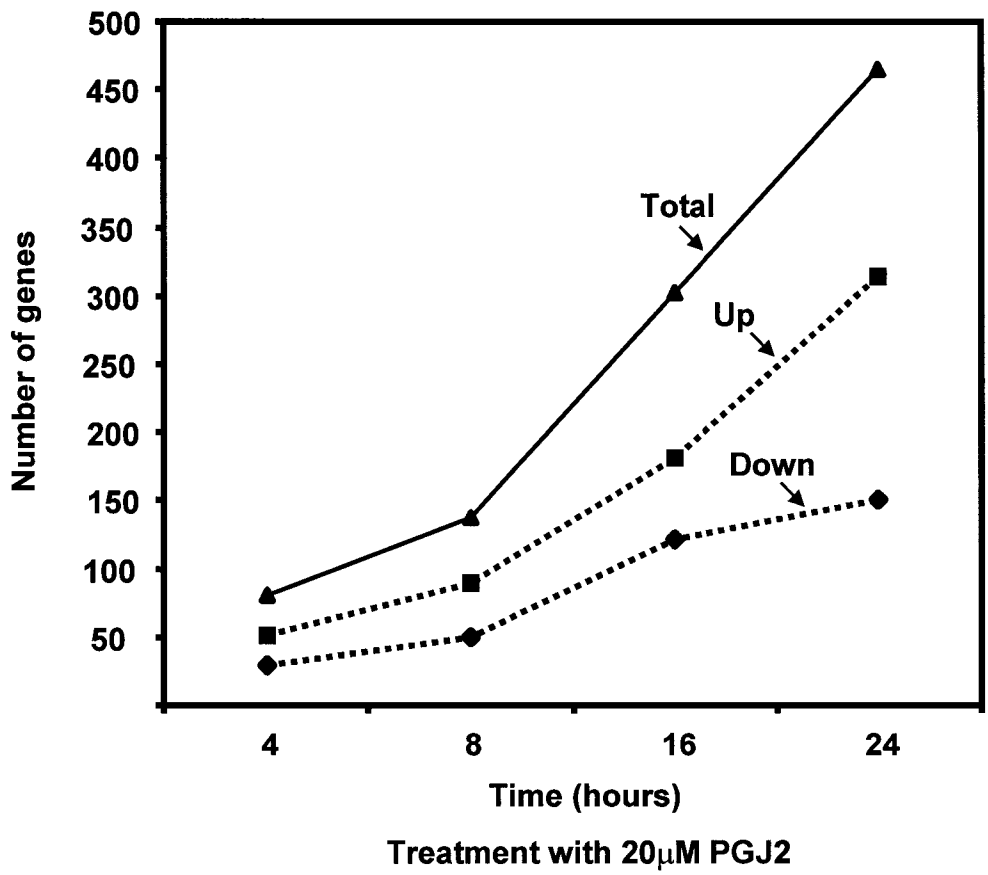

Figure 11. Functional classification of 465 known genes with significantly ($p<0.05$) altered expression and >1.5-fold change and a comparison of up- and down-regulation within each functional group. The pie chart (*left*) shows the proportion of each functional group and the total number of genes with altered expression in each group. The legend on the *right* shows the names and percentages of the functional group.

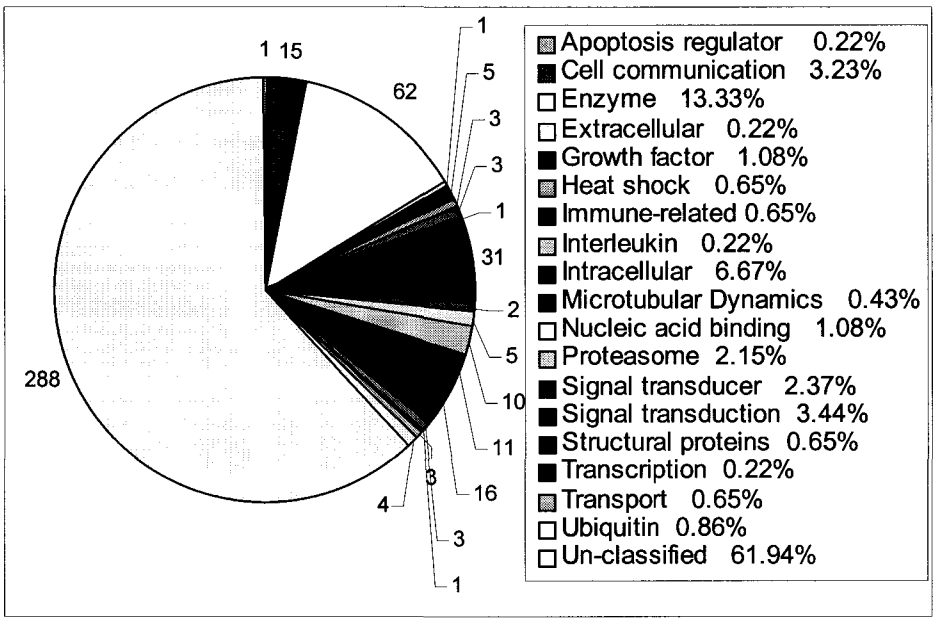

Figure 11. (Continuation) The histogram compares the percentage of up- (*red*) or down-regulated (*blue*) genes within each functional group.

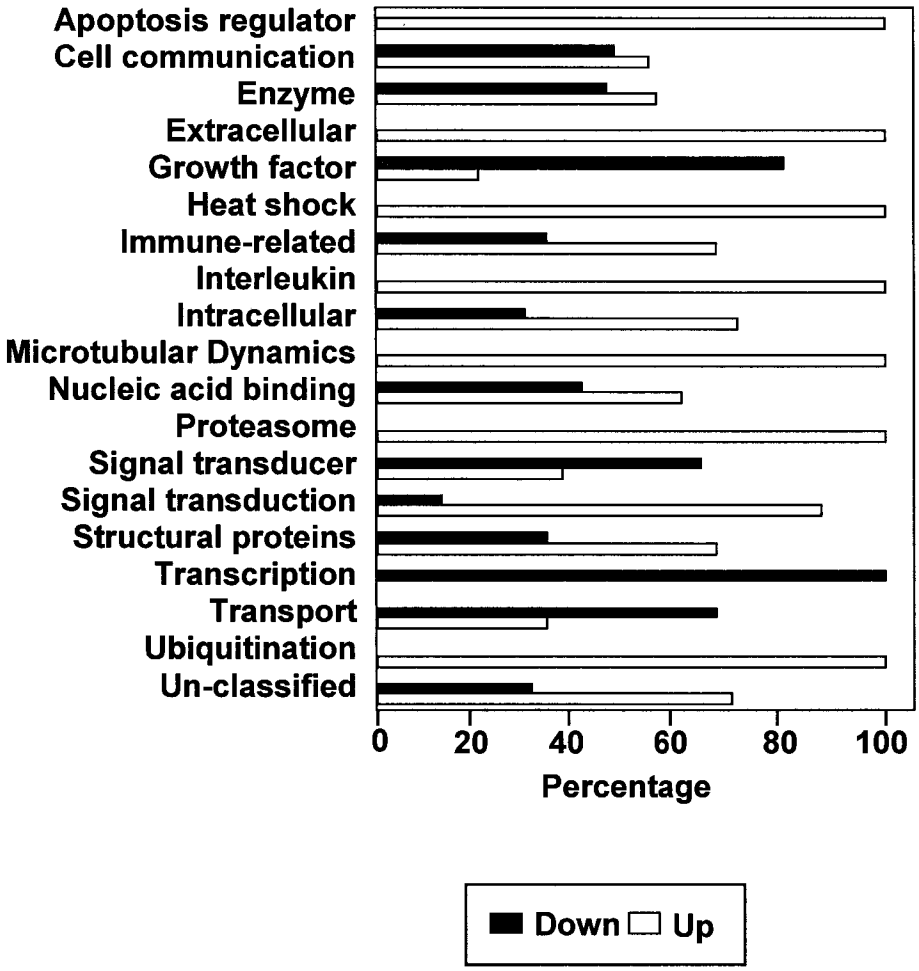

Figure 12 (next page) - Coomassie-stained acrylamide two-dimensional gel electrophoresis pattern of proteins in human neuroblastoma SK-N-SH cells treated with vehicle (DMSO, control) (*top*) or with 20μM PGJ2 for 24h (*bottom*). Total protein lysates were prepared from the respective cells as described in "Materials and Methods". 200μg of protein from each sample were then subjected to two-dimensional gel electrophoresis followed by staining with Coomassie Blue. Spots 1 through 9 represent proteins whose expression is elevated upon PGJ2-treatment as listed in Table 7.

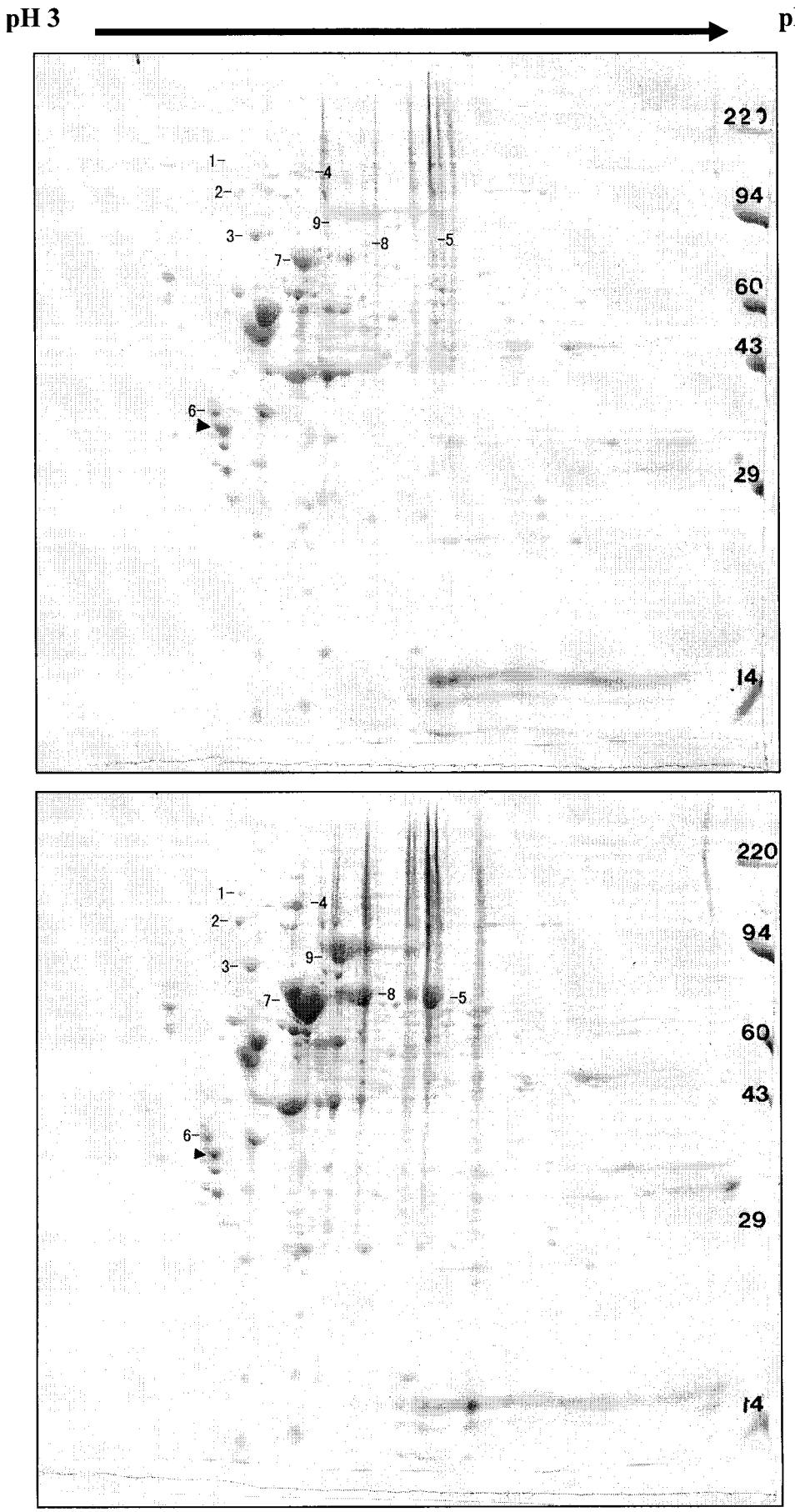

Figure 13 (next page) - Ubiquitinated proteins in human neuroblastoma SK-N-SH cells treated with vehicle (DMSO, control) (*top*) or with 20μM PGJ2 for 24h (*bottom*). Protein samples (200μg/sample) were subjected to two-dimensional gel electrophoresis followed by western blotting and immunostaining with an anti-ubiquitinated proteins antibody. High molecular weight polyubiquitinated proteins appear as a smear on the top of the gels. Lower molecular mass ubiquitin-positive species appear as "longitudinal streaks" with increasing numbers of ubiquitins in the chain. *Brackets* indicate putative unanchored pre-assembled polyubiquitin chains.

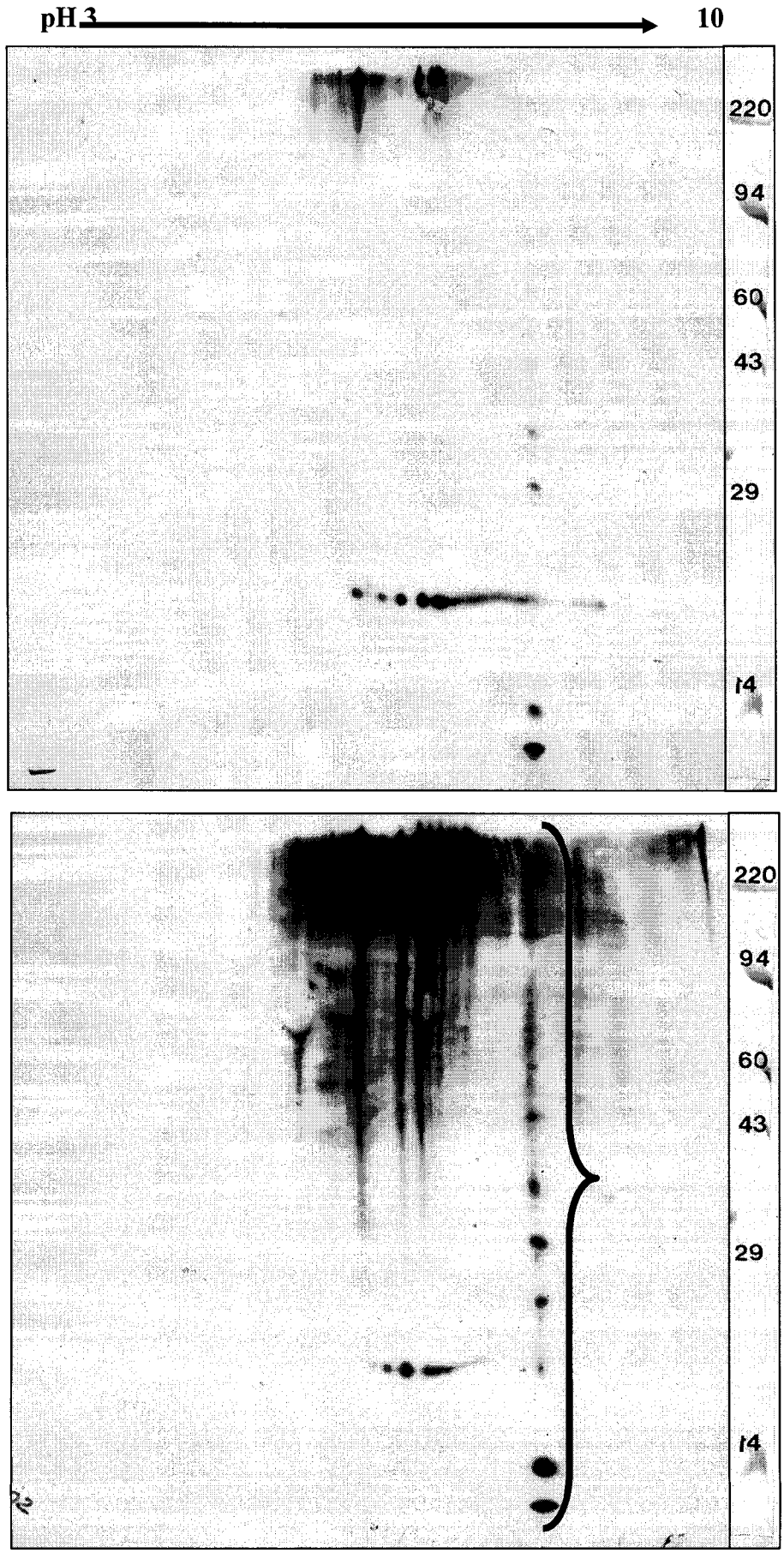

Figure 14 - PGJ2 increases the expression of sequestosome 1/p62 in a dose dependent manner - (A) - Western blot analysis was performed to detect sequestosome 1/p62 (seq.) and COX-1 levels in total extracts of human SK-N-SH neuroblastoma cells treated with PGJ2 for 24h (see Methods). Equal protein loading was demonstrated by reprobing the sequestosome 1/p62immunoblots with the anti-COX-1 antibody. **(B)** - Semi-quantitative RT-PCR analysis was performed to detect *sequestosome 1/p62* and *gapdh* gene expression in SK-N-SH cells treated with PGJ2 (see Methods). The PCR products for *sequestosome 1/p62* (336bp) and *gapdh* (598bp) are shown. **(C)** The protein (*open squares*) and PCR (*solid squares*) bands were semi-quantified by densitometry (see Methods). Data are shown as sequestosome 1/p62 and COX-1 or *sequestosome 1/p62* and *gapdh* ratios (represented by the number of pixels, arbitrary units) for each PGJ2-concentration as fold-increase over control (vehicle only). **(D)** Western blot analysis to detect sequestosome 1/p62 expression in SK-N-SH cells treated for one hour with inhibitors of transcription (Act.D, actinomycin D, 1.25μg/ml) or translation (Cycloh., cycloheximide, 6.25μg/ml) prior to exposure to PGJ2 (15μM) for 24h (see Methods). Similar results were obtained in

duplicate experiments. Molecular mass markers in kDa are shown on the right.

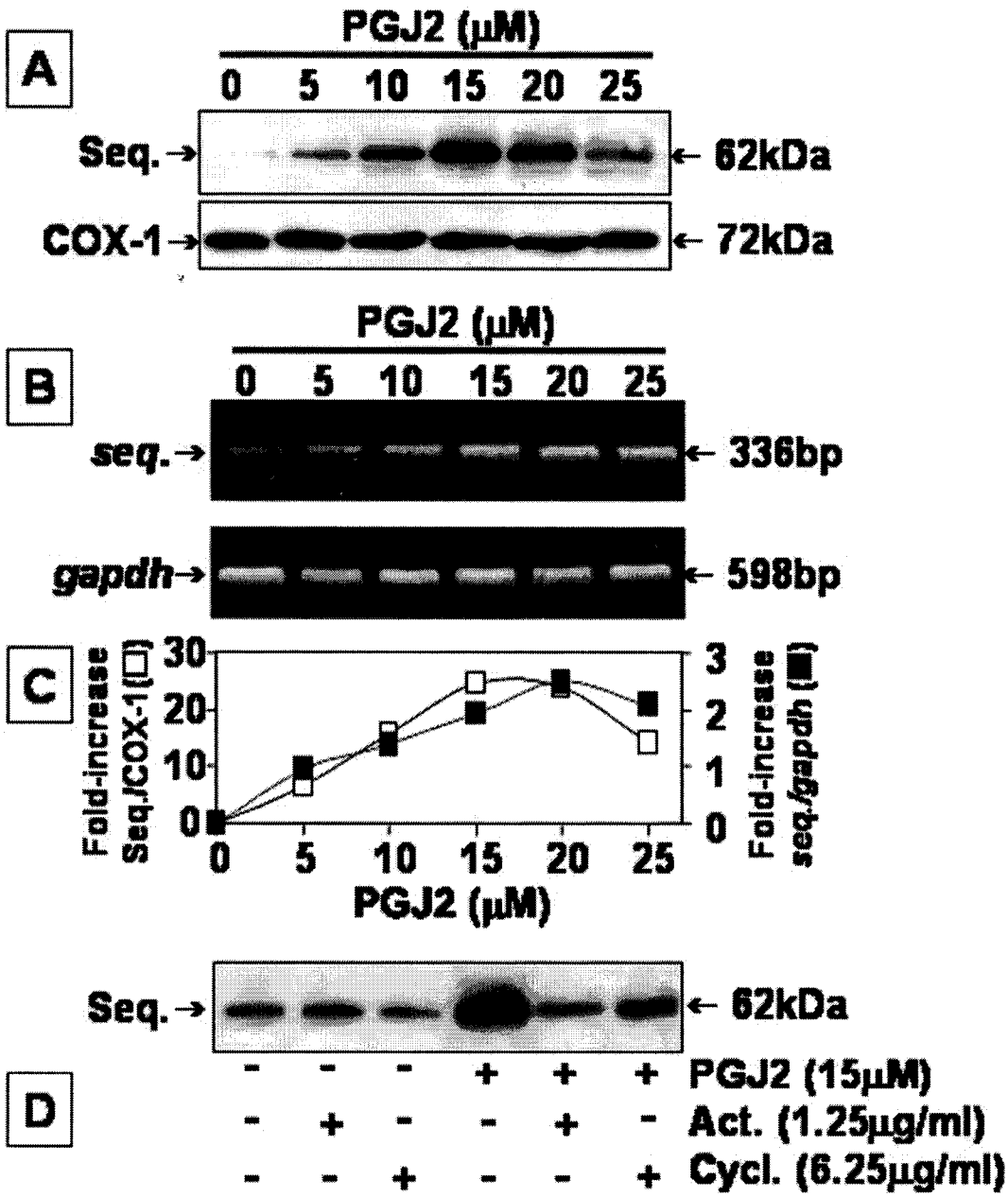

Figure 15 (next page) - PGJ2 increases sequestosome 1/p62 and ubiquitinated protein levels in a time-dependent manner - Western blot analyses were performed to detect sequestosome 1/p62 (seq., *top panel*), COX-1 (*middle panel*) and ubiquitinated protein levels (Ub-conjugates, *bottom panel*) in total extracts of human SK-N-SH neuroblastoma cells treated without (C) or with 15μM PGJ2 for 4, 8, 16, 24 and 48h (see Methods). Equal protein loading was demonstrated by reprobing the sequestosome 1/p62 blots with the anti-COX-1 antibody. The immunoreactive products for sequestosome 1/p62, COX-1 and Ub-conjugates were semiquantified by densitometry (graph, see Methods). Data are shown as sequestosome 1/p62 and COX-1 (*open squares*) or Ub-conjugates and COX-1 ratios (*solid squares*) (represented by the number of pixels, arbitrary units) for each time point as fold-increase over control (vehicle only). Molecular mass markers in kDa are shown on the left. Similar results were obtained in duplicate experiments.

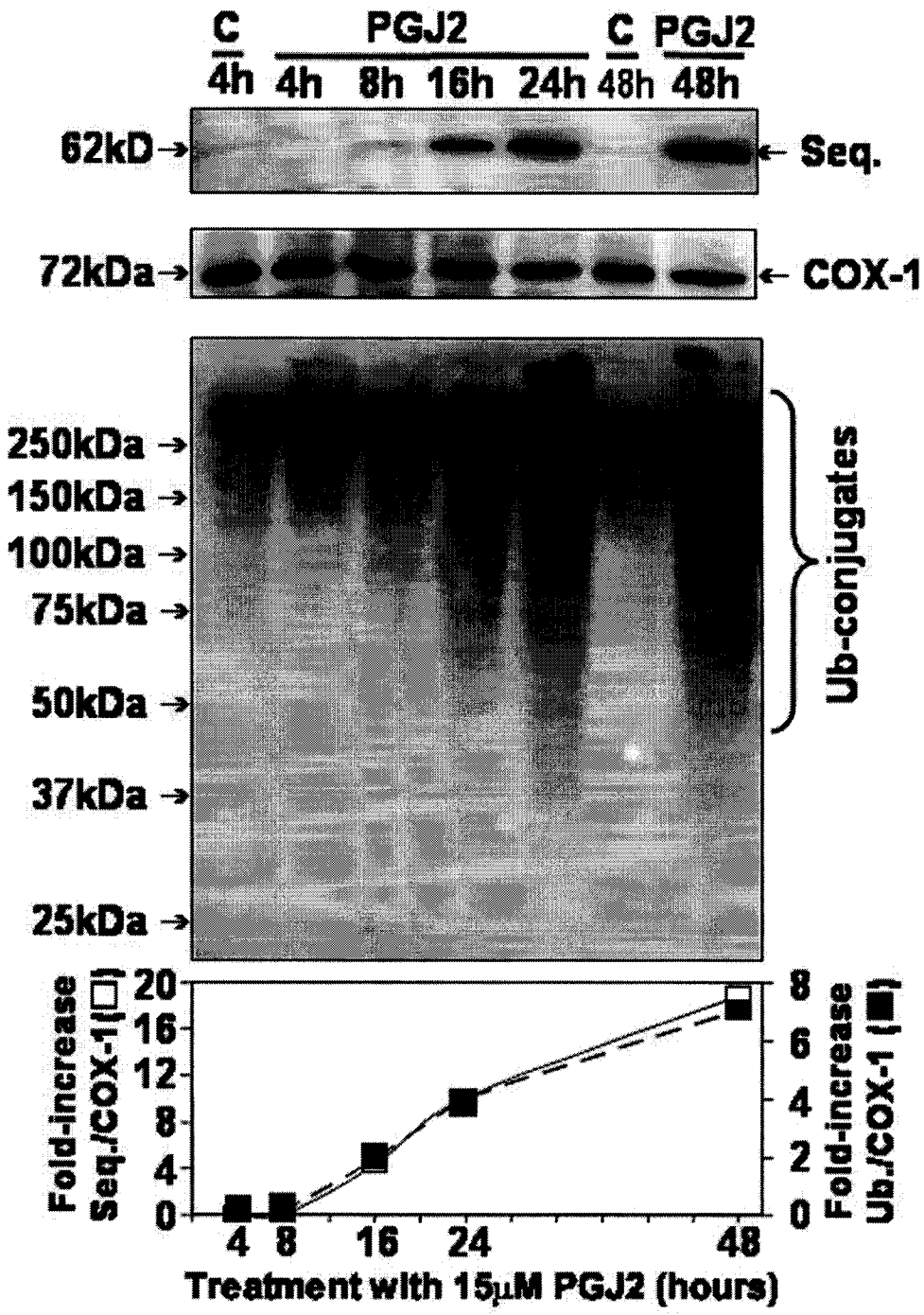

Figure 16 - The time-dependent decrease in cell viability induced by PGJ2 is inversely proportional to the increase in ubiquitinated protein and sequestosome 1/p62 levels - (*open circles*) - Viability of SK-N-SH cells treated with 15μM PGJ2 for 4, 8, 16 and 24h. Cell viability was assessed with the MTT assay (see Methods). Data represent the mean ± SEM from at least eight determinations. The viability for each condition was compared to the viability of cells at time zero. The *asterisk* (*) identifies the values that are significantly different ($p < 0.001$) from time zero. For comparison, the changes in the levels of ubiquitinated proteins and sequestosome 1/p62 as detected in Figure 15, are shown. Data represent sequestosome 1/p62 and COX-1 (*open squares*) or Ub-conjugates and COX-1 ratios (*solid squares*) calculated as number of pixels (arbitrary units) measured by densitometry.

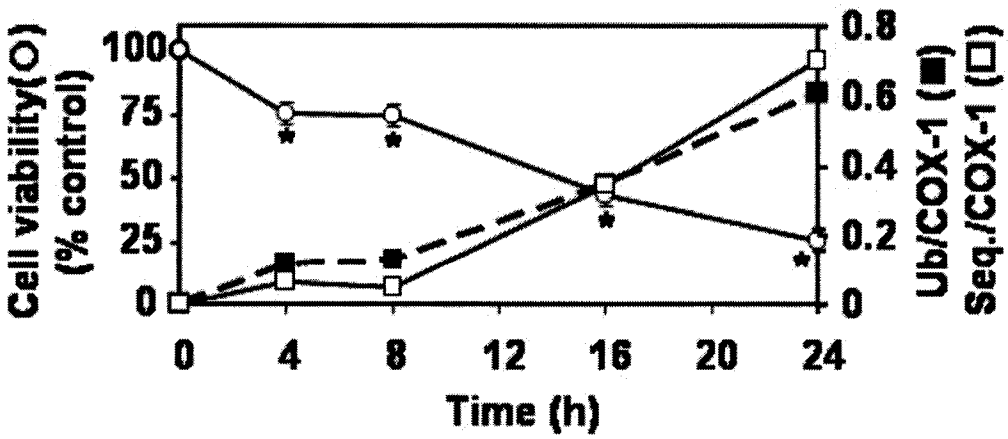

Figure 17 - Sequestosome 1/p62 and ubiquitinated proteins are co-localized in aggregates in SK-N-SH cells treated with PGJ2 - Double immunofluorescent staining of SK-NSH cells treated with vehicle only (DMSO, *1A-1D*), 10μM PGJ2 (*2A-2D*) or 20μM PGJ2 (*3A-3D*) for 24h. Sequestosome 1/p62 aggregates were visualized with the anti-sequestosome 1/p62 antibody (*arrows in 2B & 3B*, green), Ub-aggregates were visualized with the anti-Ub conjugates antibody (*arrows 2C & 3C*, red) and nuclei (n) with DAPI (*1A, 2A & 3A*, blue). Merged images are shown in (*1D, 2D & 3D*). The scale bar = 10μm.

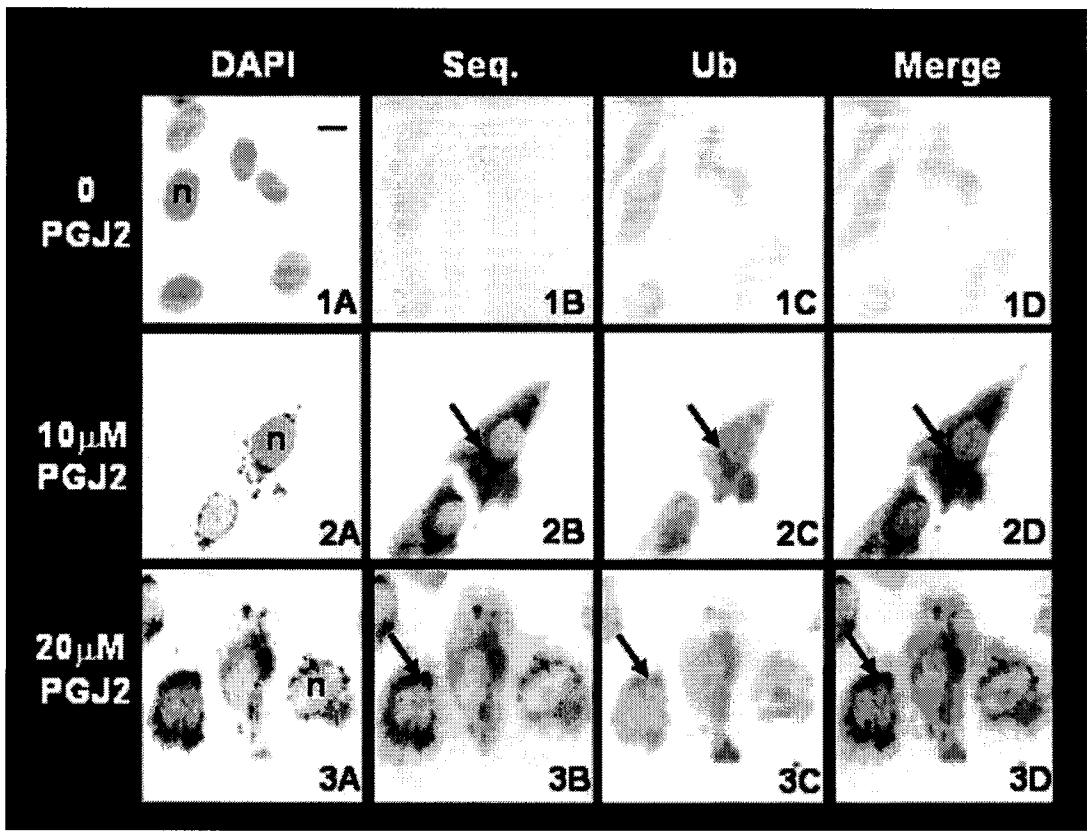

Figure 18 - Co-localization of sequestosome 1/p62 and UCH-L1 in SK-N-SH cells treated with 15 μM PGJ2 for 24h - Double immunofluorescent staining of SK-N-SH cells treated with vehicle only (DMSO, *1A-1D*) or 15μM PGJ2 for 24h (*2A-2D*). Sequestosome 1/p62 aggregates were visualized (green) with the anti-sequestosome 1/p62 antibody (*arrows in 2B)*, UCH-L1 was visualized (red) with the anti-UCH-L1 antibody (*2C*, red) and nuclei (n, blue) with DAPI (*1A & 2A*). Merged images are shown in (*1D & 2D*). The scale bar = 10μm.

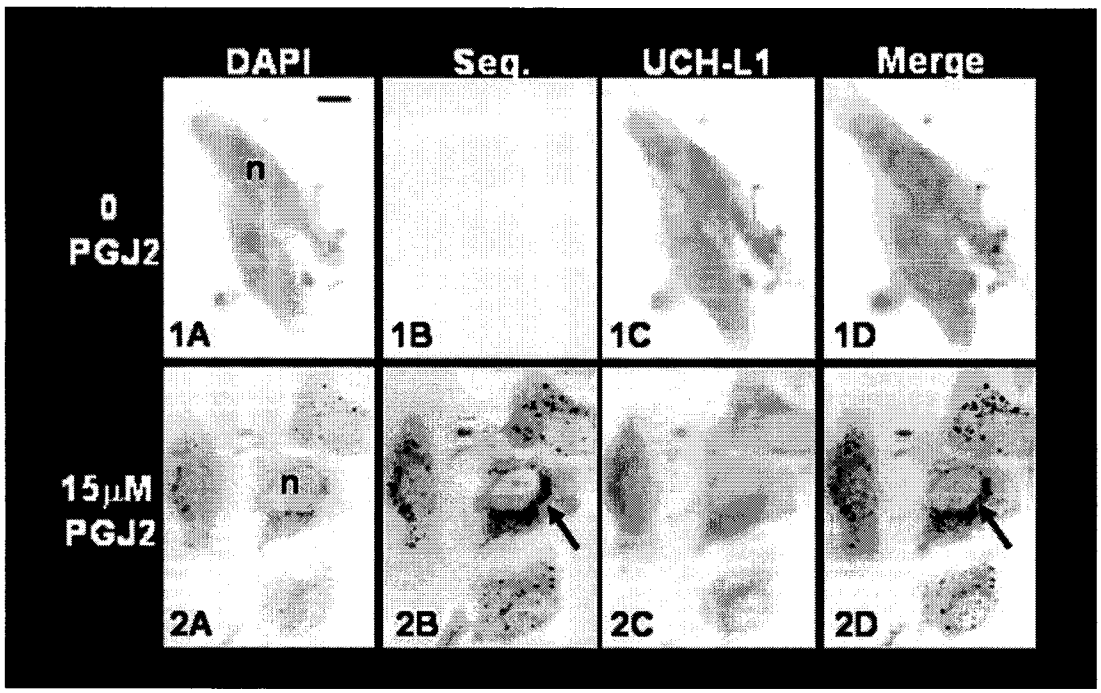

Figure 19 - PGJ2 increases protein aggregation in a time-dependent manner - Double immunofluorescent staining of SK-N-SH cells treated with 15μM PGJ2 for 4h (*first row*), 8h (*second row*), 16h (*third row*) or 24h (*fourth row*). Sequestosome 1/p62 (seq.) aggregates were visualized with the anti-sequestosome 1/p62 antibody (*green*), Ub-aggregates were visualized with the anti-Ub conjugates antibody (*red*) and nuclei (*n*) with DAPI (*blue*). Merged images are shown in the last panel of each row. The scale bar = 10μm.

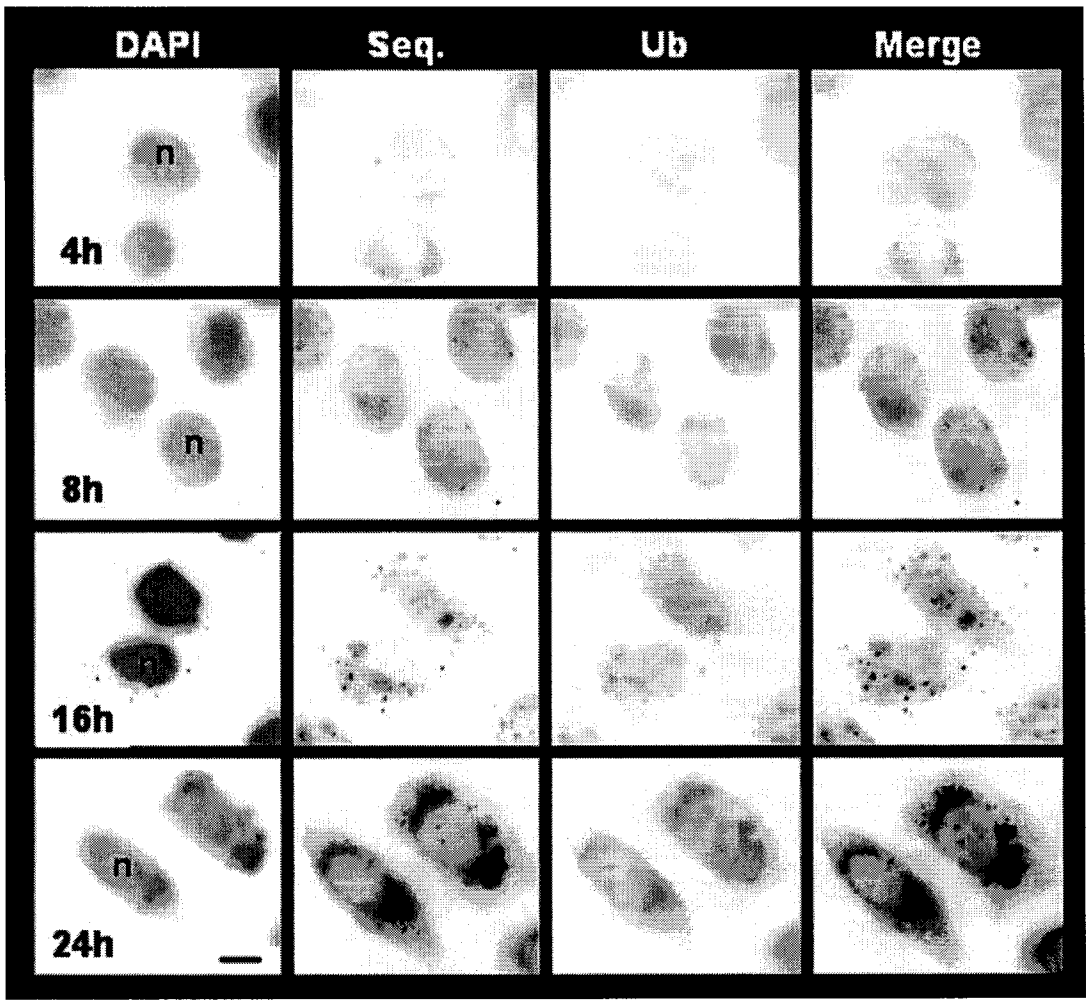

Figure 20 (next page) - Post-transcriptional silencing of sequestosome 1/p62 in SK-N-SH cells treated with PGJ2 - Western blot analyses were performed to detect sequestosome 1/p62 (seq., *top panel*), HSP105 (*middle panel*) and ubiquitinated protein levels (Ub-conjugates, *bottom panel*) in total extracts of human SK-N-SH neuroblastoma cells transfected with sequestosome 1/p62 specific siRNA (100nM) four hours prior to treatment with 15μM PGJ2 for 24h (see Methods). The specificity of the RNAi was demonstrated by reprobing the sequestosome 1/p62 blots with the anti-HSP105 antibody. Like sequestosome 1/p62, HSP105 is up-regulated by PGJ2. Molecular mass markers in kDa are shown on the right. Similar results were obtained in duplicate experiments.

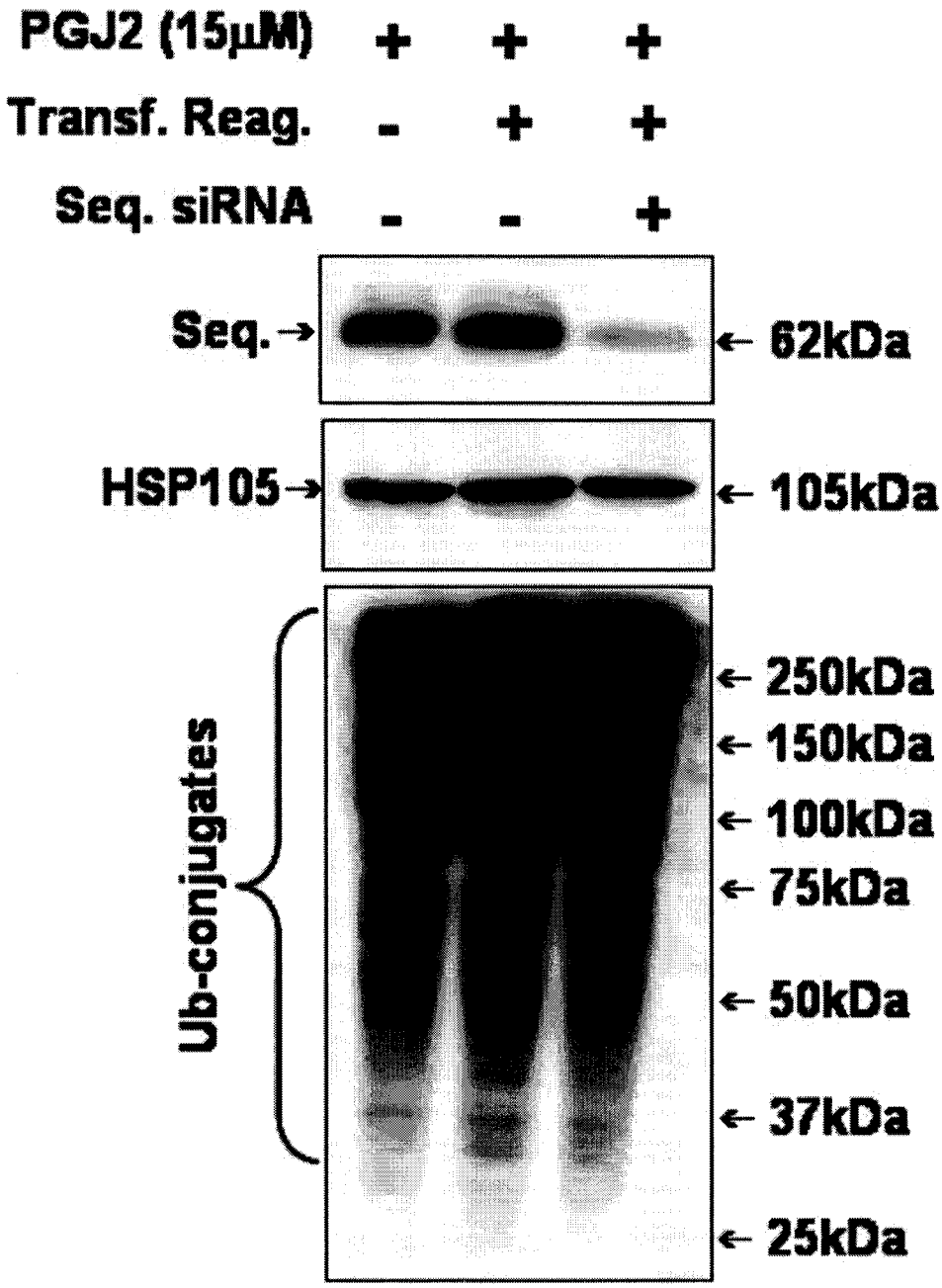

Figure 21 (next page) - Aggregation (but not accumulation) of ubiquitinated proteins induced by treating SK-N-SH cells with 15μM PGJ2 is prevented by post-transcriptional sequestosome 1/p62 silencing - Double immunofluorescent staining of SK-N-SH cells treated with vehicle only (DMSO, *1A-1D*), 15μM PGJ2 for 24h (*2A-2D*) or transfected with sequestosome 1/p62 specific siRNA (100nM) four hours prior to treatment with 15μM PGJ2 for 24h (*3A-3D*). Sequestosome 1/p62 aggregates were visualized with the anti-sequestosome 1/p62 antibody (*arrows in 2B,* green), Ub-aggregates were visualized with the anti-Ub conjugates antibody (*arrows 2C,* red) and nuclei (n) with DAPI (*1A, 2A & 3A,* blue). Sequestosome 1/p62 specific RNAi prevented sequestosome 1/p62 up-regulation (*3B*) and aggregation of ubiquitinated proteins, but not their accumulation (*3C*). Merged images are shown in (*1D, 2D & 3D*). The scale bar = 10μm.

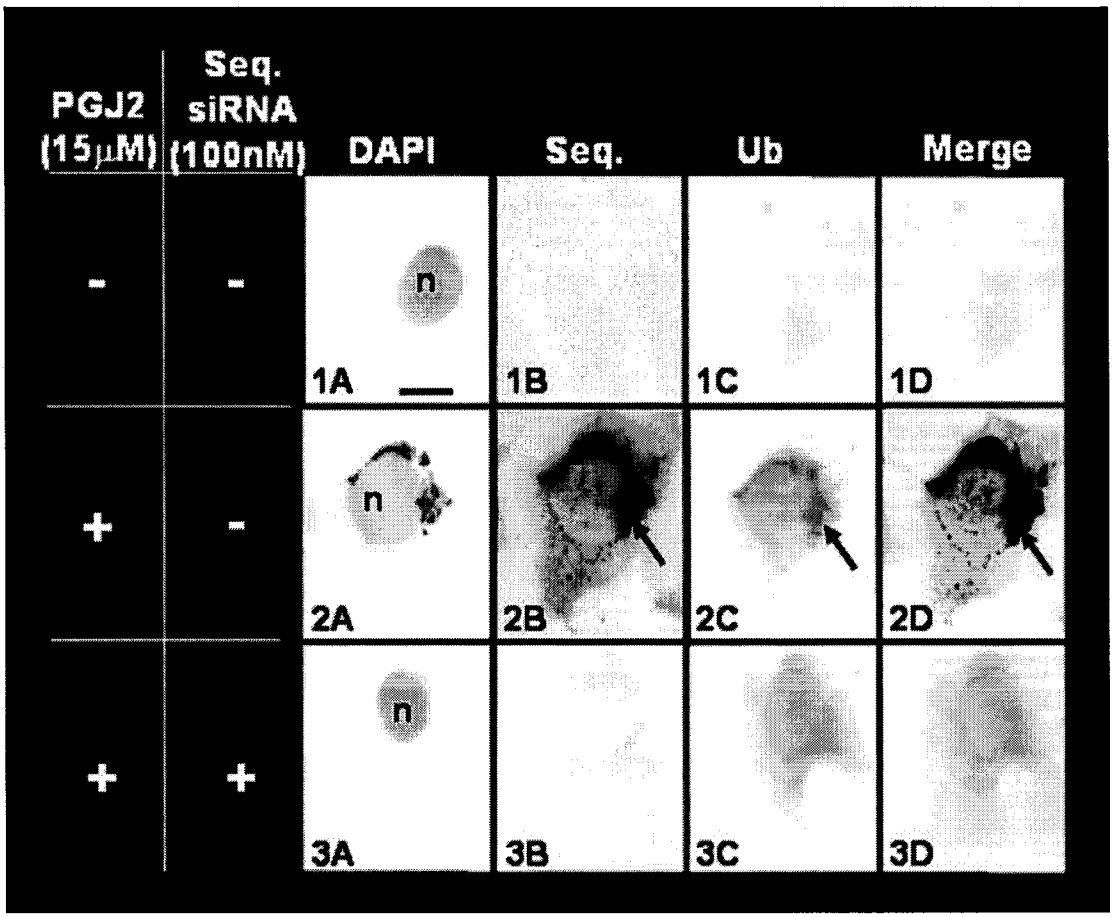

FIGURE 22 - Post-transcriptional sequestosome 1/p62 silencing failed to prevent PGJ2 cytotoxicity - Viability of SK-N-SH cells treated with vehicle only (DMSO, *solid bar*), 15μM PGJ2 for 24h (*open bar*), transfection reagent alone for 24h (*open bar*), or transfected with sequestosome 1/p62 specific siRNA (100nM) four hours prior to treatment with 15μM PGJ2 for 24h (*open bar*). Cell viability was assessed with the MTT assay (see Methods). Data represent the mean ± SEM from at least three determinations. The viability for each condition was compared to the viability of cells treated with vehicle only (control, 100%). The *asterisk* (*) identifies the values that are significantly different ($p < 0.001$) from the control.

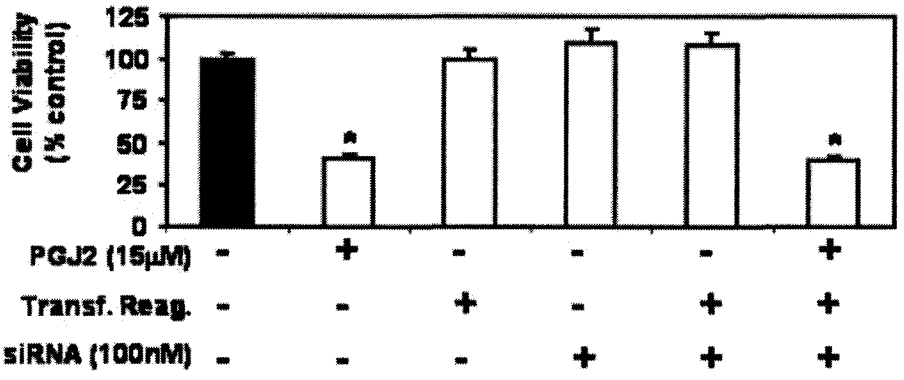

Figure 23. Scheme linking inflammation to neurodegeneration (see Chapter V for explanation). This scheme depicts only putative pathways of neurodegeneration and does not exclude other mechanisms leading to neurotoxicity and the development of neurodegenerative disorders associated with the accumulation of ubiquitinated proteins in neuronal inclusions.

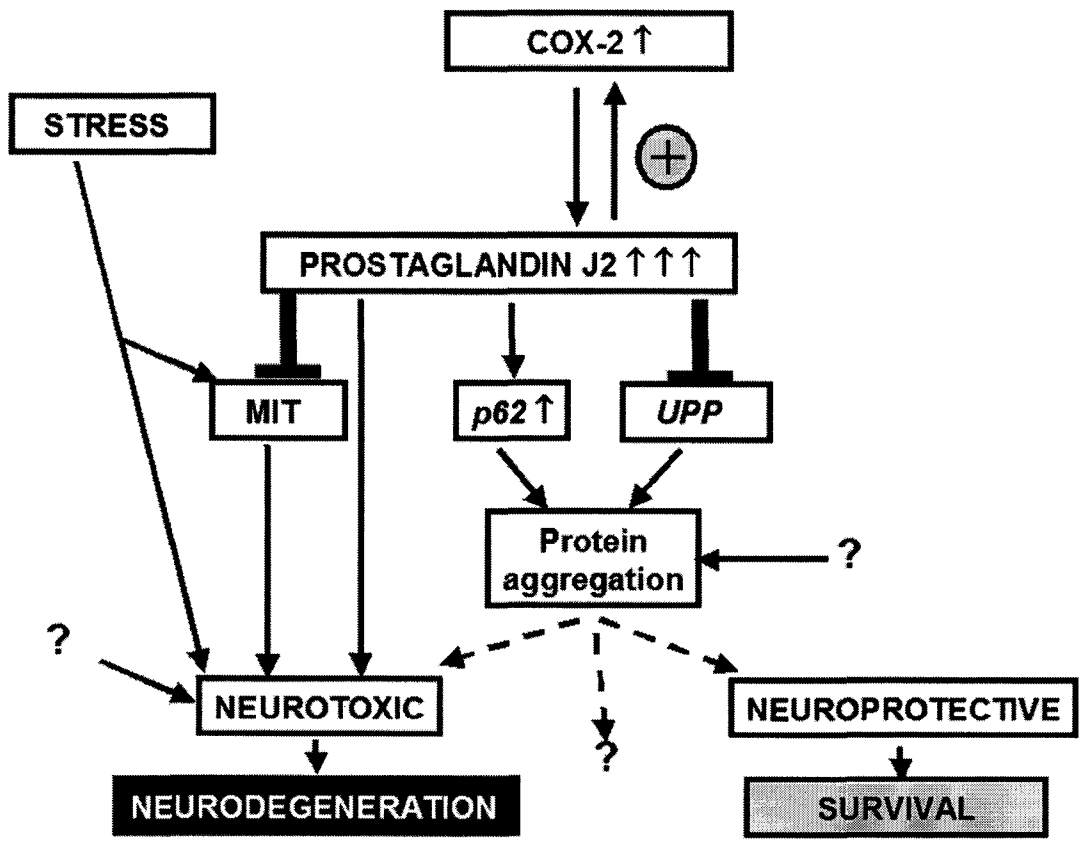

Table 1. Frequency and number of known genes that showed altered expression following treatment with 20μM PGJ2 for 4, 8, 16 and 24h

	1 Time	2 Times	3 Times	4 Times
Down	243	83	22	4
Up	389	174	55	18
Total	632	257	77	22
Percentage	72.9	29.7	8.9	2.5

Table 2. Time course of the number of known genes with significantly ($p<0.05$) altered expression and > 1.5-fold change following treatment with 20μM PGJ2

	4 Hours	8 Hours	16 Hours	24 Hours
Down	29	49	121	151
Up	51	89	182	314
Total	80	138	303	465

Table 3. Genes significantly ($p<0.05$) up-regulated following treatment with 20μM PGJ2 for 24h. The genes are listed in descending order of fold-increase over control levels. The fold-increase is highlighted in different colors following the legend shown below.

49-10	9.9-5.0	4.99-3.0	2.99-2.0	1.99-1.5
		YELLOW	GREY	WHITE

Gene Name	Expression
heat shock 70kD protein 6 (HSP70B') (HSPA6) mRNA	
cDNA: FLJ22349 fis, clone HRC06310	
proteasome (prosome, macropain) 26S subunit, ATPase, 5 (PSMC5)	
Human ubiquitin mRNA, complete cds	
clusterin (complement lysis inhibitor, SP-40,40, sulfated glyc	
FOS-like antigen-1 (FOSL1), mRNA	
cDNA FLJ11627 fis, clone HEMBA1004225	
syntaxin 3A (STX3A) mRNA	
heat shock protein (hsp110 family) (APG-1), mRNA	
mRNA for KIAA0527 protein, partial cds	
cDNA FLJ13123 fis, clone NT2RP3002763	
Human heart mRNA for heat shock protein 90, partial cds	
pleckstrin homology-like domain, family A, member 1 (PHLDA1),	
cDNA FLJ13874 fis, clone THYRO1001365	
HT014 (HT014), mRNA	
serine/threonine protein kinase MASK (LOC51765), mRNA	
NAD(P)H menadione oxidoreductase 1, dioxin-inducible (NMOR1) m	
arylacetamide deacetylase (esterase) (AADAC) mRNA	
HSPC311 mRNA, partial cds	
mRNA for KIAA0463 protein, partial cds	4.78
hypothetical protein (H41), mRNA	4.76
G protein-coupled receptor 56 (GPR56) mRNA	4.63
RAB31, member RAS oncogene family (RAB31), mRNA	4.59
CGI-125 protein (LOC51003), mRNA	4.50
mRNA for FLJ00044 protein, partial cds	4.42
BCL2/adenovirus E1B 19kD-interacting protein 3 (BNIP3), nuclea	4.41
CGI-17 protein (LOC51007), mRNA	4.20
vacuolar H(+)-ATPase subunit (ATP6GL) mRNA	4.20
clone 23674 mRNA sequence	4.15
cDNA FLJ10934 fis, clone OVARC1000640	4.13
calcium channel, voltage-dependent, L type, alpha 1B subunit (	4.08
SRY (sex-determining region Y)-box 9 (campomelic dysplasia, au	4.08
HCCA2 mRNA, complete cds	3.98
microtubule-associated proteins 1A/1B light chain 3 mRNA, comp	3.92

Table 3. continued

cDNA: FLJ21934 fis, clone HEP04364	3.91
hypothetical protein (HSPC219), mRNA	3.85
mRNA; cDNA DKFZp434C1613 (from clone DKFZp434C1613)	3.83
proteasome (prosome, macropain) subunit, beta type, 7 (PSMB7)	3.80
Tax1 (human T-cell leukemia virus type I) binding protein 1 (T	3.75
cDNA: FLJ23476 fis, clone HSI14935	3.72
hypothetical protein FLJ20279 (FLJ20279), mRNA	3.66
RAB1, member RAS oncogene family (RAB1) mRNA	3.62
valosin-containing protein (VCP), mRNA	3.60
cDNA: FLJ21325 fis, clone COL02408, highly similar to AF147723	3.57
pirin (PIR) mRNA	3.57
mRNA; cDNA DKFZp761A052 (from clone DKFZp761A052)	3.55
prion protein (p27-30) (Creutzfeld-Jakob disease, Gerstmann-St	3.55
DKFZP564A2416 protein (DKFZP564A2416), mRNA	3.52
protease, serine, 15 (PRSS15), mRNA	3.50
cathepsin D (lysosomal aspartyl protease) (CTSD) mRNA	3.48
testis-specific kinase 1 (TESK1) mRNA	3.47
PPAR(gamma) angiopoietin related protein (PGAR), mRNA	3.46
GAP-like protein (LOC51306), mRNA	3.45
ATP-binding cassette, sub-family B (MDR/TAP), member 6 (ABCB6)	3.39
growth factor receptor-bound protein 10 (GRB10) mRNA	3.37
proteasome (prosome, macropain) subunit, beta type, 2 (PSMB2),	3.36
proteasome (prosome, macropain) subunit, alpha type, 5 (PSMA5)	3.26
ALL1-fused gene from chromosome 1q (AF1Q), mRNA	3.23
hypothetical protein FLJ10567 (FLJ10567), mRNA	3.23
Niemann-Pick disease, type C1 (NPC1) mRNA, and translated prod	3.19
hypothetical protein FLJ20287 (FLJ20287), mRNA	3.18
mRNA for KIAA1526 protein, partial cds	3.17
Human gene from PACs 37M17 and 305B16, chromosome X, similar to	3.16
hypothetical protein FLJ20186 (FLJ20186), mRNA	3.12
mRNA; cDNA DKFZp434H2450 (from clone DKFZp434H2450)	3.12
mutS (E. coli) homolog 3 (MSH3) mRNA	3.12
cDNA: FLJ22652 fis, clone HSI07445, highly similar to AF131829	3.11
ATPase, H+ transporting, lysosomal (vacuolar proton pump) 9kD	3.10
cDNA: FLJ23510 fis, clone LNG03216	3.10
matrix metalloproteinase 1 (interstitial collagenase) (MMP1) mR	3.10
chromosome 11 hypothetical protein ORF3 (LOC56851), mRNA	3.01
mRNA for KIAA1092 protein, partial cds	3.01
mRNA; cDNA DKFZp434E0516 (from clone DKFZp434E0516)	2.99
BCL2-associated athanogene 2 (BAG2), mRNA	2.98
glycerol kinase deficiency (GK) mRNA	2.95
delta-like 1 (mouse) homolog (DLL1), mRNA	2.93
sorting nexin 2 (SNX2) mRNA, and translated products	2.92
mRNA for KIAA0771 protein, partial cds	2.91
ring finger protein 14 (RNF14), mRNA	2.89

Table 3. continued

cDNA FLJ11856 fis, clone HEMBA1006789	2.87
hypothetical protein FLJ11106 (FLJ11106), mRNA	2.87
receptor-interacting serine-threonine kinase 2 (RIPK2) mRNA	2.86
mRNA for KIAA1236 protein, partial cds	2.84
origin recognition complex, subunit 4 (yeast homolog)-like (OR	2.82
proteasome (prosome, macropain) 26S subunit, non-ATPase, 1 (PS	2.82
glutamine-fructose-6-phosphate transaminase 2 (GFPT2) mRNA	2.79
cDNA FLJ12827 fis, clone NT2RP2002939, weakly similar to ZINC	2.78
putative zinc finger protein (LOC55818), mRNA	2.78
ubiquitin specific protease 16 (USP16) mRNA	2.76
death-associated protein kinase-related 1 (DRAK1) mRNA	2.72
inorganic pyrophosphatase 2 (PPA2) mRNA, complete cds, nuclear	2.72
Rag C mRNA, complete cds	2.70
TTF-I interacting peptide 20 mRNA, partial cds	2.69
lipopolysaccharide specific response-7 protein (LSR7), mRNA	2.68
M-phase phosphoprotein homolog (LOC51663), mRNA	2.65
cDNA: FLJ22282 fis, clone HRC03861	2.63
regeneration associated protein 3 (RAP3) mRNA, alternatively s	2.62
mRNA for KIAA1321 protein, partial cds	2.62
cDNA FLJ13046 fis, clone NT2RP3001374	2.60
Human mRNA for KIAA0093 gene, partial cds	2.58
mRNA; cDNA DKFZp586A0618 (from clone DKFZp586A0618)	2.58
parathyroid hormone-like hormone (PTHLH) mRNA	2.58
hypothetical protein FLJ20062 (FLJ20062), mRNA	2.58
hypothetical protein (LOC51244), mRNA	2.57
poly(rC)-binding protein 2 (PCBP2) mRNA	2.57
RAD9 (S. pombe) homolog (RAD9) mRNA	2.56
cDNA FLJ13409 fis, clone PLACE1001716	2.54
mitogen-activated protein kinase kinase kinase 11 (MAP3K11), m	2.53
mortality factor 4 (MORF4), mRNA	2.53
protein phosphatase 4 (formerly X), catalytic subunit (PPP4C)	2.52
aspartate beta-hydroxylase (ASPH) mRNA	2.50
golgi autoantigen, golgin subfamily a, 3 (GOLGA3) mRNA	2.50
hypothetical protein FLJ20686 (FLJ20686), mRNA	2.50
protein phosphatase 2 (formerly 2A), catalytic subunit, beta i	2.50
cell membrane glycoprotein, 110000M(r) (surface antigen) (GP11	2.49
H.sapiens polyA site DNA	2.49
nuclear domain 10 protein (NDP52) mRNA	2.49
Human mRNA for KIAA0077 gene, partial cds	2.49
hypothetical protein FLJ10767 (FLJ10767), mRNA	2.48
intercellular adhesion molecule 5, telencephalin (ICAM5), mRNA	2.48
selectin P ligand (SELPLG), mRNA	2.48
hypothetical protein (HSPC014), mRNA	2.46
progesterone binding protein (HPR6.6), mRNA	2.46
cDNA: FLJ21504 fis, clone COL05662	2.44

Table 3. continued

partial mRNA for hypothetical protein (ORF1), RZPD clone MPMGp	2.44
mRNA for KIAA0375 protein, partial cds	2.42
tissue inhibitor of metalloproteinase 1 (erythroid potentiatin	2.39
putative receptor protein (PMI), mRNA	2.39
ancient conserved domain protein 4 (LOC56939), mRNA	2.36
mRNA for KIAA1143 protein, partial cds	2.36
neutral sphingomyelinase (N-SMase) activation associated factor	2.36
hypothetical protein (LOC51234), mRNA	2.34
ubiquitin fusion degradation 1-like (UFD1L) mRNA	2.34
Human WW domain binding protein-2 mRNA, complete cds	2.33
fatty acid binding protein 4, adipocyte (FABP4) mRNA	2.31
CD4 receptor {exons 1 and 2} [human, T-lymphocyte, mRNA, 3429 n	2.30
mRNA; cDNA DKFZp434J194 (from clone DKFZp434J194)	2.30
KIAA0107 gene product (KIAA0107), mRNA	2.29
cDNA FLJ12475 fis, clone NT2RM1000962	2.29
Human co-beta glucosidase (proactivator) mRNA, complete cds	2.29
mRNA for methyltransferase-like protein 1	2.29
ephrin-B2 (EFNB2) mRNA	2.28
chromosome 16 open reading frame 5 (C16orf5), mRNA	2.28
crystallin, zeta (quinone reductase) (CRYZ) mRNA	2.25
discs, large (Drosophila) homolog 5 (DLG5) mRNA	2.25
hypothetical protein FLJ10430 (FLJ10430), mRNA	2.25
KIAA0025 gene product; MMS-inducible gene (KIAA0025), mRNA	2.24
mRNA for KIAA1340 protein, partial cds	2.24
inhibitor of kappa light polypeptide gene enhancer in B-cells,	2.24
mRNA for KIAA1620 protein, partial cds	2.24
catenin (cadherin-associated protein), alpha 1 (102kD) (CTNNA1	2.23
fragile X mental retardation, autosomal homolog 2 (FXR2), mRNA	2.23
cDNA FLJ14153 fis, clone NT2RM1000092, weakly similar to MULTI	2.22
spermatogenesis associated PD1 (KIAA0757) mRNA	2.22
interferon, gamma-inducible protein 16 (IFI16) mRNA	2.22
mRNA for KIAA0567 protein, partial cds	2.21
protein tyrosine phosphatase, non-receptor type 3 (PTPN3) mRNA	2.20
paired immunoglobulin-like receptor alpha (PILR(ALPHA)), mRNA	2.19
KIAA0249 gene product (KIAA0249), mRNA	2.18
mRNA for KIAA1508 protein, partial cds	2.17
SEC14 (S. cerevisiae)-like 2 (SEC14L2), mRNA	2.17
FIP2 alternatively translated mRNA, complete cds	2.17
PTD008 protein (PTD008), mRNA	2.17
ST2V protein (ST2V), mRNA	2.17
serologically defined colon cancer antigen 16 (SDCCAG16), mRNA	2.16
cDNA FLJ12679 fis, clone NT2RM4002420	2.15
hypothetical protein (LOC51255), mRNA	2.14
interleukin 15 receptor, alpha (IL15RA) mRNA	2.14
cDNA: FLJ22761 fis, clone KAIA0893	2.12

Table 3. continued

immunoglobulin mu binding protein 2 (IGHMBP2) mRNA	2.12
myosin-binding protein C, slow-type (MYBPC1) mRNA	2.12
mRNA; cDNA DKFZp564O1172 (from clone DKFZp564O1172)	2.11
mRNA full length insert cDNA clone EUROIMAGE 1967720	2.11
serine/threonine kinase 12 (STK12), mRNA	2.09
translocase of outer mitochondrial membrane 70 (yeast) homolog	2.08
oxidase (cytochrome c) assembly 1-like (OXA1L), mRNA	2.08
flavohemoprotein b5+b5R (LOC51167), mRNA	2.07
CGI-11 protein (LOC51606), mRNA	2.06
clone 214338, mRNA sequence	2.06
FH1/FH2 domain-containing protein (FHOS), mRNA	2.06
plexin B1 (PLXNB1), mRNA	2.06
signal recognition particle receptor ('docking protein') (SRPR)	2.05
tuftelin-interacting protein (TIP39), mRNA	2.05
similar to yeast BET3 (S. cerevisiae) (BET3), mRNA	2.04
proteasome (prosome, macropain) subunit, beta type, 3 (PSMB3),	2.03
adaptor-related protein complex 3, sigma 2 subunit (AP3S2), mR	2.02
Nef-associated factor 1 (NAF1) mRNA	2.01
mRNA; cDNA DKFZp434A115 (from clone DKFZp434A115)	2.01
golgi autoantigen, golgin subfamily a, 4 (GOLGA4), mRNA	2.00
mRNA for KIAA1500 protein, partial cds	2.00
neurofilament 3 (150kD medium) (NEF3) mRNA	2.00
kappa B-ras 1 (LOC57083), mRNA	1.99
steroid receptor RNA activator isoform 3 mRNA, complete cds	1.99
transmembrane glycoprotein (GPNMB) mRNA	1.99
Human lamin A mRNA, 3'end	1.98
PR-domain containing protein 14 (PRDM14) mRNA, complete cds	1.98
PNAS-112 mRNA, partial sequence	1.98
HUS1 (S. pombe) checkpoint homolog (HUS1) mRNA	1.97
proteasome (prosome, macropain) subunit, beta type, 4 (PSMB4)	1.97
serine palmitoyltransferase, long chain base subunit 2 (SPTLC2	1.96
cDNA: FLJ22555 fis, clone HSI01193	1.96
tubulin, beta, 5 (TUBB5) mRNA	1.96
disrupter of silencing 10 (SAS10), mRNA	1.96
mucolipin 1 (MCOLN1), mRNA	1.96
hypothetical protein FLJ10879 (FLJ10879), mRNA	1.95
cut (Drosophila)-like 1 (CCAAT displacement protein) (CUTL1) mR	1.95
mannosidase, alpha, class 2A, member 1 (MAN2A1), mRNA	1.95
mRNA; cDNA DKFZp434C1418 (from clone DKFZp434C1418); partial cd	1.95
zinc finger protein ZNF140-like protein (LOC55828), mRNA	1.95
beta-1,3-N-acetylglucosaminyltransferase (BETA3GNT), mRNA	1.94
vacuolar proton pump delta polypeptide (VATD), mRNA	1.94
KIAA0671 gene product (KIAA0671), mRNA	1.93
thioredoxin (TXN) mRNA	1.93
CMP-N-acetylneuraminic acid synthase (LOC55907), mRNA	1.93

Table 3. continued

mRNA; cDNA DKFZp761N0123 (from clone DKFZp761N0123)	1.93
PMEPA1 protein (PMEPA1), mRNA	1.93
brain protein (CG-6) mRNA, partial cds	1.92
PC3-96 mRNA, complete cds	1.92
cDNA FLJ13945 fis, clone Y79AA1000969	1.92
HSPC171 protein (HSPC171), mRNA	1.90
KIAA0171 gene product (KIAA0171), mRNA	1.90
Human ribosomal protein L23-related mRNA, complete cds	1.90
electron-transfer-flavoprotein, alpha polypeptide (glutaric ac	1.89
nuclear phosphoprotein similar to S. cerevisiae PWP1 (PWP1), m	1.88
Hermansky-Pudlak syndrome gene (HPS), mRNA	1.87
mRNA; cDNA DKFZp564L222 (from clone DKFZp564L222)	1.87
prenyl protein protease RCE1 RCE1 RCE1 RCE1 (RCE1), mRNA	1.87
protein phosphatase 2, regulatory subunit B (B56), epsilon iso	1.87
COX17 (yeast) homolog, cytochrome c oxidase assembly protein (	1.87
hypothetical protein (HSPC251), mRNA	1.87
RNA binding motif protein 7 (LOC51120), mRNA	1.85
carcinoembryonic antigen TMzCEA {5' region} [human, hepatoma Li	1.84
brain protein I3 (BRI3), mRNA	1.83
hypothetical protein FLJ10913 (FLJ10913), mRNA	1.83
cDNA: FLJ21949 fis, clone HEP04922	1.83
cDNA: FLJ22670 fis, clone HSI08684	1.83
mRNA; cDNA DKFZp564E122 (from clone DKFZp564E122)	1.82
hypothetical protein FLJ10231 (FLJ10231), mRNA	1.82
cDNA FLJ13622 fis, clone PLACE1010960, weakly similar to ACTIN	1.81
PIX1 mRNA sequence	1.81
POP2 (yeast homolog) (POP2) mRNA	1.81
cDNA: FLJ21941 fis, clone HEP04524	1.81
full length insert cDNA clone ZD92D08	1.81
hypothetical protein FLJ11210 (FLJ11210), mRNA	1.80
TFIIA alpha, p55 (TFIIA), mRNA	1.80
PRO1900 protein (PRO1900), mRNA	1.80
myosin VI (MYO6) mRNA	1.79
iroquois-class homeodomain protein (IRX-2A) mRNA	1.78
proteasome (prosome, macropain) 26S subunit, non-ATPase, 8 (PS	1.78
cDNA: FLJ22664 fis, clone HSI08202	1.77
renal tumor antigen (RAGE), mRNA	1.77
BCL2-like 11 (apoptosis facilitator) (BCL2L11) mRNA	1.76
endozepine-like protein type 2 mutant mRNA, complete cds	1.76
pre-mRNA splicing SR protein rA4 mRNA, partial cds	1.76
amyloid beta (A4) precursor-like protein 2 (APLP2), mRNA.	1.75
mitogen-activated protein kinase kinase 3 (MAP2K3), mRNA	1.75
ubiquitin-conjugating enzyme E2H (homologous to yeast UBC8) (UB	1.75
Human HepG2 3' region cDNA, clone hmd1f06	1.74
syntaxin 18 (STX18), mRNA	1.73

Table 3. continued

mRNA; cDNA DKFZp761E1824 (from clone DKFZp761E1824); partial cd	1.73
acetyl-CoA synthetase (LOC55902), mRNA	1.72
hypothetical protein FLJ10867 (FLJ10867), mRNA	1.72
mRNA for KIAA0582 protein, partial cds	1.72
cDNA FLJ12503 fis, clone NT2RM2001695, highly similar to clon	1.72
mRNA for KIAA0882 protein, partial cds	1.71
full length insert cDNA clone YR23G01	1.70
peflin (PEF), mRNA	1.70
phosphatidylinositol 4-kinase, catalytic, beta polypeptide (PI	1.70
proteasome (prosome, macropain) subunit, alpha type, 2 (PSMA2)	1.70
troponin I, cardiac (TNNI3) mRNA	1.69
15 kDa selenoprotein (SEP15) mRNA	1.68
BTG family, member 2 (BTG2), mRNA	1.68
cDNA: FLJ21901 fis, clone HEP03496	1.68
Human mRNA for KIAA0370 gene, partial cds	1.68
endothelial cell differentiation gene 7; calcium-mobilizing ly	1.68
hypothetical protein FLJ20533 (FLJ20533), mRNA	1.68
D123 gene product (D123) mRNA	1.67
predicted osteoblast protein (GS3786), mRNA	1.67
KIAA1100 protein (KIAA1100), mRNA	1.67
H.sapiens PROS-27 mRNA	1.67
protein-L-isoaspartate (D-aspartate) O-methyltransferase (PCMT1	1.66
KIAA0156 gene product (KIAA0156), mRNA	1.66
KIAA0625 protein (KIAA0625), mRNA	1.65
leucine aminopeptidase (LOC51056), mRNA	1.65
arsenate resistance protein ARS2 (ARS2), mRNA	1.64
Human tumor necrosis factor type 2 receptor associated protein	1.63
CGI-94 protein (LOC51118), mRNA	1.62
protein x 0001 (LOC51185), mRNA	1.62
mRNA for KIAA1193 protein, partial cds	1.61
cDNA: FLJ21449 fis, clone COL04483, highly similar to AF010235	1.61
mRNA for KIAA1440 protein, partial cds	1.60
cDNA FLJ13016 fis, clone NT2RP3000624, moderately similar to R	1.59
CGI-115 protein (LOC51018), mRNA	1.59
sorting nexin 3 (SNX3) mRNA	1.59
B-cell CLL/lymphoma 3 (BCL3) mRNA	1.59
proteasome (prosome, macropain) 26S subunit, non-ATPase, 3 (PS	1.58
clone 23781 mRNA sequence	1.58
dynactin p62 subunit (LOC51164), mRNA.	1.58
RNA polymerase I transcription factor RRN3 (RRN3), mRNA	1.56
hypothetical protein FLJ10474 (FLJ10474), mRNA	1.54
mRNA for tMDC II, isoform [a]	1.54
DNA segment on chromosome 19 (unique) 1177 expressed sequence	1.54
Human mRNA for tubulin alpha-1, 5'UTR (sequence from the 5'cap	1.53
cDNA FLJ11684 fis, clone HEMBA1004909	1.53

Table 3. continued

ADP-ribosylation factor 1 (ARF1), mRNA	1.52
hepatocellular carcinoma-associated antigen 66 (HCA66), mRNA	1.52
E4F transcription factor 1 (E4F1) mRNA	1.51
clone HQ0477 PRO0477p (LOC51204), mRNA	1.51
CGI-44 protein mRNA, complete cds	1.51
chloride intracellular channel 1 (CLIC1), mRNA	1.51
ELK3, ETS-domain protein (SRF accessory protein 2) (ELK3), mRN	1.50
cDNA: FLJ23420 fis, clone HEP22352	1.50
homeo box D9 (HOXD9), mRNA	1.50

Table 4. Genes significantly (p<0.05) down-regulated following treatment with 20μM PGJ2 for 24h. The genes are listed in descending order of fold-decrease over control levels. The fold-decrease is highlighted in different colors following the legend shown below.

4.99-4.0	3.99-3.0	2.99-2.0	1.99-1.5
		YELLOW	WHITE

Gene Name	Fold
Rec8p, a meiotic recombination and sister chromatid cohesion p	
retinol-binding protein 1, cellular (RBP1), mRNA	
dopa decarboxylase (aromatic L-amino acid decarboxylase) (DDC)	
potassium voltage-gated channel, KQT-like subfamily, member 2	
delta-like homolog (Drosophila) (DLK1), mRNA	
cysteine-rich protein 2 (CRIP2) mRNA	
ATP synthase, H+ transporting, mitochondrial F1 complex, delta	
transforming growth factor, beta-induced, 68kD (TGFBI) mRNA	
replication factor C (activator 1) 3 (38kD) (RFC3) mRNA	
NPDC1-like protein (NPDC1) mRNA, complete cds	
phosphoglucomutase 1 (PGM1) mRNA	
chromogranin B (secretogranin 1) (CHGB) mRNA	
cDNA FLJ20750 fis, clone HEP05174	
hypothetical protein FLJ10851 (FLJ10851), mRNA	
PDZ-binding kinase; T-cell originated protein kinase (TOPK), m	
cDNA FLJ11748 fis, clone HEMBA1005552	
multiple myeloma oncogene 1 (MUM1) mRNA	
NADH dehydrogenase (ubiquinone) flavoprotein 1 (51kD) (NDUFV1)	2.98
prothymosin a14 (LOC51685), mRNA	2.97
geminin (LOC51053), mRNA	2.93
prothymosin, alpha (gene sequence 28) (PTMA), mRNA.	2.91
cDNA: FLJ22749 fis, clone KAIA0458	2.87
receptor (calcitonin) activity modifying protein 1 (RAMP1), mR	2.79
Human diazepam binding inhibitor (DBI) mRNA, complete cds	2.74
Human HepG2 3' region MboI cDNA, clone hmd1c12m3	2.74
immunoglobulin superfamily, member 4 (IGSF4), mRNA	2.74
phosphate cytidylyltransferase 2, ethanolamine (PCYT2) mRNA	2.74
mRNA for KIAA1367 protein, partial cds	2.72
ATP-binding cassette, sub-family A (ABC1), member 3 (ABCA3), m	2.71

Table 4. continued

Kruppel-like factor 4 (gut) (KLF4), mRNA	2.71
epithelial protein lost in neoplasm beta (EPLIN), mRNA	2.67
collapsin response mediator protein 1 (CRMP1) mRNA	2.66
polymerase (DNA directed), delta 2, regulatory subunit (50kD)	2.65
deoxyhypusine synthase (DHPS), transcript variant 1, mRNA	2.64
deoxythymidylate kinase (DTYMK), mRNA	2.63
SRp25 nuclear protein (LOC51329), mRNA	2.61
protein phosphatase 1G (formerly 2C), magnesium-dependent, gam	2.60
histone macroH2A1.2 (H2AF12M) mRNA	2.57
CGI-69 protein (LOC51629), mRNA	2.52
clone CDABP0045 mRNA sequence	2.49
8-oxoguanine DNA glycosylase (OGG1), transcript variant 1b, nu	2.48
lysosomal acid lipase {splice junction 72-base deletion} [human	2.46
serine protease, umbilical endothelium (SPUVE), mRNA	2.42
Human cAMP-dependent protein kinase regulatory subunit RI-beta	2.38
Replication protein A complex 34 kd subunit homolog Rpa4 (HSU2	2.37
hypothetical protein FLJ10316 (FLJ10316), mRNA	2.36
Human mRNA for helix-loop-helix protein 1R21, 5'UTR (sequence f	2.36
cDNA FLJ11688 fis, clone HEMBA1004973, weakly similar to ZINC-	2.36
dihydrolipoamide branched chain transacylase (E2 component of	2.35
heterogeneous nuclear ribonucleoprotein D-like (HNRPDL) mRNA	2.30
transcription factor AP-2 beta (activating enhancer-binding pro	2.27
NADH dehydrogenase (ubiquinone) 1 alpha subcomplex, 3 (9kD, B9	2.26
multifunctional polypeptide similar to SAICAR synthetase and AI	2.25
Glucosidase I (GCS1), mRNA	2.24
Human mRNA for KIAA0084 gene, partial cds	2.23
crystallin, beta B2 (CRYBB2), mRNA	2.22
Human insulin-like growth factor binding protein 4 (IGFBP4) mRN	2.20
hypothetical protein PRO2007 (PRO2007), mRNA	2.19
hypothetical protein FLJ10335 (FLJ10335), mRNA	2.18
breast cancer 1, early onset (BRCA1), transcript variant BRCA1	2.16
fibulin 1 (FBLN1), splice variant B, mRNA	2.14
ribosomal protein S19 (RPS19) mRNA	2.14
mRNA; cDNA DKFZp434C245 (from clone DKFZp434C245); partial cds	2.13
glioblastoma amplified sequence (GBAS) mRNA	2.12
chondroitin-4-sulfotransferase (C4ST gene) (HSA269537), mRNA	2.11
hypothetical protein (LOC51257), mRNA	2.09
neurotrophin 3 (NTF3), mRNA	2.08
isocitrate dehydrogenase 3 (NAD+) gamma (IDH3G) mRNA	2.06
hypothetical protein FLJ20160 (FLJ20160), mRNA	2.03
platelet/endothelial cell adhesion molecule (CD31 antigen) (PEC	2.03
cDNA FLJ20403 fis, clone KAT01539	2.03
Human insulin-like growth factor binding protein 2 (IGFBP2) mRN	2.02
glutaminyl-tRNA synthetase (QARS), mRNA	2.01
Human HepG2 partial cDNA, clone hmd2c09m5	2.00

Table 4. continued

NADH dehydrogenase (ubiquinone) 1 beta subcomplex, 10 (22kD, P	1.97
carbonyl reductase (LOC51181), mRNA	1.96
CGI-119 protein (LOC51643), mRNA	1.96
mRNA full length insert cDNA clone EUROIMAGE 383179	1.95
epimorphin (syntaxin 2) (EPIM), mRNA	1.94
Human G2 protein mRNA, partial cds	1.94
melanoma-associated antigen MG50 mRNA, partial cds	1.94
Human myosin light chain 3 non-muscle (MLC3nm) mRNA, complete c	1.93
cDNA: FLJ22347 fis, clone HRC06188	1.92
succinate dehydrogenase complex, subunit A, flavoprotein (Fp)	1.90
quinolinate phosphoribosyltransferase (nicotinate-nucleotide p	1.89
8D6 antigen (LOC51293), mRNA	1.88
Human mRNA for KIAA0365 gene, partial cds	1.88
mRNA full length insert cDNA clone EUROIMAGE 2004433	1.88
hypothetical protein FLJ11112 (FLJ11112), mRNA	1.87
H.sapiens P1-Cdc21 mRNA	1.87
Human partial mRNA for homeodomain protein	1.85
hypothetical protein (H17), mRNA	1.85
hypothetical protein FLJ10079 (FLJ10079), mRNA	1.82
mRNA for KIAA0828 protein, partial cds	1.81
cDNA FLJ11302 fis, clone PLACE1009971	1.81
hypothetical protein FLJ20643 (FLJ20643), mRNA	1.80
imidazoline receptor candidate (I-1), mRNA	1.79
aminoacylase 1 (ACY1), mRNA	1.78
cDNA: FLJ22207 fis, clone HRC01454	1.76
site-1 protease (subtilisin-like, sterol-regulated, cleaves st	1.75
protein tyrosine phosphatase, receptor type, alpha polypeptide	1.74
cDNA: FLJ20917 fis, clone ADSE00750	1.74
nuclear transport factor 2 (placental protein 15) (PP15) mRNA	1.71
EphB3 (EPHB3) mRNA	1.71
cDNA: FLJ23602 fis, clone LNG15735	1.70
GLUT4 enhancer factor mRNA, partial cds	1.70
esterase D mRNA, complete cds	1.68
uroporphyrinogen III synthase (congenital erythropoietic porphy	1.68
mRNA for KIAA0922 protein, partial cds	1.67
mRNA; cDNA DKFZp547D065 (from clone DKFZp547D065)	1.67
lectin, galactoside-binding, soluble, 1 (galectin 1) (LGALS1)	1.67
NME7 (NME7), mRNA	1.66
glutathione peroxidase 4 (phospholipid hydroperoxidase) (GPX4)	1.65
mRNA; cDNA DKFZp434P0111 (from clone DKFZp434P0111); partial cd	1.65
creatine kinase, brain (CKB) mRNA	1.65
MJ0495-like protein SelB mRNA, partial cds	1.64
coatomer protein complex, subunit epsilon (COPE), mRNA	1.64
insulin-like growth factor binding protein 7 (IGFBP7) mRNA	1.63
hypothetical protein FLJ10512 (FLJ10512), mRNA	1.63

Table 4. continued

ribosomal protein L30 (RPL30) mRNA	1.63
testis-specific poly(A)-binding protein (PABP) mRNA, complete	1.63
collagen, type V, alpha 2 (COL5A2) mRNA	1.62
CGI-53 protein (LOC51098), mRNA	1.62
adaptor-related protein complex 3, sigma 1 subunit (AP3S1), mR	1.61
mRNA; cDNA DKFZp761C029 (from clone DKFZp761C029); partial cds	1.60
low density lipoprotein receptor-related protein 3 (LRP3) mRNA	1.60
cytidine deaminase (CDA) mRNA, complete cds	1.59
mRNA for KIAA1139 protein, partial cds	1.59
apolipoprotein H (beta-2-glycoprotein I) (APOH) mRNA	1.59
protease, serine, 11 (IGF binding) (PRSS11) mRNA	1.57
histidine triad nucleotide-binding protein (HINT) mRNA	1.57
PR-domain-containing protein 16 (PRDM16) mRNA, complete cds	1.57
cDNA: FLJ21832 fis, clone HEP01571	1.56
zinc finger protein (ZNF-U69274), mRNA	1.56
NADH dehydrogenase (ubiquinone) 1 beta subcomplex, 7 (18kD, B1	1.56
full length insert cDNA clone ZD77G04	1.56
HOX C6=class I homeodomain {fragment M13, homeodomain} [human,	1.56
cDNA FLJ12736 fis, clone NT2RP2000327	1.54
hnRNP 2H9B mRNA, complete cds	1.54
thioredoxin peroxidase (antioxidant enzyme) (AOE372), mRNA	1.54
CD20-like precusor mRNA, complete cds	1.54
sec22 homolog (SEC22A), mRNA	1.53
ets variant gene 1 (ETV1) mRNA	1.53
Human HepG2 3' region MboI cDNA, clone hmd6h07m3	1.53
protein phosphatase 2, regulatory subunit B (B56), gamma isofo	1.52
HGF activator (HGFAC) mRNA	1.52
cDNA FLJ11379 fis, clone HEMBA1000469	1.51
SWI/SNF related, matrix associated, actin dependent regulator	1.51
hypothetical protein FLJ10814 (FLJ10814), mRNA	1.51
hypothetical protein FLJ20315 (FLJ20315), mRNA	1.51
mRNA for KIAA0919 protein, partial cds	1.50

Table 5. Functional classification of the genes that are significantly ($p<0.05$) up-regulated by at least 1.5-fold following treatment for 24h with 20μM PGJ2

Class	**Up-regulated Genes**
	Apoptosis regulator
Apoptosis regulator	BCL2-like 11 (apoptosis facilitator) (BCL2L11) mRNA
	Cell communication
Cell communication	Human tumor necrosis factor type 2 receptor associated protein intercellular adhesion molecule 5, telencephalin (ICAM5), mRNA death-associated protein kinase-related 1 (DRAK1) mRNA ATPase, H+ transporting, lysosomal (vacuolar proton pump) 9kD growth factor receptor-bound protein 10 (GRB10) mRNA Human heart mRNA for heat shock protein 90, partial cds heat shock protein (hsp110 family) (APG-1), mRNA heat shock 70kD protein 6 (HSP70B') (HSPA6) mRNA
	Enzyme
Enzyme	RNA polymerase I transcription factor RRN3 (RRN3), mRNA proteasome (prosome, macropain) 26S subunit, non-ATPase, 3 (PS protein-L-isoaspartate (D-aspartate) O-methyltransferase (PCMT1 mitogen-activated protein kinase kinase 3 (MAP2K3), mRNA ubiquitin-conjugating enzyme E2H (homologous to yeast UBC8) (UB proteasome (prosome, macropain) 26S subunit, non-ATPase, 8 (PS COX17 (yeast) homolog, cytochrome c oxidase assembly protein protein phosphatase 2, regulatory subunit B (B56), epsilon iso prenyl protein protease RCE1 RCE1 RCE1 RCE1 (RCE1), mRNA CMP-N-acetylneuraminic acid synthase (LOC55907), mRNA beta-1,3-N-acetylglucosaminyltransferase (BETA3GNT), mRNA serine palmitoyltransferase, long chain base subunit 2 (SPTLC2 oxidase (cytochrome c) assembly 1-like (OXA1L), mRNA serine/threonine kinase 12 (STK12), mRNA protein tyrosine phosphatase, non-receptor type 3 (PTPN3) mRNA crystallin, zeta (quinone reductase) (CRYZ) mRNA mRNA for methyltransferase-like protein 1 protein phosphatase 2 (formerly 2A), catalytic subunit, beta i aspartate beta-hydroxylase (ASPH) mRNA protein phosphatase 4 (formerly X), catalytic subunit (PPP4C) mitogen-activated protein kinase kinase kinase 11 (MAP3K11), m inorganic pyrophosphatase 2 (PPA2) mRNA, complete cds, nuclear ubiquitin specific protease 16 (USP16) mRNA proteasome (prosome, macropain) 26S subunit, non-ATPase, 1 (PS receptor-interacting serine-threonine kinase 2 (RIPK2) mRNA glycerol kinase deficiency (GK) mRNA ATPase, H+ transporting, lysosomal (vacuolar proton pump) 9kD cathepsin D (lysosomal aspartyl protease) (CTSD) mRNA protease, serine, 15 (PRSS15), mRNA vacuolar H(+)-ATPase subunit (ATP6GL) mRNA arylacetamide deacetylase (esterase) (AADAC) mRNA NAD(P)H menadione oxidoreductase 1, dioxin-inducible (NMOR1) m serine/threonine protein kinase MASK (LOC51765), mRNA proteasome (prosome, macropain) 26S subunit, ATPase, 5 (PSMC5)

Table 5. continued

	Extracellular
Extracellular	matrix metalloproteinase 1 (interstitial collagenase) (MMP1) mR
	Growth factor
Growth factor	growth factor receptor-bound protein 10 (GRB10) mRNA
	Heat shock
Heat shock	Human heart mRNA for heat shock protein 90, partial cds heat shock protein (hsp110 family) (APG-1), mRNA heat shock 70kD protein 6 (HSP70B') (HSPA6) mRNA
	Immune-related
Immune-related	immunoglobulin mu binding protein 2 (IGHMBP2) mRNA paired immunoglobulin-like receptor alpha (PILR(ALPHA)), mRNA
	Interleukin
Interleukin	*NONE*
	Intracellular
Intracellular	dynactin p62 subunit (LOC51164), mRNA. troponin I, cardiac (TNNI3) mRNA myosin VI (MYO6) mRNA cDNA FLJ13622 fis, clone PLACE1010960, weakly similar to ACTIN COX17 (yeast) homolog, cytochrome c oxidase assembly protein (nuclear phosphoprotein similar to S. cerevisiae PWP1 (PWP1), m vacuolar proton pump delta polypeptide (VATD), mRNA golgi autoantigen, golgin subfamily a, 4 (GOLGA4), mRNA tuftelin-interacting protein (TIP39), mRNA oxidase (cytochrome c) assembly 1-like (OXA1L), mRNA translocase of outer mitochondrial membrane 70 (yeast) homolog myosin-binding protein C, slow-type (MYBPC1) mRNA nuclear domain 10 protein (NDP52) mRNA golgi autoantigen, golgin subfamily a, 3 (GOLGA3) mRNA TTF-I interacting peptide 20 mRNA, partial cds inorganic pyrophosphatase 2 (PPA2) mRNA, complete cds, nuclear receptor-interacting serine-threonine kinase 2 (RIPK2) mRNA ATPase, H+ transporting, lysosomal (vacuolar proton pump) 9kD cathepsin D (lysosomal aspartyl protease) (CTSD) mRNA microtubule-associated proteins 1A/1B light chain 3 mRNA, comp vacuolar H(+)-ATPase subunit (ATP6GL) mRNA BCL2/adenovirus E1B 19kD-interacting protein 3 (BNIP3), nuclea
	Microtubular Dynamics
Microtubular Dynamics	dynactin p62 subunit (LOC51164), mRNA. microtubule-associated proteins 1A/1B light chain 3 mRNA, comp
	Nucleic acid binding
Nucleic acid binding	E4F transcription factor 1 (E4F1) mRNA RNA polymerase I transcription factor RRN3 (RRN3), mRNA RNA binding motif protein 7 (LOC51120), mRNA
	Proteasome

Table 5 continued

Proteasome	proteasome (prosome, macropain) 26S subunit, non-ATPase, 3 (PS proteasome (prosome, macropain) subunit, alpha type, 2 (PSMA2) proteasome (prosome, macropain) 26S subunit, non-ATPase, 8 (PS proteasome (prosome, macropain) subunit, beta type, 4 (PSMB4) proteasome (prosome, macropain) subunit, beta type, 3 (PSMB3), proteasome (prosome, macropain) 26S subunit, non-ATPase, 1 (PS proteasome (prosome, macropain) subunit, alpha type, 5 (PSMA5) proteasome (prosome, macropain) subunit, beta type, 2 (PSMB2), proteasome (prosome, macropain) subunit, beta type, 7 (PSMB7) proteasome (prosome, macropain) 26S subunit, ATPase, 5 (PSMC5)
	Signal transducer
Signal transducer	ephrin-B2 (EFNB2) mRNA parathyroid hormone-like hormone (PTHLH) mRNA mutS (E. coli) homolog 3 (MSH3) mRNA growth factor receptor-bound protein 10 (GRB10) mRNA
	Signal transduction
Signal transduction	DNA segment on chromosome 19 (unique) 1177 expressed sequence carcinoembryonic antigen TMzCEA {5' region} [human, hepatoma Li kappa B-ras 1 (LOC57083), mRNA tuftelin-interacting protein (TIP39), mRNA serine/threonine kinase 12 (STK12), mRNA protein tyrosine phosphatase, non-receptor type 3 (PTPN3) mRNA spermatogenesis associated PD1 (KIAA0757) mRNA inhibitor of kappa light polypeptide gene enhancer in B-cells, receptor-interacting serine-threonine kinase 2 (RIPK2) mRNA prion protein (p27-30) (Creutzfeld-Jakob disease, Gerstmann-St Tax1 (human T-cell leukemia virus type I) binding protein 1 (T calcium channel, voltage-dependent, L type, alpha 1B subunit (BCL2/adenovirus E1B 19kD-interacting protein 3 (BNIP3), nuclea serine/threonine protein kinase MASK (LOC51765), mRNA
	Structural proteins
Structural proteins	amyloid beta (A4) precursor-like protein 2 (APLP2), mRNA. matrix metalloproteinase 1 (interstitial collagenase) (MMP1) mR
	Transcription
Transcription	NONE
	Transport
Transport	ATPase, H+ transporting, lysosomal (vacuolar proton pump) 9kD

Table 5. continued

	Ubiquitin
Ubiquitin	ubiquitin-conjugating enzyme E2H (homologous to yeast UBC8) (UB ubiquitin fusion degradation 1-like (UFD1L) mRNA ubiquitin specific protease 16 (USP16) mRNA Human ubiquitin mRNA, complete cds

Table 6. Functional classification of the genes that are significantly ($p<0.05$) down-regulated by at least 1.5-fold following treatment for 24h with 20μM PGJ2

Class	Down-regulated Genes
	Apoptosis regulator
Apoptosis regulator	NONE
	Cell communacation
Cell communacation	ATP synthase, H+ transporting, mitochondrial F1 complex, delta transforming growth factor, beta-induced, 68kD (TGFBI) mRNA Human insulin-like growth factor binding protein 4 (IGFBP4) mRN platelet/endothelial cell adhesion molecule (CD31 antigen) (PEC Human insulin-like growth factor binding protein 2 (IGFBP2) mRN nuclear transport factor 2 (placental protein 15) (PP15) mRNA insulin-like growth factor binding protein 7 (IGFBP7) mRNA
	Energy
Enzyme	dopa decarboxylase (aromatic L-amino acid decarboxylase) (DDC) ATP synthase, H+ transporting, mitochondrial F1 complex, delta phosphoglucomutase 1 (PGM1) mRNA NADH dehydrogenase (ubiquinone) flavoprotein 1 (51kD) (NDUFV1) phosphate cytidylyltransferase 2, ethanolamine (PCYT2) mRNA polymerase (DNA directed), delta 2, regulatory subunit (50kD) deoxyhypusine synthase (DHPS), transcript variant 1, mRNA deoxythymidylate kinase (DTYMK), mRNA protein phosphatase 1G (formerly 2C), magnesium-dependent, gam serine protease, umbilical endothelium (SPUVE), mRNA Human cAMP-dependent protein kinase regulatory subunit RI-beta NADH dehydrogenase (ubiquinone) 1 alpha subcomplex, 3 (9kD, B9 chondroitin-4-sulfotransferase (C4ST gene) (HSA269537), mRNA isocitrate dehydrogenase 3 (NAD+) gamma (IDH3G) mRNA NADH dehydrogenase (ubiquinone) 1 beta subcomplex, 10 (22kD, P carbonyl reductase (LOC51181), mRNA succinate dehydrogenase complex, subunit A, flavoprotein (Fp) quinolinate phosphoribosyltransferase (nicotinate-nucleotide p site-1 protease (subtilisin-like, sterol-regulated, cleaves st protein tyrosine phosphatase, receptor type, alpha polypeptide esterase D mRNA, complete cds uroporphyrinogen III synthase (congenital erythropoietic porphy glutathione peroxidase 4 (phospholipid hydroperoxidase) (GPX4) protease, serine, 11 (IGF binding) (PRSS11) mRNA NADH dehydrogenase (ubiquinone) 1 beta subcomplex, 7 (18kD, B1 thioredoxin peroxidase (antioxidant enzyme) (AOE372), mRNA protein phosphatase 2, regulatory subunit B (B56), gamma isofo
	Extracellular
Extracellular	collagen, type V, alpha 2 (COL5A2) mRNA SWI/SNF related, matrix associated, actin dependent regulator

Table 6. continued

	Growth factor
Growth factor	transforming growth factor, beta-induced, 68kD (TGFBI) mRNA Human insulin-like growth factor binding protein 4 (IGFBP4) mRN Human insulin-like growth factor binding protein 2 (IGFBP2) mRN insulin-like growth factor binding protein 7 (IGFBP7) mRNA
	Heat shock
Heat shock	NONE
	Immune-related
Immune-related	immunoglobulin superfamily, member 4 (IGSF4), mRNA
	Interleukin
Interleukin	interleukin 15 receptor, alpha (IL15RA) mRNA
	Intracellular
Intracellular	Rec8p, a meiotic recombination and sister chromatid cohesion p ATP synthase, H+ transporting, mitochondrial F1 complex, delta SRp25 nuclear protein (LOC51329), mRNA lysosomal acid lipase {splice junction 72-base deletion} [human heterogeneous nuclear ribonucleoprotein D-like (HNRPDL) mRNA Human myosin light chain 3 non-muscle (MLC3nm) mRNA, complete c nuclear transport factor 2 (placental protein 15) (PP15) mRNA coatomer protein complex, subunit epsilon (COPE), mRNA SWI/SNF related, matrix associated, actin dependent regulator
	Microtubular Dynamics
Microtubular Dynamics	NONE
	Nucleic acid binding
Nucleic acid binding	heterogeneous nuclear ribonucleoprotein D-like (HNRPDL) mRNA transcription factor AP-2 beta (activating enhancer-binding pro
	Proteasome
Proteasome	NONE
	Signal transducer
Signal transducer	transforming growth factor, beta-induced, 68kD (TGFBI) mRNA Human insulin-like growth factor binding protein 4 (IGFBP4) mRN neurotrophin 3 (NTF3), mRNA platelet/endothelial cell adhesion molecule (CD31 antigen) (PEC Human insulin-like growth factor binding protein 2 (IGFBP2) mRN insulin-like growth factor binding protein 7 (IGFBP7) mRNA HGF activator (HGFAC) mRNA
	Signal transduction

Table 6. continued

Signal transduction	potassium voltage-gated channel, KQT-like subfamily, member 2 protein tyrosine phosphatase, receptor type, alpha polypeptide
	Structural proteins
Structural proteins	SWI/SNF related, matrix associated, actin dependent regulator
	Transcription
Transcription	transcription factor AP-2 beta (activating enhancer-binding pro
	Transport
Transport	ATP synthase, H+ transporting, mitochondrial F1 complex, delta nuclear transport factor 2 (placental protein 15) (PP15) mRNA
	Ubiquitin
Ubiquitin	NONE

Table 7. Altered protein expression in human neuroblastoma SK-N-SH cells upon treatment with PGJ2

SPOT #	Control	PGJ2-treated	FOLD-INCREASE
1	1023	24849	24.29
2	4134	22006	5.32
3	6247	10687	1.71
4	4203	24513	5.83
5	3244	35659	10.99
6	23011	21390	0.93
7	10241	52320	5.11
8	854	31679	37.09
9	897	30911	34.46

Protein spots 1 through 9 correspond to proteins whose expression was increased by treatment with 20μM PGJ2 for 24h. Numbers in the two middle columns correspond to the intensity of the spots in the respective two-dimensional gel electrophoresis Coomassie blue stained gels shown in Figure 12. Semi-quantitative analysis of the intensity of each spot was determined by image analysis with the ImagePC program from NIH as described (Pereira et al., 1992).

Chapter VI

Reference List

1. Araki E, Forster C, Dubinsky JM, Ross ME, Iadecola C (2001) Cyclooxygenase-2 inhibitor ns-398 protects neuronal cultures from lipopolysaccharide-induced neurotoxicity. Stroke 32: 2370-2375.

2. Arnold J, Dawson S, Fergusson J, Lowe J, Landon M, Mayer RJ (1998) Ubiquitin and its role in neurodegeneration. Prog Brain Res 117: 23-34.

3. Arrasate M, Mitra S, Schweitzer ES, Segal MR, Finkbeiner S (2004) Inclusion body formation reduces levels of mutant huntingtin and the risk of neuronal death. Nature 431: 805-810.

4. Bates G (2003) Huntingtin aggregation and toxicity in Huntington's disease. Lancet 361: 1642-1644.

5. Beal R, Deveraux Q, Xia G, Rechsteiner M, Pickart C (1996) Surface hydrophobic residues of multiubiquitin chains essential for proteolytic targeting. Proc Natl Acad Sci U S A 93: 861-866.

6. Bence NF, Sampat RM, Kopito RR (2001) Impairment of the ubiquitin-proteasome system by protein aggregation. Science 292: 1552-1555.

7. Berke SJ, Paulson HL (2003) Protein aggregation and the ubiquitin proteasome pathway: gaining the UPPer hand on neurodegeneration. Curr Opin Genet Dev 13: 253-261.

8. Bertolaet BL, Clarke DJ, Wolff M, Watson MH, Henze M, Divita G, Reed SI (2001) UBA domains of DNA damage-inducible proteins interact with ubiquitin. Nat Struct Biol 8: 417-422.

9. Boes B, Hengel H, Ruppert T, Multhaup G, Koszinowski UH, Kloetzel PM (1994) Interferon gamma stimulation modulates the proteolytic activity and cleavage site preference of 20S mouse proteasomes. J Exp Med 179: 901-909.

10. Braun BC, Glickman M, Kraft R, Dahlmann B, Kloetzel PM, Finley D, Schmidt M (1999) The base of the

proteasome regulatory particle exhibits chaperone-like activity [In Process Citation]. Nat Cell Biol 1: 221-226.

11. Choi J, Levey AI, Weintraub ST, Rees HD, Gearing M, Chin LS, Li L (2004) Oxidative modifications and down-regulation of ubiquitin carboxyl-terminal hydrolase L1 associated with idiopathic Parkinson's and Alzheimer's diseases. J Biol Chem 279: 13256-13264.

12. Chung CH, Baek SH (1999) Deubiquitinating Enzymes: Their Diversity and Emerging Roles. Biochem Biophys Res Commun 266: 633-640.

13. Cookson MR, Lockhart PJ, McLendon C, O'Farrell C, Schlossmacher M, Farrer MJ (2003) RING finger 1 mutations in Parkin produce altered localization of the protein. Hum Mol Genet 12: 2957-2965.

14. D'Andrea A, Pellman D (1998) Deubiquitinating enzymes: a new class of biological regulators. Crit Rev Biochem Mol Biol 33: 337-352.

15. de Silva R, Lashley T, Gibb G, Hanger D, Hope A, Reid A, Bandopadhyay R, Utton M, Strand C, Jowett T, Khan N, Anderton B, Wood N, Holton J, Revesz T, Lees A (2003) Pathological inclusion bodies in tauopathies contain distinct complements of tau with three or four microtubule-binding repeat domains as demonstrated by new specific monoclonal antibodies. Neuropathol Appl Neurobiol 29: 288-302.

16. DeMartino GN, Slaughter CA (1999) The proteasome, a novel protease regulated by multiple mechanisms. J Biol Chem 274: 22123-22126.

17. Djordjevic VB (2004) Free radicals in cell biology. Int Rev Cytol 237: 57-89.

18. Enenkel C, Lehmann A, Kloetzel PM (1999) GFP-labelling of 26S proteasomes in living yeast: insight into proteasomal functions at the nuclear envelope/rough ER. Mol Biol Rep 26: 131-135.

19. Eucker J, Bangeroth K, Zavrski I, Krebbel H, Zang C, Heider U, Jakob C, Elstner E, Possinger K, Sezer O (2004) Ligands of peroxisome proliferator-activated

receptor gamma induce apoptosis in multiple myeloma. Anticancer Drugs 15: 955-960.

20. Fabunmi RP, Wigley WC, Thomas PJ, DeMartino GN (2000) Activity and Regulation of the Centrosome-associated Proteasome. J Biol Chem 275: 409-413.

21. Ferrer I, Martin B, Castano JG, Lucas JJ, Moreno D, Olive M (2004) Proteasomal expression, induction of immunoproteasome subunits, and local MHC class I presentation in myofibrillar myopathy and inclusion body myositis. J Neuropathol Exp Neurol 63: 484-498.

22. Figueiredo-Pereira ME, Rockwell P (2001) The ubiquitin/proteasome pathway in neurological disorders. In: Role of Proteolysis in the Pathophysiology of Neurodegenerative Diseases (Lajtha A, Banik NL, eds), pp 137-153. New York, N.Y.: Kluwer Academic/Plenum Publishers.

23. Fukushima M (1990) Prostaglandin J2--anti-tumour and anti-viral activities and the mechanisms involved. Eicosanoids 3: 189-199.

24. Furukawa Y, Iseki E, Hino H, Kanai A, Odawara T, Kosaka K (2004a) Ubiquitin and ubiquitin-related proteins in neurons and dendrites of brains of atypical Pick's disease without Pick bodies. Neuropathology 24: 38-45.

25. Furukawa Y, Iseki E, Hino H, Kanai A, Odawara T, Kosaka K (2004b) Ubiquitin and ubiquitin-related proteins in neurons and dendrites of brains of atypical Pick's disease without Pick bodies. Neuropathology 24: 38-45.

26. Gao HM, Liu B, Zhang W, Hong JS (2003) Novel anti-inflammatory therapy for Parkinson's disease. Trends Pharmacol Sci 24: 395-401.

27. Garcia-Mata R, Bebok Z, Sorscher EJ, Sztul ES (1999) Characterization and dynamics of aggresome formation by a cytosolic GFP- chimera. J Cell Biol 146: 1239-1254.

28. Geetha T, Wooten MW (2002) Structure and functional properties of the ubiquitin binding protein p62. FEBS Lett 512: 19-24.

29. Gilroy DW, Colville-Nash PR, Willis D, Chivers J, Paul-Clark MJ, Willoughby DA (1999a) Inducible cyclooxygenase may have anti-inflammatory properties. Nat Med 5: 698-701.

30. Gilroy DW, Colville-Nash PR, Willis D, Chivers J, Paul-Clark MJ, Willoughby DA (1999b) Inducible cyclooxygenase may have anti-inflammatory properties [see comments]. Nat Med 5: 698-701.

31. Gilroy DW, Lawrence T, Perretti M, Rossi AG (2004) Inflammatory resolution: new opportunities for drug discovery. Nat Rev Drug Discov 3: 401-416.

32. Giri S, Rattan R, Singh AK, Singh I (2004) The 15-deoxy-delta12,14-prostaglandin J2 inhibits the inflammatory response in primary rat astrocytes via down-regulating multiple steps in phosphatidylinositol 3-kinase-Akt-NF-kappaB-p300 pathway independent of peroxisome proliferator-activated receptor gamma. J Immunol 173: 5196-5208.

33. Glickman MH, Rubin DM, Coux O, Wefes I, Pfeifer G, Cjeka Z, Baumeister W, Fried VA, Finley D (1998) A subcomplex of the proteasome regulatory particle required for ubiquitin-conjugate degradation and related to the COP9-signalosome and eIF3. Cell 94: 615-623.

34. Groll M, Ditzel L, Lowe J, Stock D, Bochtler M, Bartunik HD, Huber R (1997) Structure of 20S proteasome from yeast at 2.4 A resolution [see comments]. Nature 386: 463-471.

35. Harris SG, Smith RS, Phipps RP (2002) 15-deoxy-Delta 12,14-PGJ2 induces IL-8 production in human T cells by a mitogen-activated protein kinase pathway. J Immunol 168: 1372-1379.

36. Hartmann-Petersen R, Semple CA, Ponting CP, Hendil KB, Gordon C (2003) UBA domain containing proteins in fission yeast. Int J Biochem Cell Biol 35: 629-636.

37. Herschman HR, Reddy ST, Xie W (1997) Function and regulation of prostaglandin synthase-2. Adv Exp Med Biol 407: 61-66.

38. Ho L, Pieroni C, Winger D, Purohit DP, Aisen PS, Pasinetti GM (1999) Regional distribution of cyclooxygenase-2 in the hippocampal formation in Alzheimer's disease. J Neurosci Res 57: 295-303.

39. Hofmann K, Bucher P (1996) The UBA domain: a sequence motif present in multiple enzyme classes of the ubiquitination pathway. Trends Biochem Sci 21: 172-173.

40. Hofmann K, Falquet L (2001) A ubiquitin-interacting motif conserved in components of the proteasomal and lysosomal protein degradation systems. Trends Biochem Sci 26: 347-350.

41. Howatson AF, Fornasier VL (1982) Microfilaments associated with Paget's disease of bone: comparison with nucleocapsids of measles virus and respiratory syncytial virus. Intervirology 18: 150-159.

42. Huang L, Kinnucan E, Wang G, Beaudenon S, Howley PM, Huibregtse JM, Pavletich NP (1999) Structure of an E6AP-UbcH7 complex: insights into ubiquitination by the E2-E3 enzyme cascade. Science 286: 1321-1326.

43. Joazeiro CA, Wing SS, Huang H, Leverson JD, Hunter T, Liu YC (1999) The Tyrosine Kinase Negative Regulator c-Cbl as a RING-Type, E2- Dependent Ubiquitin-Protein Ligase. Science 286: 309-312.

44. Johnston JA, Ward CL, Kopito RR (1998a) Aggresomes: a cellular response to misfolded proteins. J Cell Biol 143: 1883-1898.

45. Johnston JA, Ward CL, Kopito RR (1998b) Aggresomes: a cellular response to misfolded proteins. J Cell Biol 143: 1883-1898.

46. Kaufmann WE, Andreasson KI, Isakson PC, Worley PF (1997) Cyclooxygenases and the central nervous system. Prostaglandins 54: 601-624.

47. Keller JN, Hanni KB, Markesbery WR (2000) Impaired proteasome function in Alzheimer's disease [In Process Citation]. J Neurochem 75: 436-439.

48. Koegl M, Hoppe T, Schlenker S, Ulrich HD, Mayer TU, Jentsch S (1999) A novel ubiquitination factor, E4,

is involved in multiubiquitin chain assembly. Cell 96: 635-644.

49. Kondo M, Oya-Ito T, Kumagai T, Osawa T, Uchida K (2001) Cyclopentenone prostaglandins as potential inducers of intracellular oxidative stress. J Biol Chem 276: 12076-12083.

50. Kondo M, Shibata T, Kumagai T, Osawa T, Shibata N, Kobayashi M, Sasaki S, Iwata M, Noguchi N, Uchida K (2002) 15-Deoxy-Delta(12,14)-prostaglandin J(2): the endogenous electrophile that induces neuronal apoptosis. Proc Natl Acad Sci U S A 99: 7367-7372.

51. Kulkarni SK, Jain NK, Singh A (2000) Cyclooxygenase isoenzymes and newer therapeutic potential for selective COX-2 inhibitors. Methods Find Exp Clin Pharmacol 22: 291-298.

52. Kuusisto E, Salminen A, Alafuzoff I (2001a) Ubiquitin-binding protein p62 is present in neuronal and glial inclusions in human tauopathies and synucleinopathies. Neuroreport 12: 2085-2090.

53. Kuusisto E, Salminen A, Alafuzoff I (2001b) Ubiquitin-binding protein p62 is present in neuronal and glial inclusions in human tauopathies and synucleinopathies. Neuroreport 12: 2085-2090.

54. Kuusisto E, Suuronen T, Salminen A (2001c) Ubiquitin-binding protein p62 expression is induced during apoptosis and proteasomal inhibition in neuronal cells. Biochem Biophys Res Commun 280: 223-228.

55. Kuusisto E, Suuronen T, Salminen A (2001d) Ubiquitin-binding protein p62 expression is induced during apoptosis and proteasomal inhibition in neuronal cells. Biochem Biophys Res Commun 280: 223-228.

56. Laurin N, Brown JP, Morissette J, Raymond V (2002) Recurrent mutation of the gene encoding sequestosome 1 (SQSTM1/p62) in Paget disease of bone. Am J Hum Genet 70: 1582-1588.

57. Lawrence T, Gilroy DW, Colville-Nash PR, Willoughby DA (2001) Possible new role for NF-kappaB in the resolution of inflammation. Nat Med 7: 1291-1297.

58. Lelouard H, Ferrand V, Marguet D, Bania J, Camosseto V, David A, Gatti E, Pierre P (2004) Dendritic cell aggresome-like induced structures are dedicated areas for ubiquitination and storage of newly synthesized defective proteins. J Cell Biol 164: 667-675.

59. Leroy E, Boyer R, Auburger G, Leube B, Ulm G, Mezey E, Harta G, Brownstein MJ, Jonnalagada S, Chernova T, Dehejia A, Lavedan C, Gasser T, Steinbach PJ, Wilkinson KD, Polymeropoulos MH (1998) The ubiquitin pathway in Parkinson's disease [letter]. Nature 395: 451-452.

60. Li Z, Jansen M, Ogburn K, Salvatierra L, Hunter L, Mathew S, Figueiredo-Pereira ME (2004a) Neurotoxic prostaglandin J2 enhances cyclooxygenase-2 expression in neuronal cells through the p38MAPK pathway: a death wish? J Neurosci Res 78: 824-836.

61. Li Z, Melandri F, Berdo I, Jansen M, Hunter L, Wright S, Valbrun D, Figueiredo-Pereira ME (2004b) delta12-Prostaglandin J2 inhibits the ubiquitin hydrolase UCH-L1 and elicits ubiquitin-protein aggregation without proteasome inhibition. Biochem Biophys Res Commun 319: 1171-1180.

62. Liu Y, Fallon L, Lashuel HA, Liu Z, Lansbury PT (2002) The UCH-L1 Gene Encodes Two Opposing Enzymatic Activities that Affect alpha-Synuclein Degradation and Parkinson's Disease Susceptibility. Cell 111: 209-218.

63. Lorick KL, Jensen JP, Fang S, Ong AM, Hatakeyama S, Weissman AM (1999) RING fingers mediate ubiquitin-conjugating enzyme (E2)-dependent ubiquitination. Proc Natl Acad Sci U S A 96: 11364-11369.

64. MacEwan DJ (2002) TNF receptor subtype signalling: differences and cellular consequences. Cell Signal 14: 477-492.

65. Madura K (2002) The ubiquitin-associated (UBA) domain: on the path from prudence to prurience. Cell Cycle 1: 235-244.

66. Manna SK, Mukhopadhyay A, Van NT, Aggarwal BB (1999) Silymarin suppresses TNF-induced activation of NF-

kappa B, c-Jun N-terminal kinase, and apoptosis. J Immunol 163: 6800-6809.

67. Martinez B, Perez-Castillo A, Santos A (2005) The mitochondrial respiratory complex I is a target for 15-deoxy-{Delta}12,14-prostaglandin J2 action. J Lipid Res 46: 736-743.

68. Mattammal MB, Strong R, Lakshmi VM, Chung HD, Stephenson AH (1995) Prostaglandin H synthetase-mediated metabolism of dopamine: implication for Parkinson's disease. J Neurochem 64: 1645-1654.

69. McNaught KS, Olanow CW, Halliwell B, Isacson O, Jenner P (2001) Failure of the ubiquitin-proteasome system in Parkinson's disease. Nat Rev Neurosci 2: 589-594.

70. Meade EA, McIntyre TM, Zimmerman GA, Prescott SM (1999) Peroxisome proliferators enhance cyclooxygenase-2 expression in epithelial cells. J Biol Chem 274: 8328-8334.

71. Mengual E, Arizti P, Rodrigo J, Gimenez-Amaya JM, Castano JG (1996) Immunohistochemical distribution and electron microscopic subcellular localization of the proteasome in the rat CNS. J Neurosci 16: 6331-6341.

72. Mezey E, Dehejia A, Harta G, Papp MI, Polymeropoulos MH, Brownstein MJ (1998) Alpha synuclein in neurodegenerative disorders: murderer or accomplice? [In Process Citation]. Nat Med 4: 755-757.

73. Mosmann T (1983) Rapid colorimetric assay for cellular growth and survival: application to proliferation and cytotoxicity assays. J Immunol Methods 65: 55-63.

74. Mrak RE, Landreth GE (2004) PPARgamma, neuroinflammation, and disease. J Neuroinflammation 1: 5.

75. Murakami Y, Matsufuji S, Kameji T, Hayashi S, Igarashi K, Tamura T, Tanaka K, Ichihara A (1992) Ornithine decarboxylase is degraded by the 26S proteasome without ubiquitination. Nature 360: 597-599.

76. Nagaoka U, Kim K, Jana NR, Doi H, Maruyama M, Mitsui K, Oyama F, Nukina N (2004b) Increased expression of p62 in expanded polyglutamine-expressing cells and its association with polyglutamine inclusions. J Neurochem 91: 57-68.

77. Nagaoka U, Kim K, Jana NR, Doi H, Maruyama M, Mitsui K, Oyama F, Nukina N (2004a) Increased expression of p62 in expanded polyglutamine-expressing cells and its association with polyglutamine inclusions. J Neurochem 91: 57-68.

78. Nakamura T, Tanaka T, Takagi H, Sato M (1998) Cloning and heterogeneous in vivo expression of Tat binding protein-1 (TBP-1) in the mouse. Biochim Biophys Acta 1399: 93-100.

79. Nakano T, Nakaso K, Nakashima K, Ohama E (2004a) Expression of ubiquitin-binding protein p62 in ubiquitin-immunoreactive intraneuronal inclusions in amyotrophic lateral sclerosis with dementia: analysis of five autopsy cases with broad clinicopathological spectrum. Acta Neuropathol (Berl) 107: 359-364.

80. Nakano T, Nakaso K, Nakashima K, Ohama E (2004b) Expression of ubiquitin-binding protein p62 in ubiquitin-immunoreactive intraneuronal inclusions in amyotrophic lateral sclerosis with dementia: analysis of five autopsy cases with broad clinicopathological spectrum. Acta Neuropathol (Berl) 107: 359-364.

81. Nakaso K, Yoshimoto Y, Nakano T, Takeshima T, Fukuhara Y, Yasui K, Araga S, Yanagawa T, Ishii T, Nakashima K (2004b) Transcriptional activation of p62/A170/ZIP during the formation of the aggregates: possible mechanisms and the role in Lewy body formation in Parkinson's disease. Brain Res 1012: 42-51.

82. Nakaso K, Yoshimoto Y, Nakano T, Takeshima T, Fukuhara Y, Yasui K, Araga S, Yanagawa T, Ishii T, Nakashima K (2004a) Transcriptional activation of p62/A170/ZIP during the formation of the aggregates: possible mechanisms and the role in Lewy body formation in Parkinson's disease. Brain Res 1012: 42-51.

83. Narumiya S, Fukushima M (1986) Site and mechanism of growth inhibition by prostaglandins. I. Active transport and intracellular accumulation of cyclopentenone prostaglandins, a reaction leading to growth inhibition. J Pharmacol Exp Ther 239: 500-505.

84. Noyori R, Suzuki M (1993) Organic synthesis of prostaglandins: advancing biology. Science 259: 44-45.

85. O'Farrell PH (1975) High resolution two-dimensional electrophoresis of proteins. J Biol Chem 250: 4007-4021.

86. Offenbacher S, Odle BM, Van Dyke TE (1986) The use of crevicular fluid prostaglandin E2 levels as a predictor of periodontal attachment loss. J Periodontal Res 21: 101-112.

87. Orlowski M, Cardozo C, Michaud C (1993) Evidence for the presence of five distinct proteolytic components in the pituitary multicatalytic proteinase complex. Properties of two components cleaving bonds on the carboxyl side of branched chain and small neutral amino acids. Biochemistry 32: 1563-1572.

88. Orr HT (2004) Neurodegenerative disease: Neuron protection agency. Nature 431: 747-748.

89. Palmer A, Rivett AJ, Thomson S, Hendil KB, Butcher GW, Fuertes G, Knecht E (1996) Subpopulations of proteasomes in rat liver nuclei, microsomes and cytosol. Biochem J 316 (Pt 2): 401-407.

90. Park I, Chung J, Walsh CT, Yun Y, Strominger JL, Shin J (1995a) Phosphotyrosine-independent binding of a 62-kDa protein to the src homology 2 (SH2) domain of p56lck and its regulation by phosphorylation of Ser-59 in the lck unique N-terminal region. Proc Natl Acad Sci U S A 92: 12338-12342.

91. Park I, Chung J, Walsh CT, Yun Y, Strominger JL, Shin J (1995b) Phosphotyrosine-independent binding of a 62-kDa protein to the src homology 2 (SH2) domain of p56lck and its regulation by phosphorylation of Ser-59 in the lck unique N-terminal region. Proc Natl Acad Sci U S A 92: 12338-12342.

92. Pasinetti GM, Aisen PS (1998) Cyclooxygenase-2 expression is increased in frontal cortex of Alzheimer's disease brain. Neuroscience 87: 319-324.

93. Pignatelli M, Sanchez-Rodriguez J, Santos A, Perez-Castillo A (2005) 15-deoxy-Delta-12,14-prostaglandin J2 induces programmed cell death of breast cancer cells by a pleiotropic mechanism. Carcinogenesis 26: 81-92.

94. Plemper RK, Wolf DH (1999) Retrograde protein translocation: ERADication of secretory proteins in health and disease. Trends Biochem Sci 24: 266-270.

95. Puls A, Schmidt S, Grawe F, Stabel S (1997) Interaction of protein kinase C zeta with ZIP, a novel protein kinase C-binding protein. Proc Natl Acad Sci U S A 94: 6191-6196.

96. Ramos PC, Hockendorff J, Johnson ES, Varshavsky A, Dohmen RJ (1998) Ump1p is required for proper maturation of the 20S proteasome and becomes its substrate upon completion of the assembly. Cell 92: 489-499.

97. Rebel A, Malkani K, Basle M, Bregeon C, Patezour A, Filmon R (1974) Ultrastructural characteristics of osteoclasts in Paget's disease. Rev Rhum Mal Osteoartic 41: 767-771.

98. Reits EAJ, Benham AM, Plougastel B, Neefjes J, Trowsdale J (1997) Dynamics of proteasome distribution in living cells. EMBO J 16: 6087-6094.

99. Rossi A, Kapahi P, Natoli G, Takahashi T, Chen Y, Karin M, Santoro MG (2000) Anti-inflammatory cyclopentenone prostaglandins are direct inhibitors of IkappaB kinase. Nature 403: 103-108.

100. Sairam K, Saravanan KS, Banerjee R, Mohanakumar KP (2003) Non-steroidal anti-inflammatory drug sodium salicylate, but not diclofenac or celecoxib, protects against 1-methyl-4-phenyl pyridinium-induced dopaminergic neurotoxicity in rats. Brain Res 966: 245-252.

101. Sanz L, Diaz-Meco MT, Nakano H, Moscat J (2000) The atypical PKC-interacting protein p62 channels NF-

kappaB activation by the IL-1-TRAF6 pathway. EMBO J 19: 1576-1586.

102. Sanz L, Sanchez P, Lallena MJ, Diaz-Meco MT, Moscat J (1999) The interaction of p62 with RIP links the atypical PKCs to NF-kappaB activation. EMBO J 18: 3044-3053.

103. Sawano H, Haneda M, Sugimoto T, Inoki K, Koya D, Kikkawa R (2002) 15-Deoxy-Delta12,14-prostaglandin J2 inhibits IL-1beta-induced cyclooxygenase-2 expression in mesangial cells. Kidney Int 61: 1957-1967.

104. Scher JU, Pillinger MH (2005) 15d-PGJ2: the anti-inflammatory prostaglandin? Clin Immunol 114: 100-109.

105. Scherrer K, Bey F (1994) The prosomes (multicatalytic proteinases; proteasomes) and their relationship to the untranslated messenger ribonucleoproteins, the cytoskeleton, and cell differentiation. Prog Nucleic Acid Res Mol Biol 49: 1-64.

106. Schwartz AL, Ciechanover A (1999) The ubiquitin-proteasome pathway and pathogenesis of human diseases. Annu Rev Med 50: 57-74.

107. Seibenhener ML, Babu JR, Geetha T, Wong HC, Krishna NR, Wooten MW (2004) Sequestosome 1/p62 is a polyubiquitin chain binding protein involved in ubiquitin proteasome degradation. Mol Cell Biol 24: 8055-8068.

108. Shin J (1998b) P62 and the sequestosome, a novel mechanism for protein metabolism. Arch Pharm Res 21: 629-633.

109. Shin J (1998a) P62 and the sequestosome, a novel mechanism for protein metabolism. Arch Pharm Res 21: 629-633.

110. Sitte N, Merker K, Grune T (1998) Proteasome-dependent degradation of oxidized proteins in MRC-5 fibroblasts. FEBS Lett 440: 399-402.

111. Smith WL, DeWitt DL, Garavito RM (2000) Cyclooxygenases: structural, cellular, and molecular biology. Annu Rev Biochem 69: 145-182.

112. Stewart WF, Kawas C, Corrada M, Metter EJ (1997) Risk of Alzheimer's disease and duration of NSAID use [see comments]. Neurology 48: 626-632.

113. Straus DS, Glass CK (2001) Cyclopentenone prostaglandins: new insights on biological activities and cellular targets. Med Res Rev 21: 185-210.

114. Straus DS, Pascual G, Li M, Welch JS, Ricote M, Hsiang CH, Sengchanthalangsy LL, Ghosh G, Glass CK (2000) 15-deoxy-delta 12,14-prostaglandin J2 inhibits multiple steps in the NF-kappa B signaling pathway. Proc Natl Acad Sci U S A 97: 4844-4849.

115. Streit WJ, Mrak RE, Griffin WS (2004) Microglia and neuroinflammation: a pathological perspective. J Neuroinflammation 1: 14.

116. Stumptner C, Fuchsbichler A, Heid H, Zatloukal K, Denk H (2002a) Mallory body--a disease-associated type of sequestosome. Hepatology 35: 1053-1062.

117. Stumptner C, Fuchsbichler A, Heid H, Zatloukal K, Denk H (2002b) Mallory body--a disease-associated type of sequestosome. Hepatology 35: 1053-1062.

118. Tagliavini F, Giaccone G, Bugiani O, Frangione B (1993) Ubiquitinated neurites are associated with preamyloid and cerebral amyloid beta deposits in patients with hereditary cerebral hemorrhage with amyloidosis Dutch type. Acta Neuropathol (Berl) 85: 267-271.

119. Tanaka K, Suzuki T, Chiba T, Shimura H, Hattori N, Mizuno Y (2001) Parkin is linked to the ubiquitin pathway. J Mol Med 79: 482-494.

120. Tanaka M, Kim YM, Lee G, Junn E, Iwatsubo T, Mouradian MM (2004) Aggresomes formed by alpha-synuclein and synphilin-1 are cytoprotective. J Biol Chem 279: 4625-4631.

121. Tran PB, Miller RJ (1999) Aggregates in neurodegenerative disease: crowds and power? [In Process Citation]. Trends Neurosci 22: 194-197.

122. Trushina E, Heldebrant MP, Perez-Terzic CM, Bortolon R, Kovtun IV, Badger JD, Terzic A, Estevez A,

Windebank AJ, Dyer RB, Yao J, McMurray CT (2003) Microtubule destabilization and nuclear entry are sequential steps leading to toxicity in Huntington's disease. Proc Natl Acad Sci U S A 100: 12171-12176.

123. Urade Y (1997) [New aspects on prostaglandin D synthases]. Nippon Yakurigaku Zasshi 110 Suppl 1: 56P-58P.

124. Urade Y, Hayaishi O (2000) Prostaglandin D synthase: structure and function. Vitam Horm 58: 89-120.

125. Vadlamudi RK, Joung I, Strominger JL, Shin J (1996a) p62, a phosphotyrosine-independent ligand of the SH2 domain of p56lck, belongs to a new class of ubiquitin-binding proteins. J Biol Chem 271: 20235-20237.

126. Vadlamudi RK, Joung I, Strominger JL, Shin J (1996b) p62, a phosphotyrosine-independent ligand of the SH2 domain of p56lck, belongs to a new class of ubiquitin-binding proteins. J Biol Chem 271: 20235-20237.

127. van Leeuwen FW, de Kleijn DP, van den Hurk HH, Neubauer A, Sonnemans MA, Sluijs JA, Koycu S, Ramdjielal RDJ, Salehi A, Martens GJM, Grosveld FG, Peter J, Burbach H, Hol EM (1998) Frameshift mutants of beta amyloid precursor protein and ubiquitin-B in Alzheimer's and Down patients [see comments]. Science 279: 242-247.

128. Viviani B, Bartesaghi S, Corsini E, Galli CL, Marinovich M (2004a) Cytokines role in neurodegenerative events. Toxicol Lett 149: 85-89.

129. Viviani B, Bartesaghi S, Corsini E, Galli CL, Marinovich M (2004b) Cytokines role in neurodegenerative events. Toxicol Lett 149: 85-89.

130. Wiborg O, Pedersen MS, Wind A, Berglund LE, Marcker KA, Vuust J (1985) The human ubiquitin multigene family: some genes contain multiple directly repeated ubiquitin coding sequences. EMBO J 4: 755-759.

131. Wigley WC, Fabunmi RP, Lee MG, Marino CR, Muallem S, DeMartino GN, Thomas PJ (1999) Dynamic association of

proteasomal machinery with the centrosome. J Cell Biol 145: 481-490.

132. Wilkinson CR, Seeger M, Hartmann-Petersen R, Stone M, Wallace M, Semple C, Gordon C (2001) Proteins containing the UBA domain are able to bind to multi-ubiquitin chains. Nat Cell Biol 3: 939-943.

133. Wilkinson KD (2000) Ubiquitination and deubiquitination: targeting of proteins for degradation by the proteasome. Semin Cell Dev Biol 11: 141-148.

134. Wilkinson KD, Deshpande S, Larsen CN (1992) Comparisons of neuronal (PGP 9.5) and non-neuronal ubiquitin C-terminal hydrolases. Biochem Soc Trans 20: 631-637.

135. Wilmer WA, Dixon C, Lu L, Hilbelink T, Rovin BH (2001) A cyclopentenone prostaglandin activates mesangial MAP kinase independently of PPARgamma. Biochem Biophys Res Commun 281: 57-62.

136. Wooten MW, Seibenhener ML, Mamidipudi V, Diaz-Meco MT, Barker PA, Moscat J (2001) The atypical protein kinase C-interacting protein p62 is a scaffold for NF-kappaB activation by nerve growth factor. J Biol Chem 276: 7709-7712.

137. Wu KK (2005) Control of cyclooxygenase-2 transcriptional activation by pro-inflammatory mediators. Prostaglandins Leukot Essent Fatty Acids 72: 89-93.

138. Yamagata K, Andreasson KI, Kaufmann WE, Barnes CA, Worley PF (1993) Expression of a mitogen-inducible cyclooxygenase in brain neurons: regulation by synaptic activity and glucocorticoids. Neuron 11: 371-386.

139. Yasojima K, Tourtellotte WW, McGeer EG, McGeer PL (2001) Marked increase in cyclooxygenase-2 in ALS spinal cord: implications for therapy. Neurology 57: 952-956.

140. Zatloukal K, Stumptner C, Fuchsbichler A, Heid H, Schnoelzer M, Kenner L, Kleinert R, Prinz M, Aguzzi A, Denk H (2002a) p62 Is a common component of

cytoplasmic inclusions in protein aggregation diseases. Am J Pathol 160: 255-263.

141. Zatloukal K, Stumptner C, Fuchsbichler A, Heid H, Schnoelzer M, Kenner L, Kleinert R, Prinz M, Aguzzi A, Denk H (2002b) p62 Is a common component of cytoplasmic inclusions in protein aggregation diseases. Am J Pathol 160: 255-263.